

Efficient option pricing for Rough Bergomi model

1 Introduction

1.1 The goal and outline of the project

The main goal of the project is to design a fast option pricer, based on multi-index stochastic collocation (MISC) as [18], for options whose dynamics follow rBergomi model as in [2]. We may later investigate QMC.

1.2 Review of literature

Extending the Black-Scholes model, in which volatility is assumed to be constant, to the case where the volatility is stochastic has proved to be successful in explaining certain phenomena observed in option price data, in particular the implied volatility smile. The main drawback of such stochastic volatility models, however, is that they are unable to capture the true steepness of the implied volatility smile close to maturity. While choosing to add jumps to stock price models, for example modelling the stock price process as an exponential Lévy process, does indeed produce steeper implied volatility smiles, the issue of the presence of jumps in stock price processes remains controversial[1, 10].

As an alternative to diffusive stochastic volatility models, rough stochastic volatility has emerged as a new paradigm in quantitative finance, motivated by the statistical analysis of realised volatility by Gatheral, Jaisson and Rosenbaum [16] and the theoretical results on implied volatility by Fukasawa [13]. In these models, the trajectories of volatility are less regular than those of the standard Brownian motion. As shown in [16, 2], these models are a family of (continuous-path) stochastic volatility models where the driving noise of the volatility process has Hölder regularity lower than Brownian motion, typically achieved by modeling the fundamental noise innovations of the volatility process as a fractional Brownian motion with Hurst exponent (and hence Hölder regularity) $0 < H < 1/2$. A major advantage of such rough volatility models is the fact that they allow to explain crucial phenomena observed in financial markets both from a statistical [16, 5] and an option-pricing point of view [2]. For instance, it was observed empirically that in equity markets that as time to maturity becomes small the empirical implied volatility skew follows a power law with negative exponent, and thus becomes arbitrarily large near zero. While standard stochastic volatility models with continuous paths struggle to capture this phenomenon, predicting instead a constant at-the-money implied volatility behaviour on the short end [14], fractional stochastic volatility models (and more specifically so-called rough volatility models) constitute alternative models that fit empirical implied volatilities for short dated options. Consequently, they have become the go-to models capable of reproducing stylised facts of financial markets.

Rough volatility models are based on fractional Brownian motion (fBM), which is a centred Gaussian process, whose covariance structure depends on the Hurst parameter $H \in (0, 1)$. If $H \in (0, 1/2)$, then the fractional Brownian motion has negatively correlated increments and "rough" sample paths, and if $H \in (1/2, 1)$ then it has positively correlated increments and "smooth" sample paths, when compared with a standard Brownian motion, which is recovered by taking $H = 1/2$. Gatheral, Jaisson, and Rosenbaum [16] justify empirically the benefits of such models; in particular, they argue that log-volatility in practice behaves essentially as fBM with the Hurst exponent $H \approx 0.1$ at any reasonable time scale (see also [15]). This finding is confirmed by Bennedsen, Lunde and Pakkanen [5], who study over a thousand individual US equities and find that the Hurst parameter H lies in $(0, 1/2)$ for each equity.

The rough Bergomi (rBergomi) model is one of the recent rough volatility models, developed by Bayer, Friz and Gatheral [2], that is consistent with the stylised fact of implied volatility surfaces being essentially time-invariant, and are able to capture the term structure of skew observed in equity markets. In [2], the authors constructed the rBergomi model by moving from physical to pricing measure and simulated prices under that model to fit well the implied volatility surface in the case of the S&P 500 index with few parameters-just three!. They claim that the fractional model generates strong skews or "smiles" in the implied volatility even for very short time to maturity so that this modeling provides an alternative to using jumps to model such an effect. In [2] the model is so named because of its relationship with the Bergomi variance curve model [7], and may be seen as a non-Markovian generalisation of the latter.

Due to the non-Markovian nature of the fractional driver, pricing and hedging under rough volatility constitute a significant challenge. In fact, the popularity of asset pricing models hinges on the availability of efficient numerical pricing methods. In the case of diffusions, these include Monte Carlo (MC) estimators, PDE discretization schemes, asymptotic expansions and transform methods. With fractional Brownian motion being the prime example of a process beyond the semi-martingale framework, most currently prevalent option pricing methods -particularly the ones assuming semimartingality or Markovianity - may not easily carry over to the rough setting. In fact, due to the lack of Markovianity or affine structure, conventional analytical pricing methods do not apply. At the moment, the only known method for pricing options under such models is MC simulation. In particular, recent advances in simulation methods for the rough Bergomi model have been achieved in [2, 3, 23, 6, 19]. For instance, in [23], the authors employ a novel composition of variance reduction methods, immediately applicable to any conditionally log-normal stochastic volatility model. They got a substantial computation gain in the pricing over the existing MC methods. On the other hand, more analytical results of option pricing and implied volatility under this model has been done in [20, 4, 12]. For instance, in [20], they characterise the small-time behaviour of implied volatility using large deviations theory and related results, concerning the small-time near-the-money skew, have been obtained by Bayer, Friz, Gulisashvili, Horvath and Stemper [4]. However, we should point out that pricing and model calibration under rough volatility models still remains time consuming.

In this paper, we suggest to design a fast option pricer, based on multi-index stochastic collocation (MISC) as in [18], for options whose dynamics follow rBergomi model as in [2]. We may later investigate QMC.

1.3 Background on Gaussian and fBM processes

A zero-mean real-valued Gaussian process $(Z_t)_{t \geq 0}$ is a stochastic process such that on any finite subset $\{t_1, \dots, t_n\} \subset \mathbb{R}$, $(Z_{t_1}, \dots, Z_{t_n})$ has a multivariate normal distribution with mean zero. The law of a Gaussian process is entirely determined by the covariance function $K(s, t) = \mathbb{E}[Z_t Z_s]$ and Z induces a Gaussian probability measure on $(E, \mathcal{B}(E))$, where E denotes the Banach space $C_0([0, 1])$ with the usual sup norm topology (see, e.g., section 3.1.1 of [9] for details).

Fractional Brownian motion (fBM) is a natural generalization of standard Brownian motion which preserves the properties of stationary increments, self-similarity, and Gaussian finite-dimensional distributions, but it has a more complex dependence structure. In this section, we recall the definition and summarize the basic properties of fBM.

A zero-mean Gaussian process B_t^H is called standard fractional Brownian motion (fBM) with Hurst parameter $H \in (0, 1)$ if it has covariance function

$$(1) \quad R_H = \mathbb{E}[B_t^H B_s^H] - \mathbb{E}[B_t^H] \mathbb{E}[B_s^H] = \frac{1}{2} (|t|^{2H} + |s|^{2H} - |t-s|^{2H}).$$

In order to specify the distribution of a Gaussian process, it is enough to specify its mean and its covariance function; therefore, for each H , the law of B_t^H is uniquely determined by $R_H(s, t)$. However, this definition by itself does not guarantee the existence of fBM; to show that fBM exists, one needs to verify that the covariance function is nonnegative definite.

We now recall some fundamental properties of fBM (see also Figure 1):

- fBM is continuous a.s. and H-self-similar (H-ss), i.e., for $a > 0$, $(B_{at})_{t \geq 0} \stackrel{(d)}{=} a^H (B_t)_{t \geq 0}$ where $\stackrel{(d)}{=}$ means both processes have the same finite-dimensional distributions. For $H \neq 1/2$, B_t^H does not have independent increments; for $H = 1/2$, B_t^H is the standard Brownian motion.
- From (1), we see that
$$\mathbb{E}[(B_t^H - B_s^H)^2] = |t-s|^{2H},$$
so $B_t^H - B_s^H \sim \mathcal{N}(0, |t-s|^{2H})$; thus B_t^H has stationary increments.
- If we set $X_n = B_n^H - B_{n-1}^H$, then X_n is a discrete-time Gaussian process with covariance function

$$\begin{aligned} \rho_n &= \mathbb{E}[X_{k+n} X_n] = \mathbb{E}[(B_{k+n}^H - B_{k+n-1}^H)(B_k^H - B_{k-1}^H)] \\ &\sim H(2H-1)n^{2H-2} \quad (n \rightarrow \infty), \end{aligned}$$

and thus (by convexity of the function $g(n) = n^{2H}$), we see that two increments of the form $B_k - B_{k-1}$ and $B_{k+n} - B_{k+n-1}$ are positively correlated if $H \in (1/2, 1)$ and negatively correlated if $H \in (0, 1/2)$. Thus B_t^H is persistent (i.e., it is more likely to keep a trend than to break it) when $H > 1/2$, the relatively stronger positive correlation for the consecutive increments of the associated fBm process with increasing H values gives a relatively smoother process whose correlations decay relatively slowly. On the other hand, it is antipersistent when $H < 1/2$ (i.e., if B_t^H was increasing in the past, it is more likely to decrease in the future, and vice versa). The enhanced negative correlation with smaller Hurst exponent gives a relatively rougher process.

- If $H \in (1/2, 1)$, we can show that $\sum_{n=1}^{\infty} \rho_n = \infty$, which means that the process exhibits long-range dependence, but if $H \in (0, 1/2)$, then $\sum_{n=1}^{\infty} \rho_n < \infty$.
- Using that $E[(B_t^H - B_s^H)^2] = (t-s)^{2H}$, we can show that sample paths of B^H are α -H older continuous for all $\alpha \in (0, H)$.
- fBM is the only self-similar Gaussian process with stationary increments (see, e.g., [22]), and for $H \neq 1/2$, B_t^H is neither a Markov process nor a semimartingale (see, e.g., [24]).

For more details regarding the fBm processes we refer to [8, 11, 21].

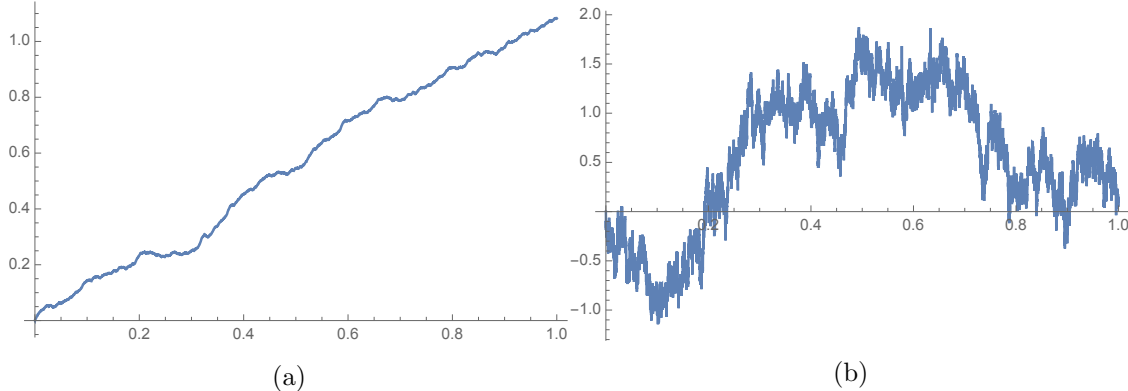


Figure 1: Monte Carlo simulation of fBM for $H = 0.9$ (left) and $H = 0.3$ (right).

2 Problem setting

2.1 The rBergomi model

We use the rBergomi model for the price process S_t as defined in [2], normalized to $r = 0$, which is defined by

$$(2) \quad dS_t = \sqrt{v_t(\tilde{W}^H)} S_t dZ_t,$$

$$(3) \quad v_t = \xi_0(t) \exp \left(\eta \tilde{W}_t^H - \frac{1}{2} \eta^2 t^{2H} \right),$$

where for $0 < H < 1$ and $\eta > 0$. We have \tilde{W}^H is a certain Volterra process (Riemann-Liouville process), defined by

$$(4) \quad \tilde{W}_t^H = \int_0^t K^H(t, s) dW_s^1, \quad t \geq 0$$

where the kernel $K^H : \mathbb{R}_+ \times \mathbb{R}_+ \rightarrow \mathbb{R}_+$ reads

$$(5) \quad K^H(t, s) = \sqrt{2H} (t-s)^{H-1/2}, \quad \forall 0 \leq s \leq t.$$

We note that the map $s \rightarrow K^H(s, t)$ belongs to L^2 , so that the stochastic integral (4) is well defined.

W^1, Z denote two *correlated* standard Brownian motions with correlation $\rho \in [-1, 1]$, so that

$$(6) \quad Z := \rho W^1 + \bar{\rho} W^\perp \equiv \rho W^1 + \sqrt{1 - \rho^2} W^\perp,$$

where (W^1, W^\perp) are two independent standard Brownian motions, Therefore, Eq 2 can be written as

$$(7) \quad \begin{aligned} S_t &= S_0 \exp \left(\int_0^t \sqrt{v(s)} dZ(s) - \frac{1}{2} \int_0^t v(s) ds \right), \quad S_0 > 0 \\ v(u) &= \xi_0(u) \exp \left(\eta \tilde{W}_u^H - \frac{\eta^2}{2} u^H \right), \quad \xi_0 > 0 \end{aligned}$$

The filtration $(\mathcal{F}_t)_{t \geq 0}$ can here be taken as the one generated by the two-dimensional Brownian motion (W^1, W^\perp) under the risk neutral measure \mathbb{Q} , resulting in a filtered probability space $(\Omega, \mathcal{F}; \mathcal{F}_t, \mathbb{Q})$. The stock price process S is clearly then a local $(\mathcal{F}_t)_{t \geq 0}$ -martingale and a supermartingale, therefore integrable. We shall henceforth use the notation $\mathbb{E}[.] = E^\mathbb{Q}[. | \mathcal{F}_0]$ unless we state otherwise.

We refer to v_u as the variance process, where $\xi_0(u) = \mathbb{E}[v_u] \in \mathcal{F}_0$ a.s. the forward variance curve. \tilde{W}^H is a centered, locally $(H - \epsilon)$ - Hölder continuous, Gaussian process with $\text{var}[\tilde{W}_t^H] = t^{2H}$.

We note that the model parameters (η, ρ, H) may have an intuitive interpretation of their influence over implied volatilities. In fact, η might seen as smile, ρ as skew, $H - 1/2$ as the explosion(smile and skew).

2.2 Option pricing under rBergomi model

Assuming $S_0 = 1$, and using the conditioning argument on the σ -algebra generated by W^1 (argument first used by [25] in the context of Markovian SV models), we can show that the call price is given by

$$(8) \quad \begin{aligned} C_{RB}(T, K) &= E[(S_T - K)^+] \\ &= E[E[(S_T - K)^+ | \sigma(W^1(t), t \leq T)]] \\ &= E \left[C_{BS} \left(S_0 = \exp \left(\rho \int_0^T \sqrt{v_t} dW_t^1 - \frac{1}{2} \rho^2 \int_0^T v_t dt \right), K = K, T = 1, \sigma^2 = (1 - \rho^2) \int_0^T v_t dt \right) \right], \end{aligned}$$

where C_{BS} denotes the Black-Scholes price.

In fact, if we use the orthogonal decomposition of S_t into S_t^1 and S_t^2 , where

$$(9) \quad S_t^1 := \mathcal{E}\{\rho \int_0^t \sqrt{v_s} dW_s^1\}, \quad S_t^2 := \mathcal{E}\{\sqrt{1 - \rho^2} \int_0^t \sqrt{v_s} dW_s^\perp\},$$

where $\mathcal{E}()$ denotes the stochastic exponential, then, we obtain by conditional log-normality

$$(10) \quad \log S_t \mid \mathcal{F}_t^1 \sim \mathcal{N} \left(\log S_t^1 - \frac{1}{2}(1-\rho^2) \int_0^t v_s ds, (1-\rho^2) \int_0^t v_s ds \right),$$

where $\mathcal{F}_t^1 = \sigma\{W_s^1 : s \leq t\}$. Therefore, we obtain (8).

We insist that the smoothing trick, based on conditionning, performed in Eq (8) enable us to get a smooth term inside the expectation. Therefore, applying sparse quadrature techniques becomes an adequate option for computing the call price as we shall see later.

2.3 Simulation of the rBergomi model

The main challenge is the computation of $S = \int_0^T \sqrt{v_t} dW_t^1$ and $V = \int_0^T v_t dt$. As was mentioned in [3], we may try to avoid any sampling related to W^2 by a brute-force approach that consists in simulating a scalar Brownian motion W^1 , followed by computing $\tilde{W}^H = \int K dW^1$ by Itô/Riemann Stieltjes approximations of (S, V) . However, this is not advisable given the singularity of the Volterra kernel $K(s, t)$ at the diagonal $s = t$. Therefore, one needs to jointly simulate the two-dimensional Gaussian process $(W_t^1, \tilde{W}_t^H : 0 \leq t \leq T)$, resulting in $W_{t_1}^1, \dots, W_{t_N}^1$ and $\tilde{W}_{t_1}^H, \dots, \tilde{W}_{t_N}^H$ along a given grid $t_1 < \dots < t_N$. There are essentially three possible ways to achieve this:

1. Euler discretization of the integral defining \tilde{W}^H together with classical simulation of increments of W^1 . This is horribly inefficient because the integral is singular and adaptivity probably does not help, as the singularity moves with time. For this method, we need an N -dimensional random Gaussian input vector to produce one (approximate, inaccurate) sample of $W_{t_1}^1, \dots, W_{t_N}^1, \tilde{W}_{t_1}^H, \dots, \tilde{W}_{t_N}^H$.
2. Given that $W_{t_1}^1, \dots, W_{t_N}^1, \tilde{W}_{t_1}^H, \dots, \tilde{W}_{t_N}^H$ together forms a $(2N)$ -dimensional Gaussian random vector with computable covariance matrix. We can use Cholesky decomposition of the covariance matrix to produce exact samples of $W_{t_1}^1, \dots, W_{t_N}^1, \tilde{W}_{t_1}^H, \dots, \tilde{W}_{t_N}^H$, but unlike the first way, we need $2N$ -dimensional Gaussian random vectors as input. This method is exact but slow (See [2] and Section 4 in [4]). The simulation requires $\mathcal{O}(N^3)$. flops.
3. The hybrid scheme of [6] uses a different approach, which is essentially based on Euler discretization as the first way but crucially improved by moment matching for the singular term in the left point rule. It is also inexact in the sense that samples produced here do not exactly have the distribution of $W_{t_1}^1, \dots, W_{t_N}^1, \tilde{W}_{t_1}^H, \dots, \tilde{W}_{t_N}^H$, however they are much more accurate than samples produced from method 1), but much faster than method 2). As in method 2), in this case we need a $2N$ -dimensional Gaussian random input vector to produce one sample of $W_{t_1}^1, \dots, W_{t_N}^1, \tilde{W}_{t_1}^H, \dots, \tilde{W}_{t_N}^H$.

In this project, we adopt the last approach for the simulation of the rBergomi model. We utilise the first order variant ($\kappa = 1$) of the hybrid scheme [6], which is based on the approximation

$$(11) \quad \tilde{W}_{\frac{i}{N}}^H \approx \overline{W}_{\frac{i}{N}} := \sqrt{2H} \left(\int_{\frac{i-1}{N}}^{\frac{i}{N}} \left(\frac{i}{N} - s \right)^{H-\frac{1}{2}} dW_u^1 + \sum_{k=2}^i \left(\frac{b_k}{N} \right)^{H-\frac{1}{2}} \left(W_{\frac{i-(k-1)}{N}}^1 - W_{\frac{i-k}{N}}^1 \right) \right)$$

where N is the number of time steps and

$$b_k := \left(\frac{k^{H+\frac{1}{2}} - (k-1)^{H+\frac{1}{2}}}{H + \frac{1}{2}} \right)^{\frac{1}{H-\frac{1}{2}}}$$

Employing the fast Fourier transform to evaluate the sum in (11), which is a discrete convolution, a skeleton $\bar{W}_0^H, \bar{W}_1^H, \dots, \bar{W}_{\frac{[Nt]}{N}}^H$ can be generated in $\mathcal{O}(N \log N)$ floating point operations.

The variates $\bar{W}_0^H, \bar{W}_1^H, \dots, \bar{W}_{\frac{[Nt]}{N}}^H$ can be generated by sampling $[nt]$ iid draws from a $\kappa + 1$ -dimensional Gaussian distribution and computing a discrete convolution. We call these pairs of Gaussian random variables from now on as (W^1, W^2) .

3 Details our approach and error bounds

Our approach of computing the expectation in (8) is based on multi-index stochastic collocation (MISC), suggested in [18]. We describe the general strategy for the multi-index construction in Section 3.1. Recall that there are two N dimensional Gaussian inputs for the used hybrid approach (N is the number of time steps in the time grid), namely

- $\{W^1\}_{i=1}^N$: The N Gaussian random parameters that are defined in Section 2.1.
- $\{W^2\}_{i=1}^N$: An artificial introduced N Gaussian random parameters that are used for left-rule points in the hybrid scheme, explained in Section 2.3.

We have a natural error decomposition for the total error of computing the the expectation in (8), namely, \mathcal{E}

$$(12) \quad \mathcal{E} \leq \mathcal{E}_Q(TOL_{\text{MISC}}, N) + \mathcal{E}_B(N),$$

where \mathcal{E}_Q is the quadrature error, function of MISC tolerance TOL_{MISC} and N (the number of time steps) and \mathcal{E}_B is the bias, function of N (the number of time steps) or $\Delta_t = \frac{T}{N}$ (size of the time grid).

We note that sampling the Brownian motion can be constructed either sequentially using a standard random walk construction or hierarchically using Brownian bridge (BB) construction. To make an effective use of MISC, which is badly affected by isotropy, we use the BB construction since it produces dimensions with different importance for MISC (creates anisotropy), contrary to random walk procedure for which all the dimension of the stochastic space have equal importance (isotropic). We explain the BB construction in Section 3.3. This transformation plays a role of dimension reduction of the problem and as a consequence accelerating the MISC procedure by reducing the computational cost.

Another way to reduce the dimension of the problem is by using Richardson extrapolation, explained in Section 3.4. In fact, Richardson extrapolation acts on both the bias (by reducing it) and MISC procedure by redcing the number of needed time steps , N , neeeded to achive a certain tolerance, resulting in a lower dimensional problem.

Motivated by some numerical observations regarding the behavior of the MISC solver with respect to the standard Gaussian hermite quadrature (See Section 4), We build a more robust MISC solver by incorporating a change of measure with respect to W^1 as described in Section 3.2.

We also discuss the error bounds in Section 3.5

3.1 Details of the MISC

We focus on solving the problem of approximating the expected value of $E[f(y)]$ on a tensorization of quadrature formulae over the stochastic domain, Γ . Assuming that $f(y)$ is a continuous function (analytic) over Γ . A quadrature approach is very adequate.

Let us define $\beta \leq 1$ be an integer positive value referred to as a "stochastic discretization level", and $m : \mathbb{N} \rightarrow \mathbb{N}$ be a strictly increasing function with $m(0) = 0$ and $m(1) = 1$, that we call a "level-to-nodes function". At level β , we consider a set of $m(\beta)$ distinct quadrature points in $(-\infty; \infty)$, $\mathcal{H}^{m(\beta)} = \{y_\beta^1, y_\beta^2, \dots, y_\beta^{m(\beta)}\} \subset [-\infty, \infty]$, and a set of quadrature weights, $\mathcal{W}^{m(\beta)} = \{\omega_\beta^1, \omega_\beta^2, \dots, \omega_\beta^{m(\beta)}\}$. We also let $C^0((-\infty, \infty))$ be the set of real-valued continuous functions over $(-\infty, \infty)$. We then define the quadrature operator as

$$(13) \quad Q(m(\beta)) : C^0((-\infty, \infty)) \rightarrow \mathbb{R}, \quad Q(m(\beta))[f] = \sum_{j=1}^{m(\beta)} f(y_\beta^j) \omega_\beta^j.$$

In the multi-variate case Γ is defined as a countable tensor product of intervals. Therefore, we define, for any definitely supported multi-index $\beta \in \mathcal{L}_+$

$$Q^{m(\beta)} : \Gamma \rightarrow \mathbb{R}, \quad Q^{m(\beta)} = \bigotimes_{n \geq 1} Q^{m(\beta_n)}$$

where the n -th quadrature operator is understood to act only on the n -th variable of f . Practically, we obtain the value of $Q^{m(\beta)}[f]$ by considering the tensor grid $\mathcal{T}^{m(\beta)} = \times_{n \geq 1} \mathcal{H}^{m(\beta_n)}$ with cardinality $\#\mathcal{T}^{m(\beta)} = \prod_{n \geq 1} m(\beta_n)$ and computing

$$Q^{\mathcal{T}^{m(\beta)}}[f] = \sum_{j=1}^{\#\mathcal{T}^{m(\beta)}} f(\hat{y}_j) \bar{\omega}_j$$

where $\hat{y}_j \in \mathcal{T}^{m(\beta)}$ and $\bar{\omega}_j$ are (infinite) products of weights of the univariate quadrature rules. We Note that it is essential in this construction that $m(1) = 1$ so that the cardinality of $\mathcal{T}^{m(\beta)}$ is finite for any $\beta \in \mathcal{L}_+$ and $\omega_{\beta_n}^1 = 1$ whenever $n = 1$, so that all weights, $\bar{\omega}_j$, are bounded.

We mention that the quadrature points are chosen to optimize the convergence properties of the quadrature error.

A direct approximation $E[f] \approx Q^{m(\beta)}[f]$ is not an appropriate option due to the well-known "curse of dimensionality" effect. We use multi-index stochastic collocation (MISC) as it was suggested in [18]. MISC as a hierarchical adaptive quadrature strategy that uses stochastic discretizations and classic sparsification approach to obtain an effective approximation scheme for $E[f]$.

In our setting, we are left with a $2N$ -dimensional Gaussian random inputs, which are chosen independently, resulting in $2N$ numerical parameters, which we use as the basis of the multi-index construction, reflecting the fact that W_i^1 and W_j^2 can vary independently of each other regardless of $i \neq j$ or $i = j$. For the sake of concreteness, let $l \in \{1, \dots, 2N\}$ and set

$$(14) \quad m_l := \begin{cases} W_l^1, & 1 \leq l \leq N, \\ W_{l-N}^2, & N + 1 \leq l \leq 2N. \end{cases}$$

For a multi-index $\ell = (l_i)_{i=1}^{2N} \in \mathbb{N}^{2N}$ we denote by $Q_\ell^N := Q^N(m_\ell)$ the result of a discretized integral, using N time steps, with parameters $m_\ell := (m_i)_{i=1}^{2N}$. We further define the set of differences ΔQ_ℓ^N as follows: for a single index $1 \leq i \leq 2N$, let

$$(15) \quad \Delta_i Q_\ell^N := \begin{cases} Q^N(m_\ell) - Q^N(m'_\ell) & \text{with } m'_\ell = m_{\ell-e_i}, \text{ if } \ell_i > 0 \\ & Q^N(m_\ell) \text{ otherwise} \end{cases}$$

where e_i denotes the i th $2N$ -dimensional unit vector. Then, ΔQ_ℓ^N is defined as

$$(16) \quad \Delta Q_\ell^N := \left(\prod_{i=1}^{2N} \Delta_i \right) Q_\ell^N.$$

For instance, when $N = 1$, then

$$\begin{aligned} \Delta Q_\ell^1 &= \Delta_2 \Delta_1 Q_{(l_1, l_2)}^1 = \Delta_2 \left(Q_{(l_1, l_2)}^1 - Q_{(l_1-1, l_2)}^1 \right) = \Delta_2 Q_{(l_1, l_2)}^1 - \Delta_2 Q_{(l_1-1, l_2)}^1 \\ &= Q_{(l_1, l_2)}^1 - Q_{(l_1, l_2-1)}^1 - Q_{(l_1-1, l_2)}^1 + Q_{(l_1-1, l_2-1)}^1. \end{aligned}$$

Note that $Q^N(m)$ converges to the biased option price (denoted by $Q^N(\infty)$) as $m \rightarrow \infty$. Hence, we have the telescoping property

$$(17) \quad Q^N(\infty) = \sum_{l_1=0}^{\infty} \cdots \sum_{l_{2N}=0}^{\infty} \Delta Q_{(l_1, \dots, l_{2N})}^N = \sum_{\ell \in \mathbb{N}^{2N}} \Delta Q_\ell^N,$$

provided that $m_{l_1} \xrightarrow{l_1 \rightarrow \infty} \infty, \dots, m_{l_{2N}} \xrightarrow{l_{2N} \rightarrow \infty} \infty$. The telescoping property is accompanied by a corresponding error factorization, i.e., the size of the increment ΔQ_ℓ^N can be bounded by a product of error terms depending on m_i and m_{i+N} .

We denote the computational work at level $\ell = (l_1, \dots, l_{2N})$ for adding an increment ΔQ_ℓ^N in the telescoping sum by W_ℓ^N , and define the actual estimator for the quantity of interest $Q^N(\infty)$: given a set of multi-indices $\mathcal{I} \subset \mathbb{N}^{2N}$, let

$$Q^N(\mathcal{I}) := \sum_{\ell \in \mathcal{I}} \Delta Q_\ell^N.$$

Then the error is given by

$$|Q^N(\infty) - Q^N(\mathcal{I})| \leq \sum_{\ell \in \mathbb{N}^{2N} \setminus \mathcal{I}} |\Delta Q_\ell^N|,$$

The construction of \mathcal{I} will be done by profit thresholding, i.e., for a certain threshold value T , we add a multi-index ℓ to \mathcal{I} provided that

$$\log \left(\frac{|\Delta Q_\ell^N|}{W_\ell^N} \right) \leq T.$$

(Actually, we take the error estimate instead of the true error.)

3.2 Gaussian Hermite Quadrature with importance sampling

Let us call the integrand that we feed to MISC by $I(W^1, W^2)$, then

$$(18) \quad C_{RB}(T, K) = \int_{\mathbb{R}_+^{2N}} I(\mathbf{W}^1, \mathbf{W}^2) \rho(\mathbf{W}^1) \rho(\mathbf{W}^2) d\mathbf{W}^1 d\mathbf{W}^2,$$

where N is the number of time steps. We can rewrite the previous expression as

$$(19) \quad C_{RB}(T, K) = \int_{\mathbb{R}_+^{2N}} \frac{I(\mathbf{W}^1, \mathbf{W}^2) \rho(\mathbf{W}^1)}{h(\mathbf{W}^1; \widehat{\mathbf{W}}^1, \Psi)} h(\mathbf{W}^1; \widehat{\mathbf{W}}^1, \Psi) \rho(\mathbf{W}^2) d\mathbf{W}^1 d\mathbf{W}^2,$$

where $h(\mathbf{W}^1; \widehat{\mathbf{W}}^1, \Psi)$ is a multivariate normal density with first and second order moments given by

$$(20) \quad \widehat{\mathbf{W}}^1 = \arg \max_{\mathbf{W}^1 \in \mathbb{R}^N} [\log I(\mathbf{W}^1; \mathbf{W}^2 = \mathbf{0})]$$

$$(21) \quad \Psi = \left(-\frac{\partial^2 [\log I(\mathbf{W}^1; \mathbf{W}^2 = \mathbf{0})]}{\partial (\mathbf{W}^1)^T \mathbf{W}^1} \right)^{-1}_{\mathbf{W}^1 = \widehat{\mathbf{W}}^1}$$

Let us define $\tilde{\mathbf{W}}^1$ as uncorrelated variables and the Cholesky factorization of Ψ is given by $\Psi = LL^T$, and $\overline{\mathbf{W}}^1 = \sqrt{2}L\tilde{\mathbf{W}}^1 + \widehat{\mathbf{W}}^1$ then Eq 19 becomes

(22)

$$C_{RB}(T, K) = 2^{N/2} \cdot |L| \int_{\mathbb{R}_+^{2N}} \left(I(\overline{\mathbf{W}}^1, \mathbf{W}^2) \exp\left(-\frac{1}{2}(\overline{\mathbf{W}}^1)^T \overline{\mathbf{W}}^1\right) \exp\left(\frac{1}{2}\tilde{\mathbf{W}}^1 T \tilde{\mathbf{W}}^1\right) \right) \rho(\tilde{\mathbf{W}}^1) \rho(\mathbf{W}^2) d\tilde{\mathbf{W}}^1 d\mathbf{W}^2$$

3.3 Brownian bridge construction

Let us denote $\{t_i\}_{i=0}^N$ the grid of time steps, then the BB construction [17] consists of the following: given a past value B_{t_i} and a future value B_{t_k} , the value B_{t_j} (with $t_i < t_j < t_k$) can be generated according to the formula:

$$(23) \quad B_{t_j} = (1 - \rho)B_{t_i} + \rho B_{t_k} + \sqrt{\rho(1 - \rho)(k - i)\Delta t} z, \quad z \sim \mathcal{N}(0, 1),$$

where $\rho = \frac{j-i}{k-i}$. In particular, if N is a power of 2, then given $B_0 = 0$, BB generates the Brownian motion at times $T, T/2, T/4, 3T/4, \dots$ according

$$(24) \quad \begin{aligned} B_T &= \sqrt{T}z_1 \\ B_{T/2} &= \frac{1}{2}(B_0 + B_T) + \sqrt{T/4}z_2 = \frac{\sqrt{T}}{2}z_1 + \frac{\sqrt{T}}{2}z_2 \\ B_{T/4} &= \frac{1}{2}(B_0 + B_{T/2}) + \sqrt{T/8}z_3 = \frac{\sqrt{T}}{4}z_1 + \frac{\sqrt{T}}{4}z_2 + \sqrt{T/8}z_3 \\ &\vdots \end{aligned}$$

where $\{z_j\}_{j=1}^N$ are independent standard normal variables. In BB construction given by (24), the most important values that determine the large scale structure of Brownian motion are the first components of $\mathbf{z} = (z_1, \dots, z_N)$.

3.4 Richardson extrapolation

We recall that the Euler (often) scheme has weak order 1 so that

$$(25) \quad \left| \mathbb{E} \left[f(\hat{X}_T^h) \right] - \mathbb{E} [f(X_T)] \right| \leq Ch$$

for some constant C , all sufficiently small h and suitably smooth f . It was shown that 25 can be improved to

$$(26) \quad \mathbb{E} \left[f(\hat{X}_T^h) \right] = \mathbb{E} [f(X_T)] + ch + \mathcal{O}(h^2),$$

where c depends on f .

Applying 26 with discretization step $2h$, we obtain

$$(27) \quad \mathbb{E} \left[f(\hat{X}_T^{2h}) \right] = \mathbb{E} [f(X_T)] + 2ch + \mathcal{O}(h^2),$$

implying

$$(28) \quad 2\mathbb{E} \left[f(\hat{X}_T^{2h}) \right] - \mathbb{E} \left[f(\hat{X}_T^h) \right] = \mathbb{E} [f(X_T)] + \mathcal{O}(h^2),$$

For higher levels extrapolations, we use the following: Let us denote by $h_J = h_0 \cdot 2^{-J}$ the grid sizes (where h_0 is the coarsest grid size), by K the level of the Richardson extrapolation, and by $I(J, K)$ the approximation of $\mathbb{E} \left[f(\hat{X}_T^{h_J}) \right]$ by terms up to level K (leading to a weak error of order K), then we have

$$(29) \quad I(J, K) = \frac{2^K [I(J, K-1) - I(J-1, K-1)]}{2^K - 1} + \mathcal{O}(h^{K+1}), \quad J = 1, 2, \dots, K = 1, 2, \dots$$

3.5 Discussion about error bounds

TO-DO: In this Section, we discuss each term in Eq 12 seperately.

3.5.1 Discussion about the Bias error

3.5.2 Discussion about the quadrature error

4 Numerical tests

In this Section, the default paramters values of the rBergomi model (unless stated), defined in Section 2.1, are: $S_0 = 1$, $\eta = 1.9$, $\xi = 0.235^2$, $\rho = -0.9$, $T = 1$.

4.1 Summary of the numerical results

We conduct our experiments for 5 different parameters sets as presented in tables 1.

In Section 4.2, we estimate the weak error (Bias) for the different parameter constellations, for 2 scenarios involving with/without Richardson extrapolation. The conclusions of this section are:

- Without Richardson extrapolation: For all cases, we get a weak error of order Δt , with different constants. Interestingly, we see that the case of parameters set 5 (see table 1) has the lowest constant. On the other hand, the case of parameters set 4 (see table 1) has the biggest constant.
- With Richardson extrapolation: For all cases, we get a weak error of order around Δt^2 . We observed similar constants except the the case of parameter set 4, which has the biggest constant, and the case of parameter set 5, which has the smallest constant

In Section 4.3, we show tables and plots reporting the different errors involved in MC method (Bias and Statistical error) and in MISC (Quadrature error). We do this for each case of parameter set. The quadrature error is computed by subtracting the MISC solution from the biased solution with huge number of samples (to kill the statistical error). The conclusions of this section are:

- We observed the optimal results for the case of parameter set 5 in table 1 (see Section 4.3.1). In fact, the MISC solver is very stable in terms of quadrature error (See tables 4, 9 and figures 12, 14). Also, the complexity analysis shows that we have substantial gain that reach over 100 times against MC to achieve total relative error below 1% (see figure 13 and tables (6, 5)). The stability of MISC is also confirmed by the plots of mixed errors and the integrand in Section 4.4.1. Using Richardson extrapolation brought a minor improvement in terms of complexity rate compared to using simple MISC (See figure 16).
- For the other parameter sets cases of table 1, we still observe some instability issues (instability means: i) a non convergence for certain MISC tolerances, or ii) Instable behavior of the quadrature error, or iii) MISC becomes too slow at certain tolerances) for MISC that deteriorates the gain that should be observed as in the case of set 5 (We refer to sections 4.3.2, 4.3.3, 4.3.4,4.3.5). We also show the mixed differences as well the integrand for those cases in Sections (4.4.3, 4.4.2, 4.4.4,4.4.5), which show the potential issues that we have in terms of the integrand growth as well bad behavior of second order differences. In fact, these plots show that we may face an unboundness of the integrand (could be numerical artifact or by the model, to be checked) that can not be absorbed by the Gaussian measure. What is interesting is that this unboundness was not observed for the case of parameters sets 5. Apart from the observed instability by MISC for those sets of parameters, we observed a substantial gains (in terms of complexity rates) by using Richardson extrapolation coupled with MISC compared to simply using MISC.

4.2 Weak error plots

In this section, I include the results of weak error rates for the different parameters sets as in table 1, with and without Richardson extrapolation. The reference solution was computed with $N = 500$ time steps (reported in table 1). We note that the weak errors plotted here corresponds to relative errors. We show in table 1 the different parameter constellations that we consider to report our results for MC and MISC.

Paramters	Reference solution
Set 1: $H = 0.43, K = 1, \rho = -0.9, \eta = 1.9, \xi = 0.235^2$	0.0712073
Set 2: $H = 0.07, K = 1, \rho = -0.9, \eta = 1.9, \xi = 0.235^2$	0.0792047
Set 3: $H = 0.07, K = 0.8, \rho = -0.9, \eta = 1.9, \xi = 0.235^2$	0.2249058 $(1.0e-04)$
Set 4: $H = 0.07, K = 1.2, \rho = -0.9, \eta = 1.9, \xi = 0.235^2$	0.0099397 $(2.3e-05)$
Set 5: $H = 0.02, K = 1, \rho = -0.7, \eta = 0.4, \xi = 0.1$	0.1247563 $(1.3e-04)$

Table 1: Reference solution, using MC with 500 time steps and $M = 10^6$, of Call option price under rBergomi model, for different parameter constellation.

4.2.1 Without Richardson extrapolation

From figures (2,3,4,5,6), we see that for all cases, we get a weak error of order Δt , with different constants. The upper and lower bounds are 95% confidence interval. Interestingly, we see that the case of parameters set 5 (see table 1) has the lowest constant. On the other hand, the case of parameters set 4 (see table 1) has the biggest constant.

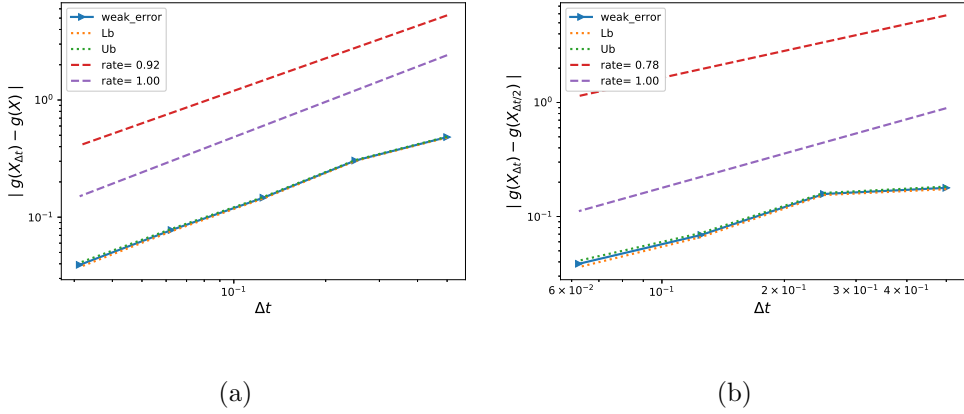


Figure 2: The rate of convergence of the weak error for set 1 parameters in table 1, without Richardson extrapolation, using MC with $M = 10^6$: a) $|E[g(X_{\Delta t})] - g(X)|$ b) $|E[g(X_{\Delta t}) - g(X_{\Delta t/2})]|$

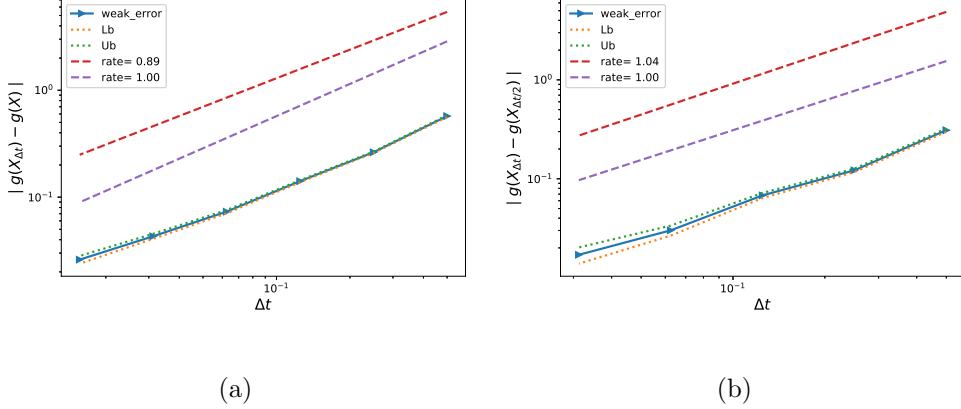


Figure 3: The rate of convergence of the weak error for set 2 parameters in table 1, without Richardson extrapolation, using MC with $M = 10^6$: a) $|\mathbb{E}[g(X_{\Delta t})] - g(X)|$ b) $|\mathbb{E}[g(X_{\Delta t}) - g(X_{\Delta t/2})]|$

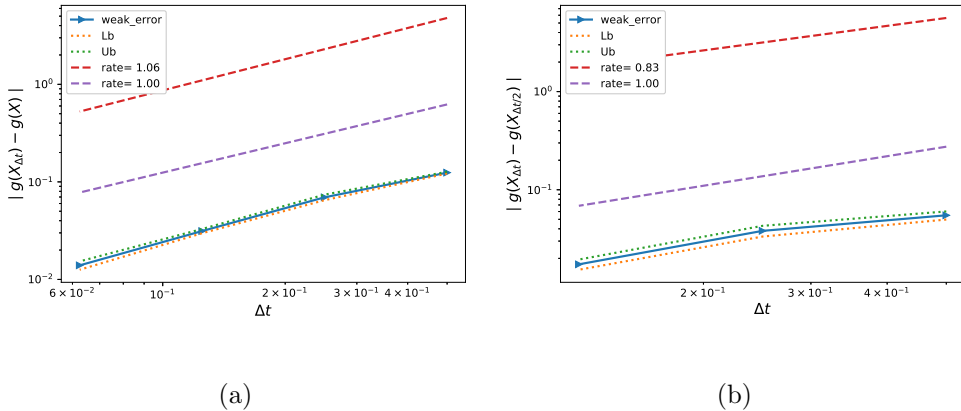


Figure 4: The rate of convergence of the weak error for set 3 parameters in table 1, without Richardson extrapolation, using MC with $M = 10^6$: a) $|\mathbb{E}[g(X_{\Delta t})] - g(X)|$ b) $|\mathbb{E}[g(X_{\Delta t}) - g(X_{\Delta t/2})]|$

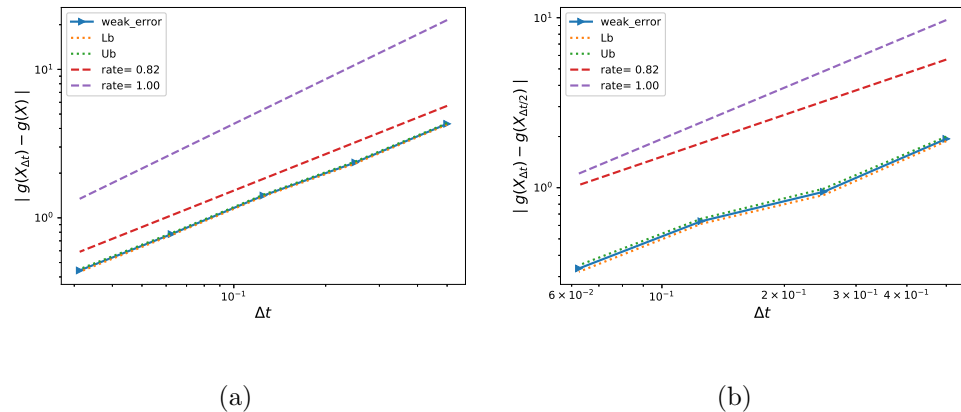


Figure 5: The rate of convergence of the weak error for set 4 parameters in table 1, without Richardson extrapolation, using MC with $M = 10^6$: a) $|\mathbb{E}[g(X_{\Delta t})] - g(X)|$ b) $|\mathbb{E}[g(X_{\Delta t}) - g(X_{\Delta t/2})]|$

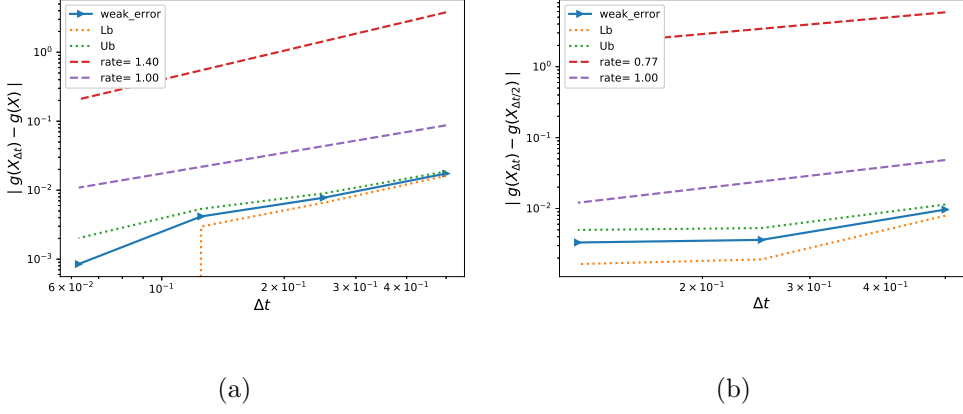


Figure 6: The rate of convergence of the weak error for set 5 parameters in table 1, without Richardson extrapolation, using MC with $M = 3.10^6$: a) $|E[g(X_{\Delta t})] - g(X)|$ b) $|E[g(X_{\Delta t}) - g(X_{\Delta t/2})]|$

4.2.2 With Richardson extrapolation (level 1)

From figures (7, 8, 9, 10, 11), we see that for all cases, we get a weak error of order around Δt^2 . The upper and lower bounds are 95% confidence interval.

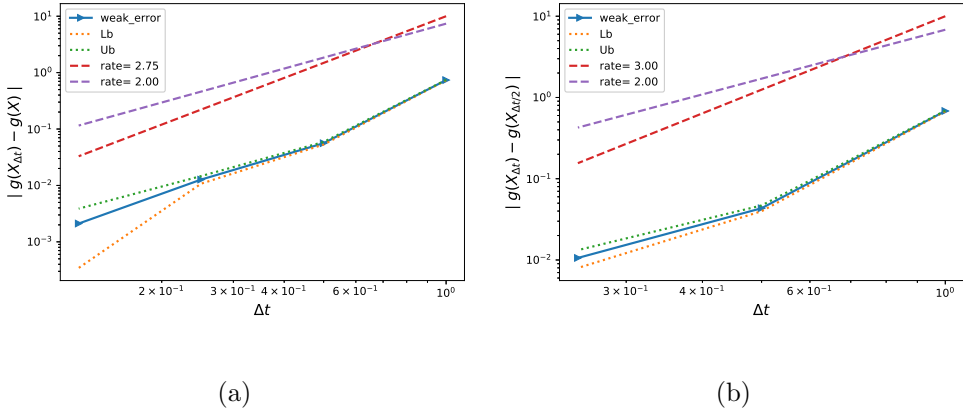


Figure 7: The rate of convergence of the weak error for set 1 parameters in table 1, with Richardson extrapolation, using MC with $M = 10^6$: a) $|E[2g(X_{\Delta t/2}) - g(X_{\Delta t})] - g(X)|$ b) $|E[3g(X_{\Delta t/2}) - g(X_{\Delta t}) - 2g(X_{\Delta t/4})]|$

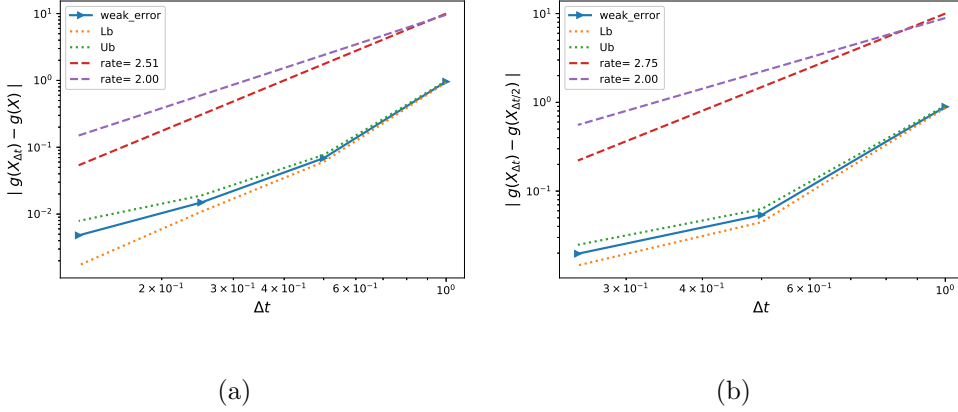


Figure 8: The rate of convergence of the weak error for set 2 parameters in table 1, with Richardson extrapolation, using MC with $M = 10^6$: a) $|\mathbb{E}[2g(X_{\Delta t/2}) - g(X_{\Delta t})] - g(X)|$ b) $|\mathbb{E}[3g(X_{\Delta t/2}) - g(X_{\Delta t}) - 2g(X_{\Delta t/4})]|$

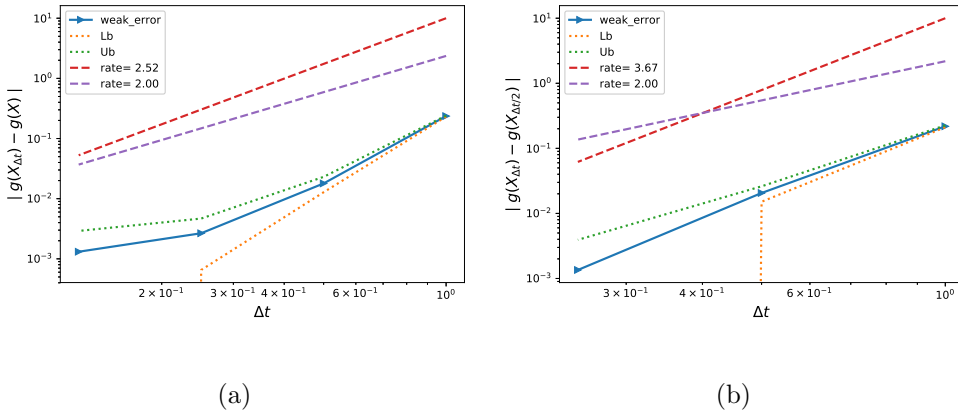


Figure 9: The rate of convergence of the weak error for set 3 parameters in table 1, with Richardson extrapolation, using MC with $M = 10^6$: a) $|\mathbb{E}[2g(X_{\Delta t/2}) - g(X_{\Delta t})] - g(X)|$ b) $|\mathbb{E}[3g(X_{\Delta t/2}) - g(X_{\Delta t}) - 2g(X_{\Delta t/4})]|$

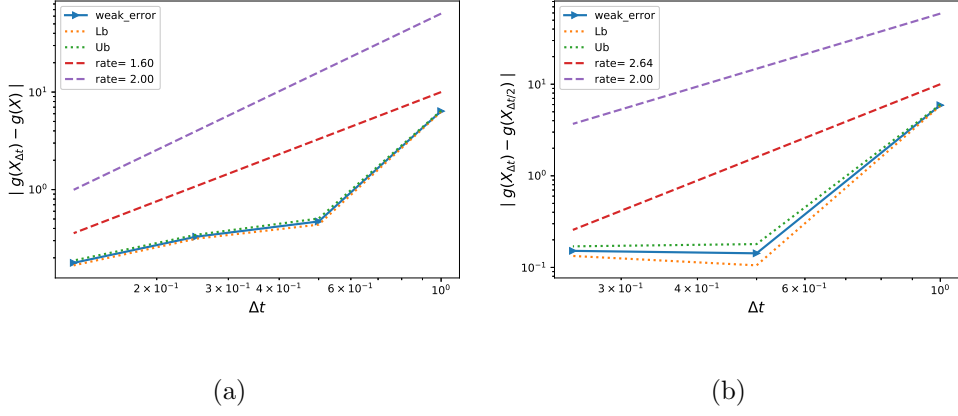


Figure 10: The rate of convergence of the weak error for set 4 parameters in table 1, with Richardson extrapolation, using MC with $M = 2.10^6$: a) $|\mathbb{E}[2g(X_{\Delta t/2}) - g(X_{\Delta t})] - g(X)|$ b) $|\mathbb{E}[3g(X_{\Delta t/2}) - g(X_{\Delta t}) - 2g(X_{\Delta t/4})]|$

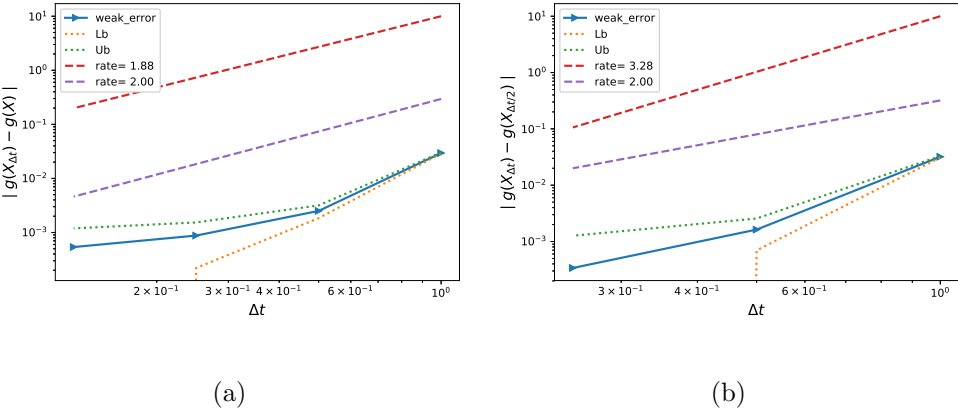


Figure 11: The rate of convergence of the weak error for set 5 parameters in table 1, with Richardson extrapolation, using MC with $M = 10^7$: a) $|\mathbb{E}[2g(X_{\Delta t/2}) - g(X_{\Delta t})] - g(X)|$ b) $|\mathbb{E}[3g(X_{\Delta t/2}) - g(X_{\Delta t}) - 2g(X_{\Delta t/4})]|$

4.3 Comparing different errors and complexity for MC and MISC

The results were reported for the different sets of parameters defined in table 1. We considered number of time steps $N \in \{2, 4, 8, 16\}$. The options are priced in terms of the moneyness K , where K is the strike price.

For each set, we report the results for 2 scenarios: i) Without using Richardson extrapolation and ii) Using level 1 Richardson extrapolation.

In each case, we show a table of computed values using MISC for different tolerances as well biased MC value, using large number of samples to kill the statistical error. Then, in a second table, we show the bias as well the statistical error for MC method. The third table shows the relative quadrature error which is computed as the normalized difference between the biased MC solution and MISC solution. Then we provide the total relative error which is the sum of the bias and statistical error for MC, and the quadrature error for MISC. Finally, we show the CPU time needed for each solver. We also provide plots for the behavior of Quadrature error of MISC and complexity plots for the different methods.

4.3.1 Case of set 5 parameters in table 1

Method \ Steps	2	4	8	16
MISC ($Tol = 5.10^{-1}$)	0.1258	0.1239	0.1231	0.1227
MISC ($Tol = 10^{-1}$)	0.1258	0.1239	0.1231	0.1229
MISC ($Tol = 5.10^{-2}$)	0.1258	0.1239	0.1231	0.1241
MISC ($Tol = 10^{-2}$)	0.1258	0.1246	0.1248	0.1250
MISC ($Tol = 10^{-3}$)	0.1271	0.1259	0.1253	0.1249
MISC ($Tol = 10^{-4}$)	0.1270	0.1258	0.1252	—
MISC ($Tol = 10^{-5}$)	0.1270	0.1258	0.1252	—
MC method ($M = 3.10^6$)	0.1269	0.1257	0.1253	0.1249

Table 2: Call option price of the different methods for different number of time steps. Case of set 5 parameters in table 1, without Richardson extrapolation.

Method \ Steps	2	4	8	16
MC Bias ($M = 3.10^6$)	0.0174 (0.0022)	0.0078 (0.001)	0.0042 (0.0005)	0.0008 (0.0001)
MC Statistical error ($M = 3.10^6$)	6.3e - 04 (7.9e-05)	6.2e - 04 (7.7e-05)	6.1e - 04 (7.6e-05)	6.0e - 04 (7.5e-05)

Table 3: Bias and Statistical errors of MC for computing Call option price for different number of time steps. Case set 5, without Richardson extrapolation. The numbers between parentheses are the corresponding absolute errors.

Method \ Steps	2	4	8	16
MISC ($Tol = 5 \cdot 10^{-1}$)	0.0088 (0.0011)	0.0144 (0.0018)	0.0176 (0.0022)	0.0176 (0.0022)
MISC ($Tol = 10^{-1}$)	0.0088 (0.0011)	0.0144 (0.0018)	0.0176 (0.0022)	0.0160 (0.0020)
MISC ($Tol = 5 \cdot 10^{-2}$)	0.0088 (0.0011)	0.0144 (0.0018)	0.0176 (0.0022)	0.0064 (0.0008)
MISC ($Tol = 10^{-2}$)	0.0088 (0.0011)	0.0088 (0.0011)	0.0040 (0.0005)	0.0008 0.0001
MISC ($Tol = 10^{-3}$)	0.0016 (0.0002)	0.0016 (0.0002)	5e - 05 1.2e-06	5e - 05 1.2e-06
MISC ($Tol = 10^{-4}$)	0.0008 (0.0001)	0.0008 0.0001	0.0008 0.0001	—
MISC ($Tol = 10^{-5}$)	0.0008 (0.0001)	0.0008 0.0001	0.0008 0.0001	—

Table 4: Quadrature error of MISC to compute Call option price of the different tolerances for different number of time steps. Case set 5 parameters in table 1, without Richardson extrapolation. The numbers between parentheses are the corresponding absolute errors.

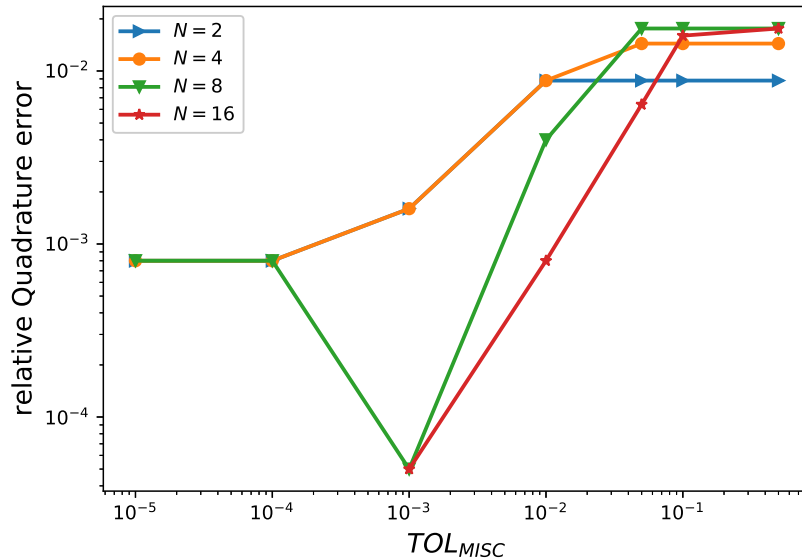


Figure 12: Quadrature error of MISC to compute Call option price of the different tolerances for different number of time steps. Case set 5 parameters, without Richardson extrapolation.

Method \ Steps	2	4	8	16
MISC ($Tol = 5.10^{-1}$)	0.0262	0.0222	0.0218	0.0184
MISC ($Tol = 10^{-1}$)	0.0262	0.0222	0.0218	0.0168
MISC ($Tol = 5.10^{-2}$)	0.0262	0.0222	0.0218	0.0072
MISC ($Tol = 10^{-2}$)	0.0262	0.0166	0.0082	0.0016
MISC ($Tol = 10^{-3}$)	0.0190	0.0094	0.0042	0.0008
MISC ($Tol = 10^{-4}$)	0.0182	0.0086	0.0050	—
MISC ($Tol = 10^{-5}$)	0.0182	0.0086	0.0050	—
MC	0.0182	0.0086	0.0050	0.0016

Table 5: Total relative error of MISC and MC to compute Call option price of the different tolerances for different number of time steps. Case Case set 5 parametrts of table 1, without Richardson extrapolation. The numbers between parentheses are the corresponding absolute errors.

Method \ Steps	2	4	8	16
MISC ($Tol = 5.10^{-1}$)	0.1	0.1	0.2	0.4
MISC ($Tol = 10^{-1}$)	0.1	0.1	0.2	0.8
MISC ($Tol = 5.10^{-2}$)	0.1	0.1	0.2	22
MISC ($Tol = 10^{-2}$)	0.1	0.5	8	92
MISC ($Tol = 10^{-3}$)	0.5	3	24	2226
MISC ($Tol = 10^{-4}$)	1	6	80	—
MISC ($Tol = 10^{-5}$)	2	32	1760	—
MC method	682	721	814	1125
Ratio of (MC/MISC)	682	120	10	12

Table 6: Comparsion of the computational time of MC and MISC, used to compute Call option price of rBergomi model for different number of time steps. Case set 5 parametrts of table 1. The average MC CPU time is computed over 10 runs.

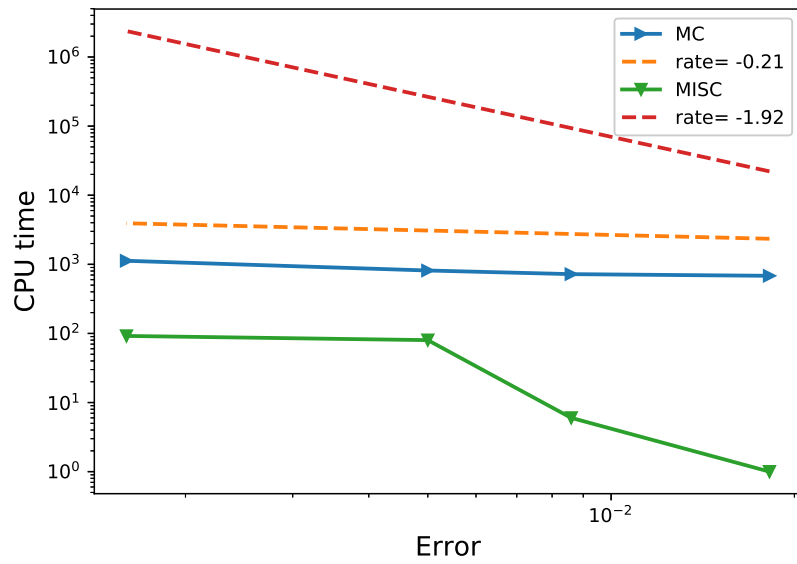


Figure 13: Complexity plot for MC and MISC for Case set 5 parameters of table 1.

Method \ Steps	1 - 2	2 - 4	4 - 8	8 - 16
MISC ($Tol = 5.10^{-1}$)	0.1261	0.1220	0.1222	0.1223
MISC ($Tol = 10^{-1}$)	0.1261	0.1220	0.1222	0.1226
MISC ($Tol = 5.10^{-2}$)	0.1261	0.1220	0.1222	0.1240
MISC ($Tol = 10^{-2}$)	0.1267	0.1230	0.1245	0.1247
MISC ($Tol = 10^{-3}$)	0.1285	0.1247	0.1247	0.1247
MISC ($Tol = 10^{-4}$)	0.1285	0.1245	0.1246	—
MISC ($Tol = 10^{-5}$)	0.1285	0.1245	0.1246	—
MC method ($M = 10^7$)	0.1284	0.1251	0.1249	0.1248

Table 7: Call option price of the different methods for different number of time steps. Case set 5 parameters of table 1, using Richardson extrapolation (level 1)

Method \ Steps	1 - 2	2 - 4	4 - 8	8 - 16
MC Bias ($M = 10^7$)	0.0295 (0.0037)	0.0025 (0.0003)	0.0009 (0.0001)	0.0005 (6.2e-05)
MC Statistical error ($M = 10^7$)	3.5e - 04 (4.4e-05)	3.4e - 04 (4.2e-05)	3.3e - 04 (4.1e-05)	3.3e - 04 (4.1e-05)

Table 8: Bias and Statistical errors of MC for computing Call option price for different number of time steps. Case set 5 parameters in tabel 1, with Richardson extrapolation (level 1). The numbers between parentheses are the corresponding absolute errors.

Method \ Steps	1 - 2	2 - 4	4 - 8	8 - 16
MISC ($Tol = 5.10^{-1}$)	0.0184 (0.0023)	0.0248 (0.0031)	0.0216 (0.0027)	0.0200 (0.0025)
MISC ($Tol = 10^{-1}$)	0.0184 (0.0023)	0.0248 (0.0031)	0.0216 (0.0027)	0.0176 (0.0022)
MISC ($Tol = 5.10^{-2}$)	0.0184 (0.0023)	0.0248 (0.0031)	0.0216 (0.0027)	0.0064 (0.0008)
MISC ($Tol = 10^{-2}$)	0.0136 (0.0017)	0.0168 (0.0021)	0.0032 (0.0004)	0.0008 (0.0001)
MISC ($Tol = 10^{-3}$)	0.0008 (0.0001)	0.0032 (0.0004)	0.0016 (0.0002)	0.0008 (0.0001)
MISC ($Tol = 10^{-4}$)	0.0008 (0.0001)	0.0048 (0.0006)	0.0024 (0.0003)	— (—)
MISC ($Tol = 10^{-5}$)	0.0008 (0.0001)	0.0048 (0.0006)	0.0024 (0.0003)	— (—)

Table 9: Quadrature error of MISC to compute Call option price of the different tolerances for different number of time steps. Case set 5 parameters in table 1, with Richardson extrapolation(level 1). The numbers between parentheses are the corresponding absolute errors.

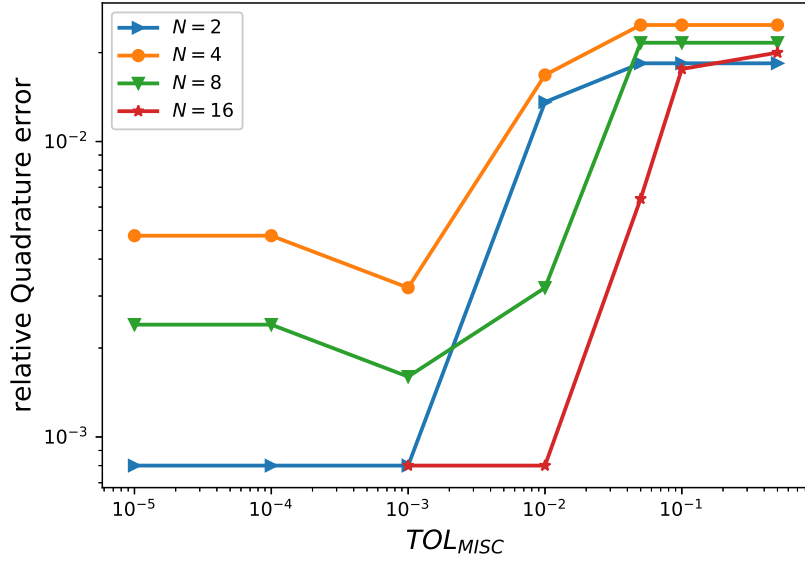


Figure 14: Quadrature error of MISC to compute Call option price of the different tolerances for different number of time steps. Case set 5 parameters, with Richardson extrapolation.

Method \ Steps	1 - 2	2 - 4	4 - 8	8 - 16
MISC ($Tol = 5.10^{-1}$)	0.0479	0.0273	0.0225	0.0205
MISC ($Tol = 10^{-1}$)	0.0479	0.0273	0.0225	0.0181
MISC ($Tol = 5.10^{-2}$)	0.0479	0.0273	0.0225	0.0069
MISC ($Tol = 10^{-2}$)	0.0431	0.0193	0.0041	0.0013
MISC ($Tol = 10^{-3}$)	0.0303	0.0057	0.0025	0.0013
MISC ($Tol = 10^{-4}$)	0.0303	0.0073	0.0033	—
MISC ($Tol = 10^{-5}$)	0.0303	0.0073	0.0033	—
MC	—	0.0073	0.0025	0.0013

Table 10: Total error of MISC and MC to compute Call option price of the different tolerances for different number of time steps. Case set 5 parameters in table 1, with Richardson extrapolation(level 1). The numbers between parentheses are the corresponding absolute errors.

Method \ Steps	1 - 2	2 - 4	4 - 8	8 - 16
MISC ($Tol = 5.10^{-1}$)	0.08	0.15	0.25	0.5
MISC ($Tol = 10^{-1}$)	0.08	0.15	0.25	1
MISC ($Tol = 5.10^{-2}$)	0.08	0.15	0.25	12.5
MISC ($Tol = 10^{-2}$)	0.15	0.6	10	112
MISC ($Tol = 10^{-3}$)	1	3.5	34	3150
MISC ($Tol = 10^{-4}$)	1	11	328	—
MISC ($Tol = 10^{-5}$)	3	39	2160	—
MC method + Richardson (level 1)	—	45	438	2240
Ratio of (MC/MISC)	—	4	13	20

Table 11: Comparison of the computational time of MC and MISC, using Richardson extrapolation (level 1), used to compute Call option price of rBergomi model for different number of time steps. Case set 5 parameters in table 1

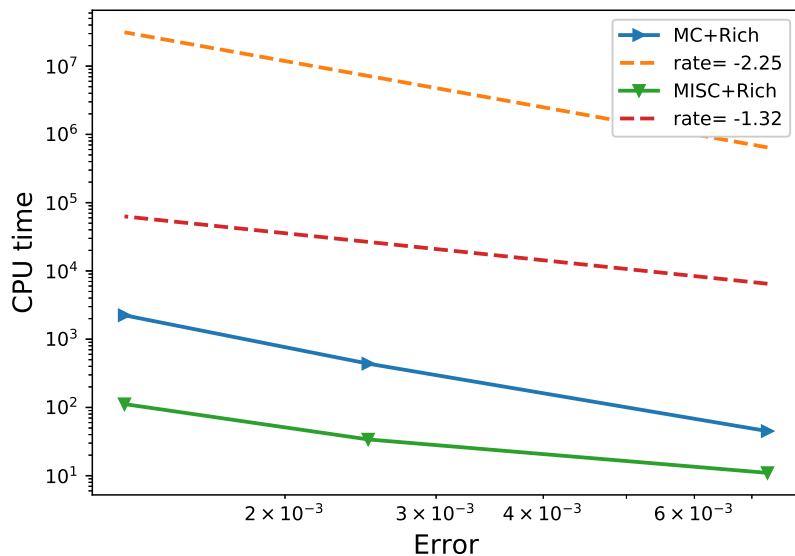


Figure 15: Complexity plot for MC and MISC with Richardson extrapolation, for Case set 5 parameters of table 1.

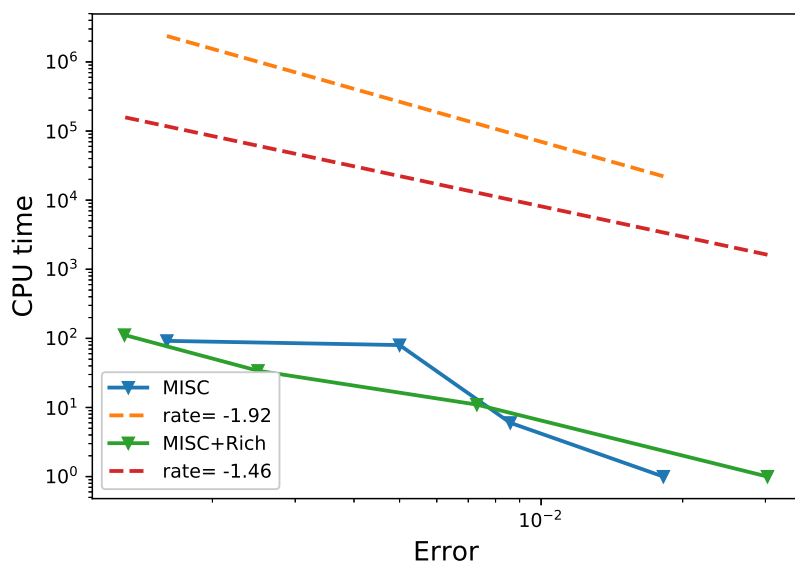


Figure 16: Complexity plot for MISC (with/without) Richardson extrapolation for Case set 5 parameters of table 1.

4.3.2 Case of set 2 parameters in table 1

Method \Steps	2	4	8	16
MISC ($Tol = 5.10^{-1}$)	0.1082	0.0917	0.0800	0.0732
MISC ($Tol = 10^{-1}$)	0.1082	0.0917	0.0786	0.080
MISC ($Tol = 5.10^{-2}$)	0.1082	0.0921	0.0914	0.0817
MISC ($Tol = 10^{-2}$)	0.1187	0.1014	0.0909	—
MISC ($Tol = 10^{-3}$)	0.1216	0.1024	0.0910	—
MISC ($Tol = 10^{-4}$)	0.1218	0.1024	—	—
MC method ($M = 10^6$)	0.1246	0.1000	0.0904	0.0850

Table 12: Call option price of the different methods for different number of time steps. Case of set 2 parameters in table 1, without Richardson extrapolation.

Method \Steps	2	4	8	16
MC Bias ($M = 10^6$)	0.5727 (0.0454)	0.2629 (0.0208)	0.1411 (0.0112)	0.0731 (0.0058)
MC Statistical error ($M = 10^6$)	5.5e - 03 (4.4e - 04)	2.02e - 03 (1.6e - 04)	1.54e - 03 (1.2e - 04)	1.33e - 03 (1.1e - 04)

Table 13: Bias and Statistical errors of MC for computing Call option price for different number of time steps. Case set 2 parameters in table 1, without Richardson extrapolation. The numbers between parentheses are the corresponding absolute errors.

Method \Steps	2	4	8	16
MISC ($Tol = 5.10^{-1}$)	0.2071 (0.0164)	0.1048 (0.0083)	0.1313 (0.0104)	0.1490 (0.0118)
MISC ($Tol = 10^{-1}$)	0.2071 (0.0164)	0.1048 (0.0083)	0.1490 (0.0118)	0.0631 (0.005)
MISC ($Tol = 5.10^{-2}$)	0.2071 (0.0164)	0.0997 (0.0079)	0.0126 (0.001)	0.0417 (0.0033)
MISC ($Tol = 10^{-2}$)	0.0745 (0.0059)	0.0177 (0.0014)	0.0063 (0.0005)	—
MISC ($Tol = 10^{-3}$)	0.0379 (0.003)	0.0303 (0.0024)	0.0076 (0.0006)	—
MISC ($Tol = 10^{-4}$)	0.0354 (0.0028)	0.0303 (0.0024)	—	—

Table 14: Quadrature error of MISC to compute Call option price of the different tolerances for different number of time steps. Case set 2 parameters in table 1, without Richardson extrapolation. The numbers between parentheses are the corresponding absolute errors.

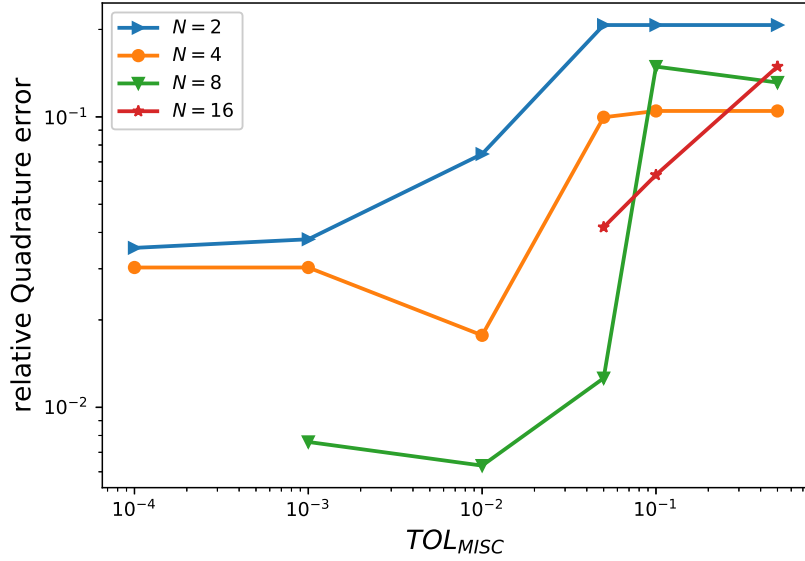


Figure 17: Quadrature error of MISC to compute Call option price of the different tolerances for different number of time steps. Case set 2 parameters, without Richardson extrapolation.

Method \ Steps	2	4	8	16
MISC ($Tol = 5.10^{-1}$)	0.7798	0.3677	0.2724	0.2221
MISC ($Tol = 10^{-1}$)	0.7798	0.3677	0.2901	0.1362
MISC ($Tol = 5.10^{-2}$)	0.7798	0.3626	0.1537	0.1148
MISC ($Tol = 10^{-2}$)	0.6472	0.2806	0.1474	-
MISC ($Tol = 10^{-3}$)	0.6106	0.2932	0.1487	-
MISC ($Tol = 10^{-4}$)	0.6081	0.2932	-	-
MC	0.6472	0.2932	0.1487	-

Table 15: Total error of MISC and MC to compute Call option price of the different tolerances for different number of time steps. Case set 2 parameters in table 1, without Richardson extrapolation. The numbers between parentheses are the corresponding absolute errors.

Method \ Steps	2	4	8	16
MISC ($Tol = 5.10^{-1}$)	0.08	0.13	0.2	0.5
MISC ($Tol = 10^{-1}$)	0.08	0.13	1	220
MISC ($Tol = 5.10^{-2}$)	0.08	0.3	10	5600
MISC ($Tol = 10^{-2}$)	0.45	6	800	—
MISC ($Tol = 10^{-3}$)	7	350	5370	—
MISC ($Tol = 10^{-4}$)	63	6350	—	—
MC method	1.3	4.7	37.5	—
Ratio of (MC/MISC)	2.9	0.01	0.007	—

Table 16: Comparison of the computational time of MC and MISC, used to compute Call option price of rBergomi model for different number of time steps. Case $K = 1, H = 0.07$

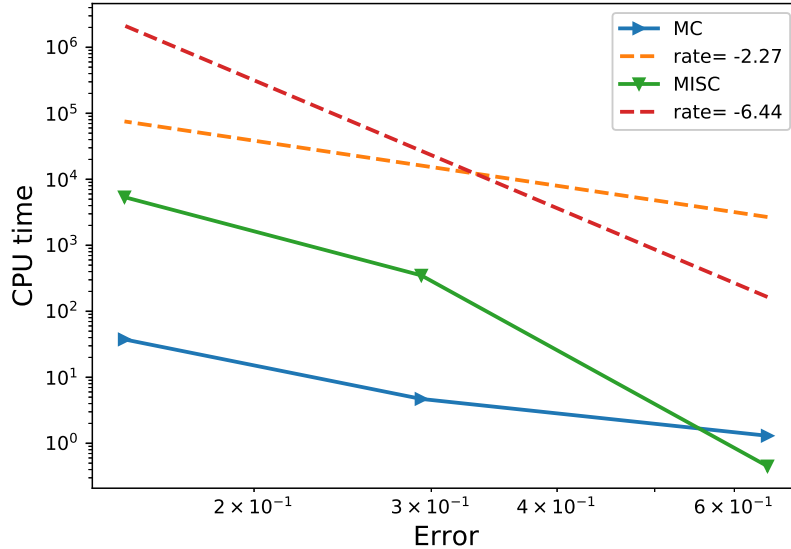


Figure 18: Complexity plot for MC and MISC for Case set 2 parameters of table 1.

Method \ Steps	1 – 2	2 – 4	4 – 8	8 – 16
MISC ($Tol = 5.10^{-1}$)	0.1242	0.0752	0.0682	0.0665
MISC ($Tol = 10^{-1}$)	0.1242	0.0752	0.0658	0.0764
MISC ($Tol = 5.10^{-2}$)	0.1242	0.0676	0.0800	—
MISC ($Tol = 10^{-2}$)	0.1459	0.0845	0.0803	—
MISC ($Tol = 10^{-3}$)	0.1505	0.0827	—	—
MISC ($Tol = 5.10^{-4}$)	0.1505	0.0830	—	—
MISC ($Tol = 10^{-4}$)	0.1500	—	—	—
MC method ($M = 10^6$)	0.1552	0.0846	0.0804	0.0796

Table 17: Call option price of the different methods for different number of time steps. Case set 2 parameters of table 1, using Richardson extrapolation (level 1)

Method \ Steps	1 - 2	2 - 4	4 - 8	8 - 16
MC Bias ($M = 10^6$)	0.9594 (0.0760)	0.0686 (0.0054)	0.0149 (0.0012)	0.0048 (0.0004)
MC Statistical error ($M = 10^6$)	1.3e - 02 (1e-03)	4.1e - 03 (3.2e-04)	2.1e - 03 (1.7e-04)	1.6e - 03 (1.3e-04)

Table 18: Bias and Statistical errors of MC for computing Call option price for different number of time steps. Case set 2 parameters in tabel 1, with Richardson extrapolation (level 1). The numbers between parentheses are the corresponding absolute errors.

Method \ Steps	1 - 2	2 - 4	4 - 8	8 - 16
MISC ($Tol = 5.10^{-1}$)	0.3914 0.0310	0.1187 0.0094	0.1540 0.0122	0.1654 0.0131
MISC ($Tol = 10^{-1}$)	0.3914 0.0310	0.1187 0.0094	0.1843 0.0146	0.0404 0.0032
MISC ($Tol = 5.10^{-2}$)	0.3914 0.0310	0.2146 0.0170	0.0050 0.0004	—
MISC ($Tol = 10^{-2}$)	0.1174 0.0093	0.0013 0.0001	0.0013 0.0001	—
MISC ($Tol = 10^{-3}$)	0.0593 0.0047	0.0240 0.0019	—	—
MISC ($Tol = 5.10^{-4}$)	0.0593 0.0047	0.0202 0.0016	—	—
MISC ($Tol = 10^{-4}$)	0.0657 0.0052	—	—	—

Table 19: Quadrature error of MISC to compute Call option price of the different tolerances for different number of time steps. Case set 2 parameters in table 1, with Richardson extrapolation(level 1). The numbers between parentheses are the corresponding absolute errors.

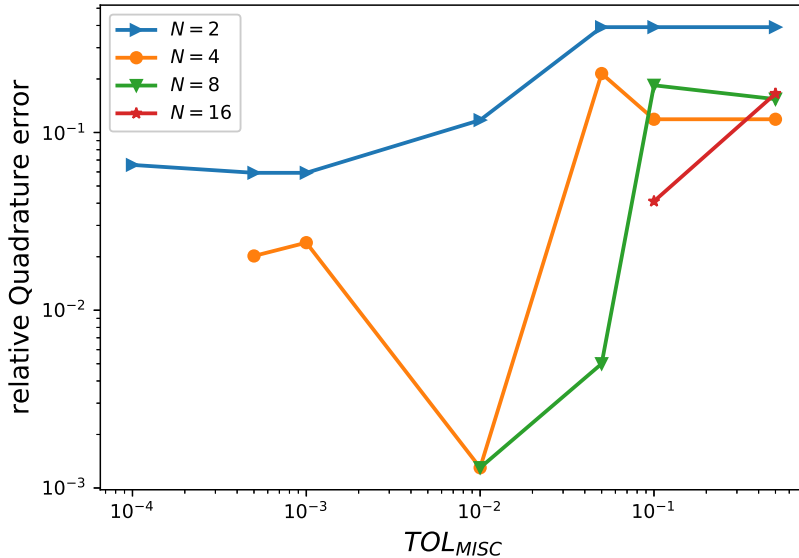


Figure 19: Quadrature error of MISC to compute Call option price of the different tolerances for different number of time steps. Case set 2 parameters, with Richardson extrapolation.

Method \ Steps	1 - 2	2 - 4	4 - 8	8 - 16
MISC ($Tol = 5.10^{-1}$)	1.3508	0.1873	0.1689	0.1702
MISC ($Tol = 10^{-1}$)	1.3508	0.1873	0.1992	0.0458
MISC ($Tol = 5.10^{-2}$)	1.3508	0.2832	0.0199	—
MISC ($Tol = 10^{-2}$)	1.0768	0.0699	0.0162	—
MISC ($Tol = 10^{-3}$)	1.0187	0.0926	—	—
MISC ($Tol = 5.10^{-4}$)	1.0187	0.0888	—	—
MISC ($Tol = 10^{-4}$)	1.0251	—	—	—
MC	1.0187	0.0926	0.0162	—

Table 20: Total error of MISC and MC to compute Call option price of the different tolerances for different number of time steps. Case set 2 parameters in table 1, with Richardson extrapolation(level 1). The numbers between parentheses are the corresponding absolute errors.

Method \ Steps	1 - 2	2 - 4	4 - 8	8 - 16
MISC ($Tol = 5.10^{-1}$)	0.1	0.13	0.2	0.5
MISC ($Tol = 10^{-1}$)	0.1	0.13	1.3	1198
MISC ($Tol = 5.10^{-2}$)	0.1	0.5	34	—
MISC ($Tol = 10^{-2}$)	2	9	3450	—
MISC ($Tol = 10^{-3}$)	16	2460	—	—
MISC ($Tol = 5.10^{-4}$)	52	9566	—	—
MISC ($Tol = 10^{-4}$)	180	—	—	—
MC method + Richardson (level 1)	16	20	2780	—
Ratio of (MC/MISC)	1	0.008	0.81	—

Table 21: Comparison of the computational time of MC and MISC, using Richardson extrapolation (level 1), used to compute Call option price of rBergomi model for different number of time steps. Case set 2 parameters in table 1

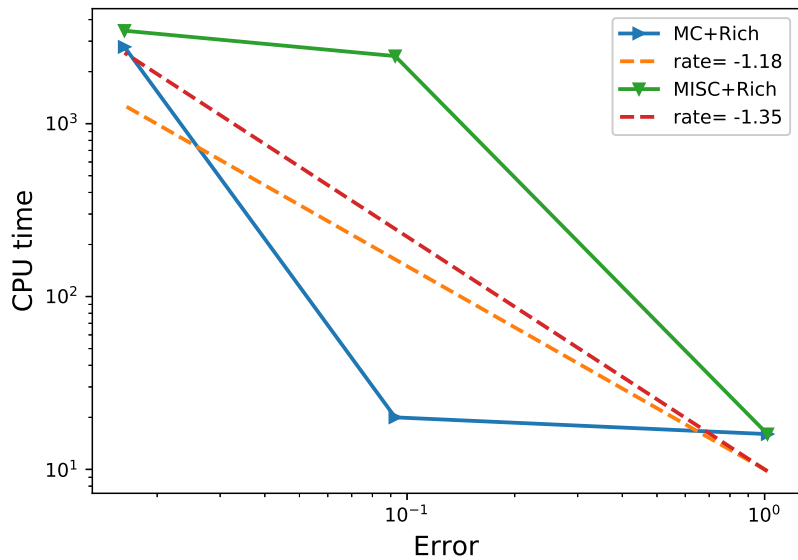


Figure 20: Complexity plot for MC and MISC with Richardson extrapolation, for Case set 2 parameters of table 1.

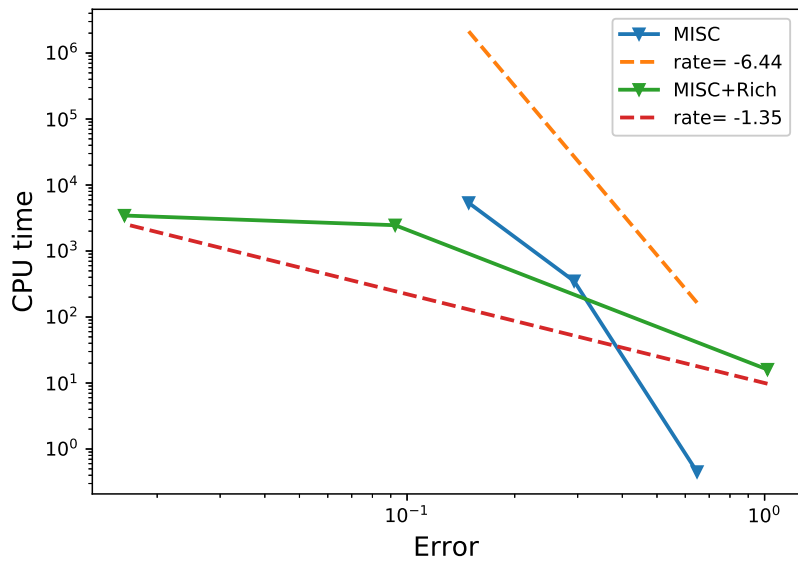


Figure 21: Complexity plot for MISC (with/without) Richardson extrapolation for Case set 2 parameters of table 1.

4.3.3 Case of set 1 parameters in table 1

Method \ Steps	2	4	8	16
MISC ($Tol = 5.10^{-1}$)	0.1140	0.0961	0.0848	0.0781
MISC ($Tol = 10^{-1}$)	0.1140	0.0961	0.0871	0.0802
MISC ($Tol = 5.10^{-2}$)	0.1140	0.0963	0.0843	0.0824
MISC ($Tol = 10^{-2}$)	0.1077	0.0944	0.0838	0.0772
MISC ($Tol = 10^{-3}$)	0.1077	0.0921	0.0819	0.0762
MISC ($Tol = 10^{-4}$)	0.1077	0.0921	0.0822	—
MC method ($M = 10^6$)	0.1056	0.0929	0.0816	0.0767

Table 22: Call option price of the different methods for different number of time steps. Case of set 1 parameters in table 1, without Richardson extrapolation.

Method \ Steps	2	4	8	16
MC Bias ($M = 10^6$)	0.4825 (0.0344)	0.3042 (0.0217)	0.1466 (0.0104)	0.0777 (0.0055)
MC Statistical error ($M = 10^6$)	1.9e - 03 (1.4e - 04)	1.4e - 03 (9.9e - 05)	1.1e - 03 (7.8e - 05)	9.4e - 04 (6.7e - 05)

Table 23: Bias and Statistical errors of MC for computing Call option price for different number of time steps. Case set 1, without Richardson extrapolation. The numbers between parentheses are the corresponding absolute errors.

Method \ Steps	2	4	8	16
MISC ($Tol = 5.10^{-1}$)	0.1180 0.0084	0.0449 0.0032	0.0449 0.0032	0.0197 0.0014
MISC ($Tol = 10^{-1}$)	0.1180 0.0084	0.0449 0.0032	0.0772 0.0055	0.0492 0.0035
MISC ($Tol = 5.10^{-2}$)	0.1180 0.0084	0.0477 0.0034	0.0379 0.0027	0.0800 0.0057
MISC ($Tol = 10^{-2}$)	0.0295 0.0021	0.0211 0.0015	0.0309 0.0022	0.0070 0.0005
MISC ($Tol = 10^{-3}$)	0.0295 0.0021	0.0112 0.0008	0.0042 0.0003	0.0070 0.0005
MISC ($Tol = 10^{-4}$)	0.0295 0.0021	0.0112 0.0008	0.0084 (0.0006)	—

Table 24: Quadrature error of MISC to compute Call option price of the different tolerances for different number of time steps. Case set 1 parameters in table 1, without Richardson extrapolation. The numbers between parentheses are the corresponding absolute errors.

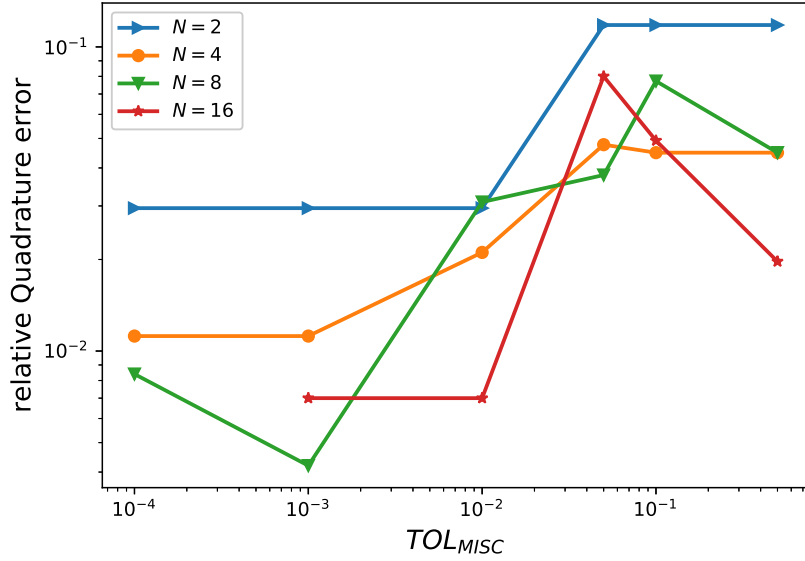


Figure 22: Quadrature error of MISC to compute Call option price of the different tolerances for different number of time steps. Case set 1 parameters, without Richardson extrapolation.

Method \ Steps	2	4	8	16
MISC ($Tol = 5.10^{-1}$)	0.6005	0.3491	0.1915	0.0974
MISC ($Tol = 10^{-1}$)	0.6005	0.3491	0.2238	0.1269
MISC ($Tol = 5.10^{-2}$)	0.6005	0.3519	0.1845	0.1577
MISC ($Tol = 10^{-2}$)	0.5120	0.3253	0.1775	0.0847
MISC ($Tol = 10^{-3}$)	0.5120	0.3154	0.1508	0.0847
MISC ($Tol = 10^{-4}$)	0.5120	0.3154	0.1550	—
MC	0.5120	0.3154	0.1550	0.0847

Table 25: Total error of MISC and MC to compute Call option price of the different tolerances for different number of time steps. Case Case set 1 parametr of table 1, without Richardson extrapolation..

Method \ Steps	2	4	8	16
MISC ($Tol = 5.10^{-1}$)	0.1	0.1	0.2	0.4
MISC ($Tol = 10^{-1}$)	0.1	0.1	0.6	6
MISC ($Tol = 5.10^{-2}$)	0.1	0.3	2	14
MISC ($Tol = 10^{-2}$)	0.2	1	9	215
MISC ($Tol = 10^{-3}$)	2	11	243	4650
MISC ($Tol = 10^{-4}$)	6	96	5760	—
MC	3.4	10	13.4	18
Ratio of (MC/MISC)	17	1	0.002	0.08

Table 26: Comparsion of the computational time of MC and MISC, used to compute Call option price of rBergomi model for different number of time steps. Case set 1 parametrs of table 1

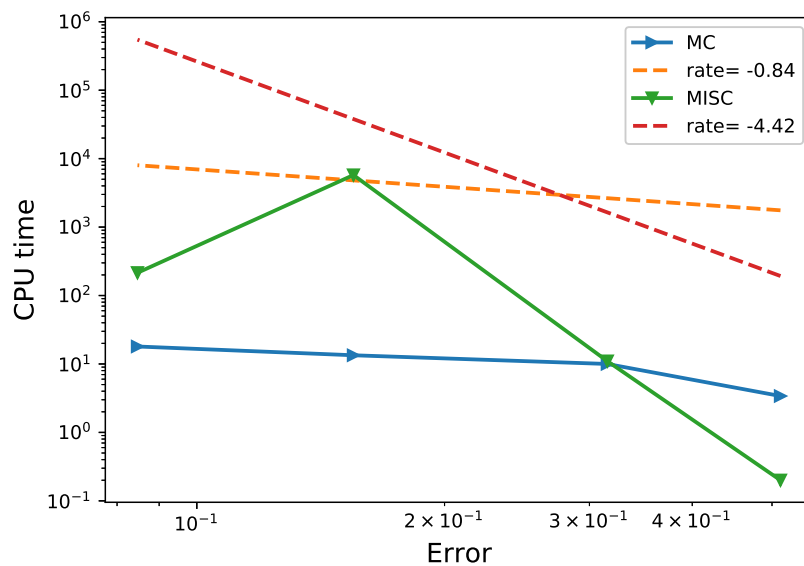


Figure 23: Complexity plot for MC and MISC for Case set 1 parameters of table 1.

Method \ Steps	1 – 2	2 – 4	4 – 8	8 – 16
MISC ($Tol = 5.10^{-1}$)	0.1357	0.0783	0.0735	0.0714
MISC ($Tol = 10^{-1}$)	0.1357	0.0783	0.0785	0.0761
MISC ($Tol = 5.10^{-2}$)	0.1357	0.0831	0.0773	0.0758
MISC ($Tol = 10^{-2}$)	0.1237	0.0781	0.0745	0.0714
MISC ($Tol = 10^{-3}$)	0.1224	0.0766	0.0720	0.0705
MISC ($Tol = 10^{-4}$)	0.1224	0.0763	0.0724	—
MC method ($M = 10^6$)	0.1237	0.0752	0.0721	0.0713

Table 27: Call option price of the different methods for different number of time steps. Case set 1 parameters of table 1, using Richardson extrapolation (level 1)

Method \ Steps	1 - 2	2 - 4	4 - 8	8 - 16
MC ($M = 10^6$) Bias	0.7378 (0.0525)	0.0561 (0.0040)	0.0127 (0.0009)	0.0021 (0.0001)
MC Statistical error ($M = 10^6$)	3.3e - 03 (2.3e-04)	1.6e - 03 (1.1e-04)	1.0e - 03 (7.1e-05)	9.0e - 04 (6.4e-05)

Table 28: Bias and Statistical errors of MC for computing Call option price for different number of time steps. Case set 1 parameters in tabel 1, with Richardson extrapolation (level 1). The numbers between parentheses are the corresponding absolute errors.

Method \ Steps	1 - 2	2 - 4	4 - 8	8 - 16
MISC ($Tol = 5.10^{-1}$)	0.1685 (0.0120)	0.0435 (0.0031)	0.0197 (0.0014)	0.0014 (0.0001)
MISC ($Tol = 10^{-1}$)	0.1685 (0.0120)	0.0435 (0.0031)	0.0899 (0.0064)	0.0674 (0.0048)
MISC ($Tol = 5.10^{-2}$)	0.1685 (0.0120)	0.1109 (0.0079)	0.0730 (0.0052)	0.0632 (0.0045)
MISC ($Tol = 10^{-2}$)	1e - 05 (7e-07)	0.0407 (0.0029)	0.0337 (0.0024)	0.0014 (0.0001)
MISC ($Tol = 10^{-3}$)	0.0183 (0.0013)	0.0197 (0.0014)	0.0014 (0.0001)	0.0112 (0.0008)
MISC ($Tol = 10^{-4}$)	0.0183 (0.0013)	0.0154 (0.0011)	0.0014 (0.001)	— (-)

Table 29: Quadrature error of MISC to compute Call option price of the different tolerances for different number of time steps. Case set 1 parameters in table 1, with Richardson extrapolation(level 1). The numbers between parentheses are the corresponding absolute errors.

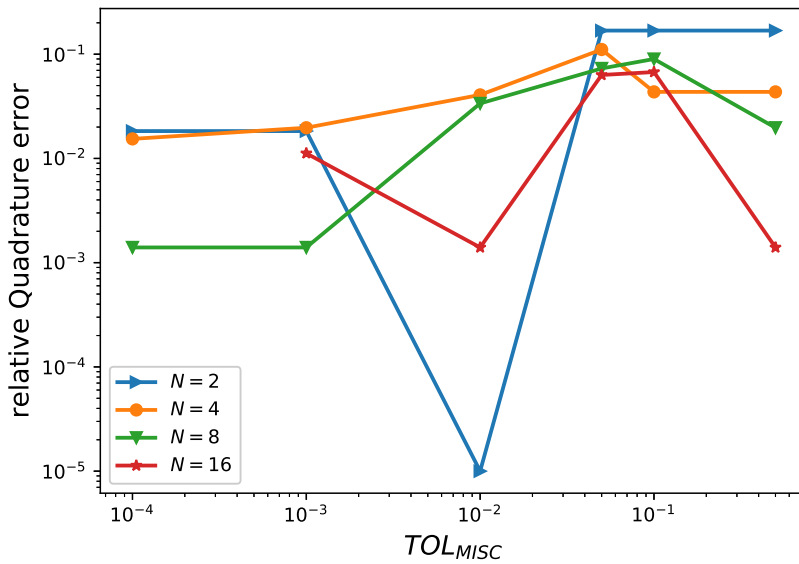


Figure 24: Quadrature error of MISC to compute Call option price of the different tolerances for different number of time steps. Case set 1 parameters, with Richardson extrapolation.

Method \ Steps	1 - 2	2 - 4	4 - 8	8 - 16
MISC ($Tol = 5.10^{-1}$)	0.9063	0.0996	0.0324	0.0035
MISC ($Tol = 10^{-1}$)	0.9063	0.0996	0.1026	0.0695
MISC ($Tol = 5.10^{-2}$)	0.9063	0.1670	0.0857	0.0653
MISC ($Tol = 10^{-2}$)	0.7378	0.0968	0.0464	0.0035
MISC ($Tol = 10^{-3}$)	0.7561	0.0758	0.0141	—
MISC ($Tol = 10^{-4}$)	0.7561	0.0715	0.0141	—
MC	0.7561	0.0715	0.0141	—

Table 30: Total error of MISC and MC to compute Call option price of the different tolerances for different number of time steps. Case set 1 parameters in table 1, with Richardson extrapolation(level 1).

Method \ Steps	1 - 2	2 - 4	4 - 8	8 - 16
MISC ($Tol = 5.10^{-1}$)	0.1	0.1	0.2	0.5
MISC ($Tol = 10^{-1}$)	0.1	0.1	0.6	8
MISC ($Tol = 5.10^{-2}$)	0.1	0.4	2	38
MISC ($Tol = 10^{-2}$)	1	2	18	490
MISC ($Tol = 10^{-3}$)	4	12	664	54065
MISC ($Tol = 10^{-4}$)	7	191	7650	—
MC	34.7	37	532	—
Ratio of (MC/MISC)	8.7	0.2	0.8	—

Table 31: Comparsion of the computational time of MC and MISC, using Richardson extrapolation (level 1), used to compute Call option price of rBergomi model for different number of time steps. Case set 1 parameters in table 1

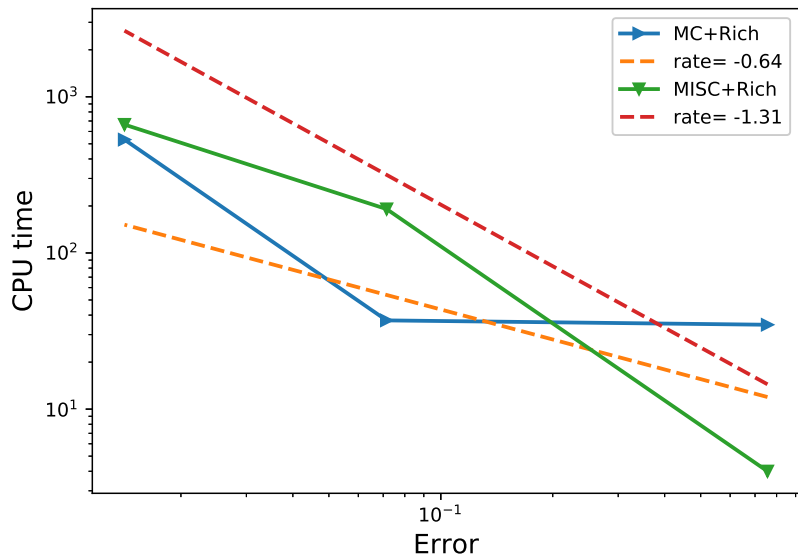


Figure 25: Complexity plot for MC and MISC with Richardson extrapolation, for Case set 1 parameters of table 1.

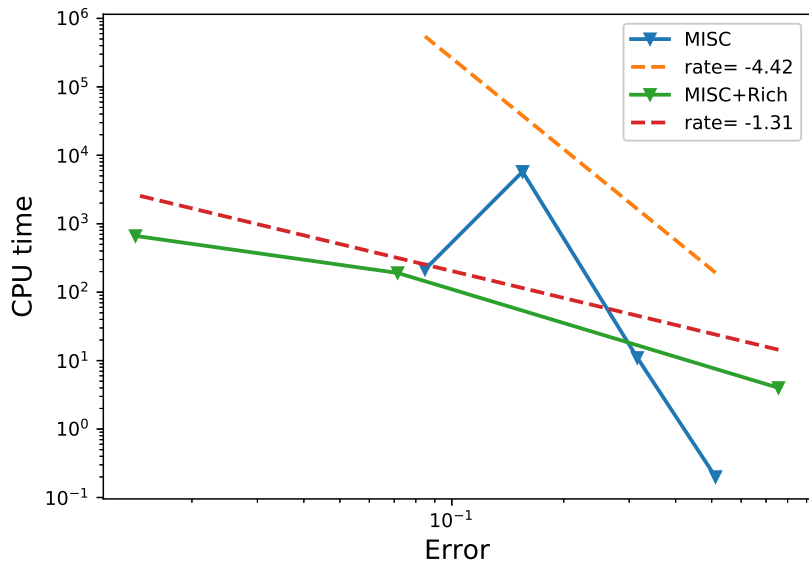


Figure 26: Complexity plot for MISC (with/without) Richardson extrapolation for Case set 1 parameters of table 1.

4.3.4 Case of set 3 parameters in table 1

Method \ Steps	2	4	8	16
MISC ($Tol = 5.10^{-1}$)	0.2393	0.2228	0.2152	0.2093
MISC ($Tol = 10^{-1}$)	0.2393	0.2228	0.2205	0.2228
MISC ($Tol = 5.10^{-2}$)	0.2393	0.2205	0.2273	0.2225
MISC ($Tol = 10^{-2}$)	0.2453	0.2369	0.2325	did not converge
MISC ($Tol = 10^{-3}$)	0.2505	0.2373	did not converge	—
MISC ($Tol = 10^{-4}$)	0.2501	—	—	—
MC method ($M = 10^6$)	0.2529	0.2405	0.2319	0.2280

Table 32: Call option price of the different methods for different number of time steps. Case of set 3 parameters in table 1, without Richardson extrapolation.

Method \ Steps	2	4	8	16
MC Bias ($M = 10^6$)	0.1244 (0.0280)	0.0695 (0.0156)	0.0313 (0.0070)	0.0139 (0.0031)
MC Statistical error ($M = 10^6$)	3.9e - 03 (8.9e-04)	3.2e - 03 (7.3e-04)	2.7e - 03 (6.0e-04)	2.3e - 03 (5.2e-04)

Table 33: Bias and Statistical errors of MC for computing Call option price for different number of time steps. Case set 3, without Richardson extrapolation. The numbers between parentheses are the corresponding absolute errors.

Method \ Steps	2	4	8	16
MISC ($Tol = 5.10^{-1}$)	0.0605 (0.0136)	0.0787 (0.0177)	0.0743 (0.0167)	0.0831 (0.0187)
MISC ($Tol = 10^{-1}$)	0.0605 (0.0136)	0.0787 (0.0177)	0.0507 (0.0114)	0.0231 (0.0052)
MISC ($Tol = 5.10^{-2}$)	0.0605 (0.0136)	0.0889 (0.0200)	0.0205 (0.0046)	0.0245 (0.0055)
MISC ($Tol = 10^{-2}$)	0.0338 (0.0076)	0.0160 (0.0036)	0.0027 (0.0006)	did not converge —
MISC ($Tol = 10^{-3}$)	0.0107 (0.0024)	0.0142 (0.0032)	did not converge —	—
MISC ($Tol = 10^{-4}$)	0.0124 (0.0028)	—	—	—

Table 34: Quadrature error of MISC to compute Call option price of the different tolerances for different number of time steps. Case set 3 parameters in table 1, without Richardson extrapolation. The numbers between parentheses are the corresponding absolute errors.

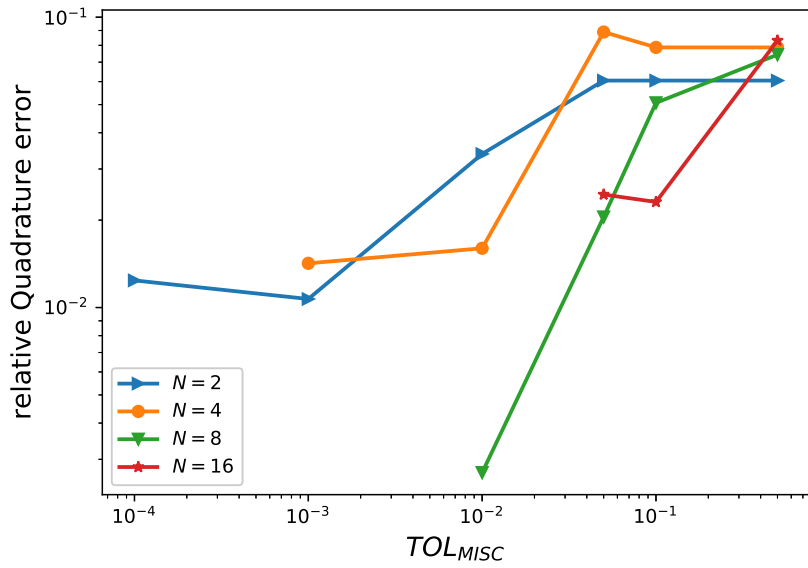


Figure 27: Quadrature error of MISC to compute Call option price of the different tolerances for different number of time steps. Case set 3 parameters, without Richardson extrapolation.

Method \ Steps	2	4	8	16
MISC ($Tol = 5.10^{-1}$)	0.1849	0.1482	0.1056	0.0970
MISC ($Tol = 10^{-1}$)	0.1849	0.1482	0.0820	0.0370
MISC ($Tol = 5.10^{-2}$)	0.1849	0.1584	0.0518	0.0384
MISC ($Tol = 10^{-2}$)	0.1582	0.0855	0.0340	did not converge
MISC ($Tol = 10^{-3}$)	0.1351	0.0837	did not converge	—
MISC ($Tol = 10^{-4}$)	0.1368	—	—	—
MC	0.1582	0.0855	—	—

Table 35: Total error of MISC and MC to compute Call option price of the different tolerances for different number of time steps. Case Case set 3 parametrts of table 1, without Richardson extrapolation.

Method \ Steps	2	4	8	16
MISC ($Tol = 5.10^{-1}$)	0.1	0.1	0.2	2
MISC ($Tol = 10^{-1}$)	0.1	0.1	4	640
MISC ($Tol = 5.10^{-2}$)	0.1	0.4	11	1256
MISC ($Tol = 10^{-2}$)	1	9	1400	did not converge
MISC ($Tol = 10^{-3}$)	20	1760	did not converge	—
MISC ($Tol = 10^{-4}$)	78	—	—	—
MC method	1.4	4		
Ratio of (MC/MISC)	1.4	0.44		—

Table 36: Comparison of the computational time of MC and MISC, used to compute Call option price of rBergomi model for different number of time steps. Case set 3 parametrs of table 1

Method \ Steps	1 – 2	2 – 4	4 – 8	8 – 16
MISC ($Tol = 5.10^{-1}$)	0.2587	0.2062	0.2075	0.2077
MISC ($Tol = 10^{-1}$)	0.2587	0.2047	0.2147	0.2163
MISC ($Tol = 5.10^{-2}$)	0.2587	0.2267	0.2186	did not converge
MISC ($Tol = 10^{-2}$)	0.2789	0.2306	0.2260	—
MISC ($Tol = 10^{-3}$)	0.2811	0.2255	did not converge	—
MISC ($Tol = 10^{-4}$)	0.2808	did not converge	—	—
MC method ($M = 10^6$)	0.2780	0.2289	0.2255	0.2252

Table 37: Call option price of the different methods for different number of time steps. Case set 3 parameters of table 1, using Richardson extrapolation (level 1)

Method \ Steps	1 – 2	2 – 4	4 – 8	8 – 16
MC ($M = 10^6$) Bias	0.2362 (0.0531)	0.0179 (0.0040)	0.0027 (0.0006)	0.0013 (0.0003)
Statistical error ($M = 10^6$)	2.6e – 03 (5.8e–04)	2.6e – 03 (5.8e–04)	1.0e – 03 (2.2e–04)	8.2e – 04 (1.8e–04)

Table 38: Bias and Statistical errors of MC for computing Call option price for different number of time steps. Case set 3 parameters in tabel 1, with Richardson extrapolation (level 1). The numbers between parentheses are the corresponding absolute errors.

Method \ Steps	1 - 2	2 - 4	4 - 8	8 - 16
MISC ($Tol = 5.10^{-1}$)	0.0858 (0.0193)	0.1009 (0.0227)	0.0800 (0.0180)	0.0778 (0.0175)
MISC ($Tol = 10^{-1}$)	0.0858 (0.0193)	0.1076 (0.0242)	0.0480 (0.0108)	0.0396 (0.0089)
MISC ($Tol = 5.10^{-2}$)	0.0858 (0.0193)	0.0098 (0.0022)	0.0307 (0.0069)	did not converge
MISC ($Tol = 10^{-2}$)	0.0040 (0.0009)	0.0076 (0.0017)	0.0022 (0.0005)	—
MISC ($Tol = 10^{-3}$)	0.0138 (0.0031)	0.0151 (0.0034)	did not converge	
MISC ($Tol = 10^{-4}$)	0.0124 (0.0028)	did not converge		

Table 39: Quadrature error of MISC to compute Call option price of the different tolerances for different number of time steps. Case set 3 parameters in table 1, with Richardson extrapolation(level 1). The numbers between parentheses are the corresponding absolute errors.

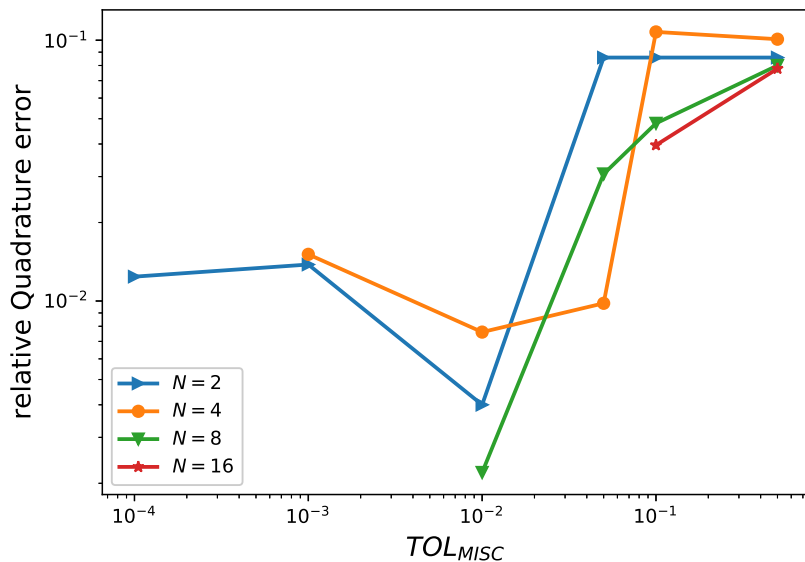


Figure 28: Quadrature error of MISC to compute Call option price of the different tolerances for different number of time steps. Case set 3 parameters, with Richardson extrapolation.

Method \ Steps	1 – 2	2 – 4	4 – 8	8 – 16
MISC ($Tol = 5.10^{-1}$)	0.3220	0.1188	0.0827	0.0791
MISC ($Tol = 10^{-1}$)	0.3220	0.1255	0.0507	0.0409
MISC ($Tol = 5.10^{-2}$)	0.3220	0.0277	0.0334	did not converge
MISC ($Tol = 10^{-2}$)	0.2402	0.0255	0.0049	–
MISC ($Tol = 10^{-3}$)	0.2500	0.0330	did not converge	–
MISC ($Tol = 10^{-3}$)	0.2486	did not converge	–	–

Table 40: Total error of MISC and MC to compute Call option price of the different tolerances for different number of time steps. Case set 3 parameters in table 1, with Richardson extrapolation(level 1). The numbers between parentheses are the corresponding absolute errors.

Method \ Steps	1 – 2	2 – 4	4 – 8	8 – 16
MISC ($Tol = 5.10^{-1}$)	0.1	0.1	0.2	7
MISC ($Tol = 10^{-1}$)	0.1	0.2	5	1375
MISC ($Tol = 5.10^{-2}$)	0.1	2	19	did not converge
MISC ($Tol = 10^{-2}$)	3	24	1900	–
MISC ($Tol = 10^{-3}$)	30	9510	did not converge	–
MISC ($Tol = 10^{-4}$)	234	did not converge	–	–

Table 41: Comparison of the computational time of MC and MISC, using Richardson extrapolation (level 1), used to compute Call option price of rBergomi model for different number of time steps. Case set 3 parameters in table 1

4.3.5 Case of set 4 parameters in table 1

Method \ Steps	2	4	8	16
MISC ($Tol = 5.10^{-1}$)	0.0298	0.0107	0.0033	0.0008
MISC ($Tol = 10^{-1}$)	0.0298	0.0107	0.0033	0.0008
MISC ($Tol = 5.10^{-2}$)	0.0298	0.0107	0.0033	0.0008
MISC ($Tol = 10^{-2}$)	0.0524	0.0157	0.0033	0.0008
MISC ($Tol = 10^{-3}$)	0.0519	0.0341	0.0220	did not converge
MISC ($Tol = 10^{-4}$)	0.0525	did not converge	did not converge	—
MC method ($M = 10^6$)	0.0527	0.0334	0.0240	0.0177

Table 42: Call option price of the different methods for different number of time steps. Case of set 4 parameters in table 1, without Richardson extrapolation.

Method \ Steps	2	4	8	16
MC Bias ($M = 10^6$)	4.2973 (0.0427)	2.3592 (0.0234)	1.4125 (0.0140)	0.777 (0.0077)
Statistical error ($M = 10^6$)	2.4e - 02 (2.4e-04)	1.8e - 02 (1.8e-04)	9.5e - 03 (9.4e-05)	6.0e - 03 (6.0e-05)

Table 43: Bias and Statistical errors of MC for computing Call option price for different number of time steps. Case set 4, without Richardson extrapolation. The numbers between parentheses are the corresponding absolute errors.

Method \ Steps	2	4	8	16
MISC ($Tol = 5.10^{-1}$)	2.3039 (0.0229)	2.2838 (0.0227)	2.0826 (0.0207)	1.7002 (0.0169)
MISC ($Tol = 10^{-1}$)	2.3039 (0.0229)	2.2838 (0.0227)	2.0826 (0.0207)	1.7002 (0.0169)
MISC ($Tol = 5.10^{-2}$)	2.3039 (0.0229)	2.2838 (0.0227)	2.0826 (0.0207)	1.7002 (0.0169)
MISC ($Tol = 10^{-2}$)	0.0302 (0.0003)	1.7807 (0.0177)	2.0826 (0.0207)	1.7002 (0.0169)
MISC ($Tol = 10^{-3}$)	0.0805 (0.0008)	0.0704 (0.0007)	0.2012 (0.0020)	did not converge
MISC ($Tol = 10^{-4}$)	0.0201 (0.0002)	did not converge	did not converge	—

Table 44: Quadrature error of MISC to compute Call option price of the different tolerances for different number of time steps. Case set 4 parameters in table 1, without Richardson extrapolation. The numbers between parentheses are the corresponding absolute errors.

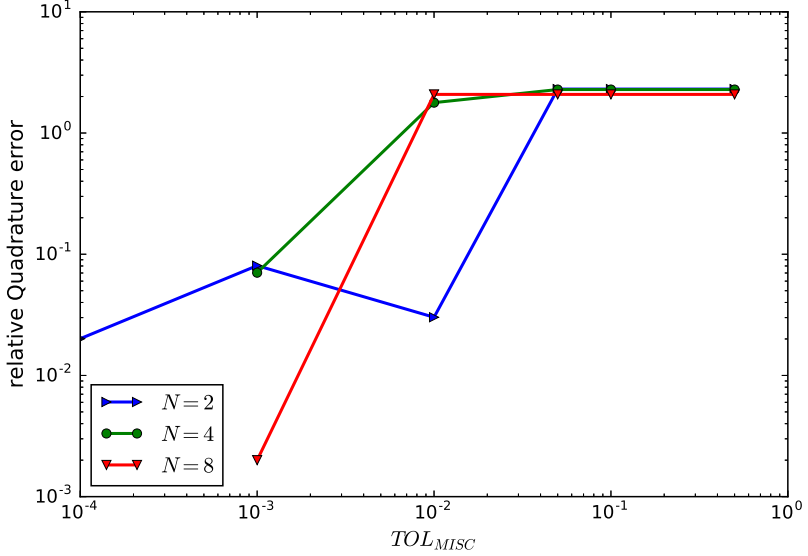


Figure 29: Quadrature error of MISC to compute Call option price of the different tolerances for different number of time steps. Case set 4 parameters, without Richardson extrapolation.

Method \ Steps	2	4	8	16
MISC ($Tol = 5.10^{-1}$)	6.6012	4.6430	3.4951	2.4772
MISC ($Tol = 10^{-1}$)	6.6012	4.6430	3.4951	2.4772
MISC ($Tol = 5.10^{-2}$)	6.6012	4.6430	3.4951	2.4772
MISC ($Tol = 10^{-2}$)	4.3275	4.1399	3.4951	2.4772
MISC ($Tol = 10^{-3}$)	4.3778	2.4296	1.6137	did not converge
MISC ($Tol = 10^{-4}$)	4.3174	did not converge	did not converge	—

Table 45: Total error of MISC and MC to compute Call option price of the different tolerances for different number of time steps. Case Case set 4 parametrts of table 1, without Richardson extrapolation. The numbers between parentheses are the corresponding absolute errors.

Method \ Steps	2	4	8	16
MISC ($Tol = 5.10^{-1}$)	0.1	0.1	0.2	0.4
MISC ($Tol = 10^{-1}$)	0.1	0.1	0.2	0.4
MISC ($Tol = 5.10^{-2}$)	0.1	0.1	0.2	0.4
MISC ($Tol = 10^{-2}$)	0.8	0.5	0.2	0.4
MISC ($Tol = 10^{-3}$)	4	2368	6750	did not converge
MISC ($Tol = 10^{-4}$)	80	did not converge	did not converge	—

Table 46: Comparison of the computational time of MC and MISC, used to compute Call option price of rBergomi model for different number of time steps. Case set 4 parametrts of table 1

Method \ Steps	1 – 2	2 – 4	4 – 8	8 – 16
MISC ($Tol = 5.10^{-1}$)	0.0262	0.0084	-0.0042	-0.0016
MISC ($Tol = 10^{-1}$)	0.0262	0.0084	-0.0042	-0.0016
MISC ($Tol = 5.10^{-2}$)	0.0262	0.0084	-0.0042	-0.0016
MISC ($Tol = 10^{-2}$)	0.0668	-0.0069	0.0163	-0.0016
MISC ($Tol = 10^{-3}$)	0.0726	0.0154	did not converge	did not converge
MISC ($Tol = 10^{-4}$)	0.0732	did not converge	-	-
MC method ($M = 10^6$)	0.0733	0.0146	0.0132	0.0117

Table 47: Call option price of the different methods for different number of time steps. Case set 4 parameters of table 1, using Richardson extrapolation (level 1)

Method \ Steps	1 – 2	2 – 4	4 – 8	8 – 16
MC ($M = 10^6$) Bias	6.3745 (0.0634)	0.4716 (0.047)	0.3291 (0.0033)	0.1775 (0.0018)
Statistical error ($M = 10^6$)	4.1e – 02 (4.1e–04)	1.7e – 02 (1.7e–04)	7.8e – 03 (7.8e–05)	5.1e – 03 (5.1e–05)

Table 48: Bias and Statistical errors of MC for computing Call option price for different number of time steps. Case set 4 parameters in tabel 1, with Richardson extrapolation (level 1). The numbers between parentheses are the corresponding absolute errors.

Method \ Steps	1 – 2	2 – 4	4 – 8	8 – 16
MISC ($Tol = 5.10^{-1}$)	4.7386 (0.0471)	0.6238 (0.0062)	1.7506 (0.0174)	1.3381 (0.0133)
MISC ($Tol = 10^{-1}$)	4.7386 (0.0471)	0.6238 (0.0062)	1.7506 (0.0174)	1.3381 (0.0133)
MISC ($Tol = 5.10^{-2}$)	4.7386 (0.0471)	0.6238 (0.0062)	1.7506 (0.0174)	1.3381 (0.0133)
MISC ($Tol = 10^{-2}$)	0.6540 (0.0065)	2.1630 (0.0215)	0.3119 (0.0031)	1.3381 (0.0133)
MISC ($Tol = 10^{-3}$)	0.0704 (0.0007)	0.0805 (0.0008)	did not converge	did not converge
MISC ($Tol = 10^{-4}$)	0.0101 (0.0001)	did not converge	-	-

Table 49: Quadrature error of MISC to compute Call option price of the different tolerances for different number of time steps. Case set 4 parameters in table 1, with Richardson extrapolation(level 1). The numbers between parentheses are the corresponding absolute errors.

Method \ Steps	1 – 2	2 – 4	4 – 8	8 – 16
MISC ($Tol = 5.10^{-1}$)	11.1131	1.0954	2.0797	1.4556
MISC ($Tol = 10^{-1}$)	11.1131	1.0954	2.0797	1.4556
MISC ($Tol = 5.10^{-2}$)	11.1131	1.0954	2.0797	1.4556
MISC ($Tol = 10^{-2}$)	7.0285	2.6346	0.6410	1.4556
MISC ($Tol = 10^{-3}$)	6.4449	0.5521	did not converge	did not converge
MISC ($Tol = 10^{-4}$)	6.3846	did not converge	-	-

Table 50: Total error of MISC and MC to compute Call option price of the different tolerances for different number of time steps. Case set 4 parameters in table 1, with Richardson extrapolation(level 1). The numbers between parentheses are the corresponding absolute errors.

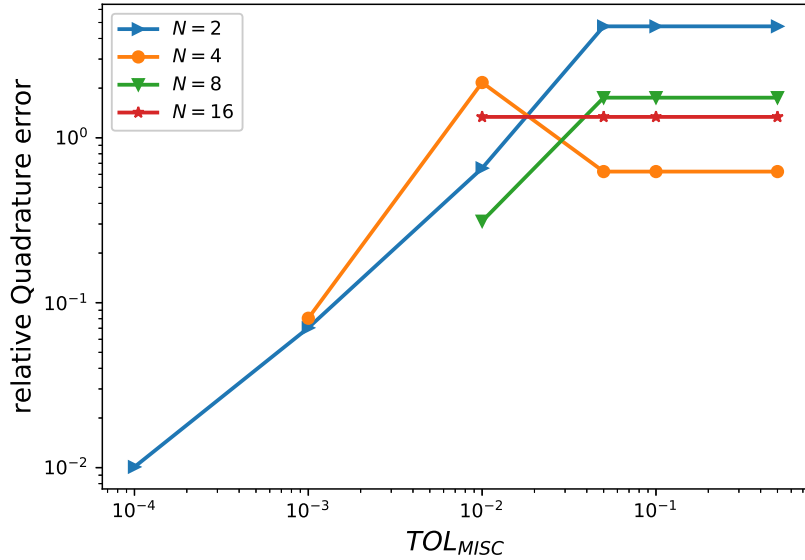


Figure 30: Quadrature error of MISC to compute Call option price of the different tolerances for different number of time steps. Case set 4 parameters, with Richardson extrapolation.

Method \ Steps	1 - 2	2 - 4	4 - 8	8 - 16
MISC ($Tol = 5.10^{-1}$)	0.1	0.1	0.2	0.5
MISC ($Tol = 10^{-1}$)	0.1	0.1	0.2	0.5
MISC ($Tol = 5.10^{-2}$)	0.1	0.1	0.2	0.5
MISC ($Tol = 10^{-2}$)	2	0.9	1640	0.5
MISC ($Tol = 10^{-3}$)	12	3652	did not converge	did not converge
MISC ($Tol = 10^{-4}$)	159	did not converge	-	-

Table 51: Comparsion of the computational time of MC and MISC, using Richardson extrapolation (level 1), used to compute Call option price of rBergomi model for different number of time steps. Case set 4 parameters in table 1

4.4 First and mixed differences rates

In this section, we plot the first and second order differences for the case without change of measure. These plots are important because they provide an indication about the efficiency and speed of MISC. We show the plots for all parameters sets considered in table 1 and for $N = 4$ time steps (we observed similar behaviors for other scenarios of number of time steps). We also show plots of the integrand without Gaussian weights for all cases. From the below figures, we have the following observations:

- i) As was expected, the slowest directions are those corresponding to W^1 , compared to those of W^2 .
- ii) The case of parameters set 5 shows the most stable results in terms of the mixed rates convergence as well the growth of the integrand wrt W_1 and W_2 . On the other hand, for all the other paramters sets, we face a bad behavior for the second differences, which may explain the potential instability observed by MISC as well its bad convergence behavior for high number of time steps (see Section 4.3).

4.4.1 Mixed differences for the case of set 5 in table 1

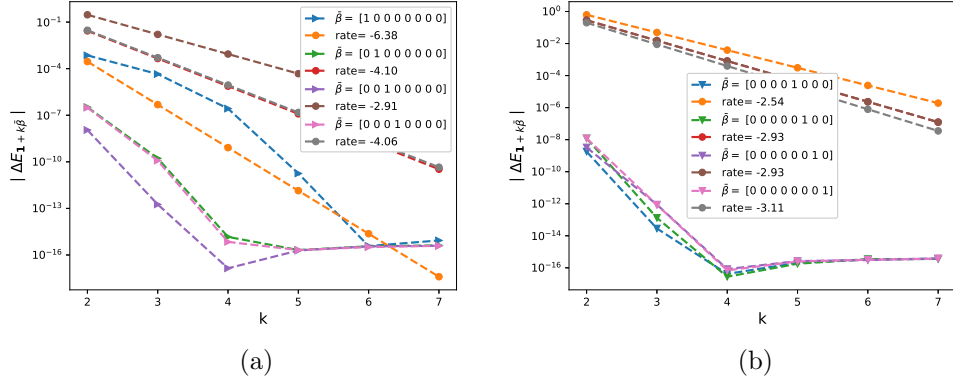


Figure 31: The rate of convergence of first order differences $|\Delta E_\beta|$ ($\beta = \mathbf{1} + k\bar{\beta}$), for $K = 1$, $H = 0.02$: a) for W^1 b) for W^2

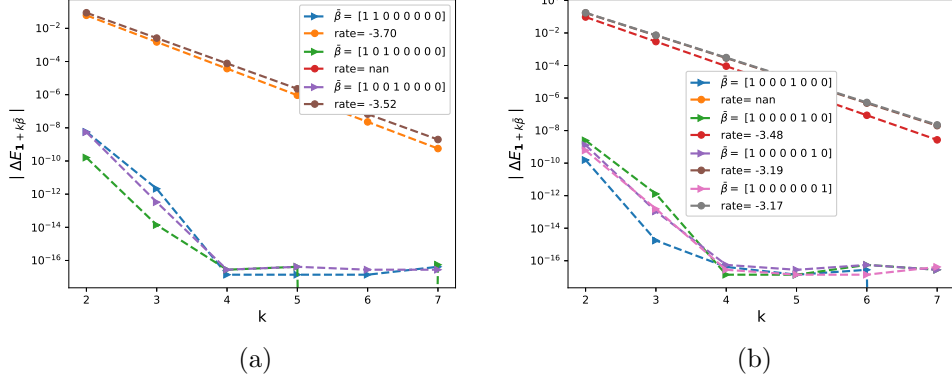


Figure 32: The rate of convergence of second order differences $|\Delta E_\beta|$ ($\beta = \mathbf{1} + k\bar{\beta}$), for $K = 1$, $H = 0.02$: a) for W^1 b) for W^2

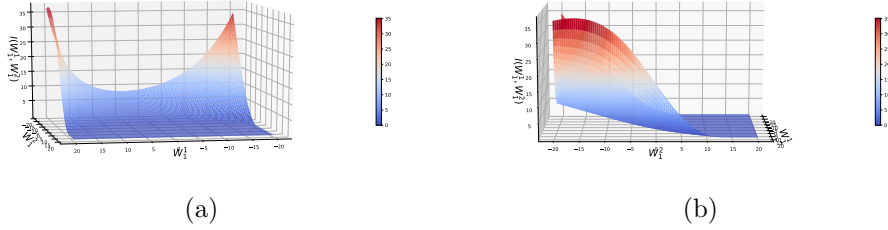


Figure 33: Two dimensional Plotting of the integrand I (in (8)) without the Gaussian weight for $H = 0.02$ and $N = 4$, function of W_1 coordinates (W_1^1, W_1^2)

4.4.2 Mixed differences for the case of set 2 in table 1

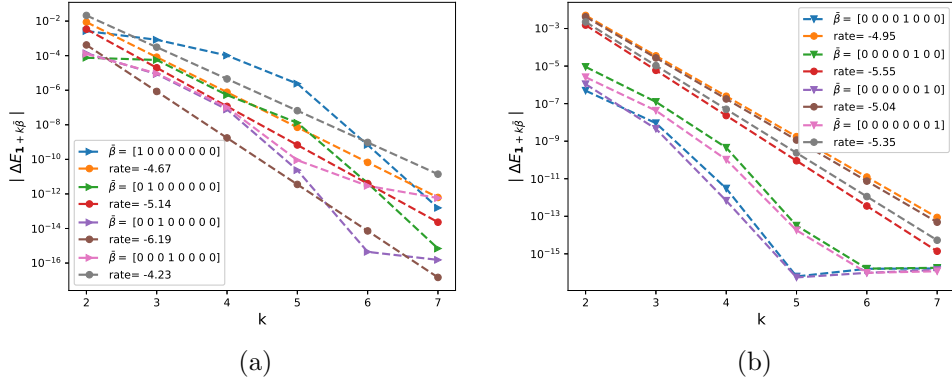


Figure 34: The rate of convergence of first order differences $|\Delta E_\beta|$ ($\beta = \mathbf{1} + k\bar{\beta}$), for $K = 1$, $H = 0.07$: a) for W^1 b) for W^2

We tried to investigate the reason of the bad behavior observed for the mixed differences. From

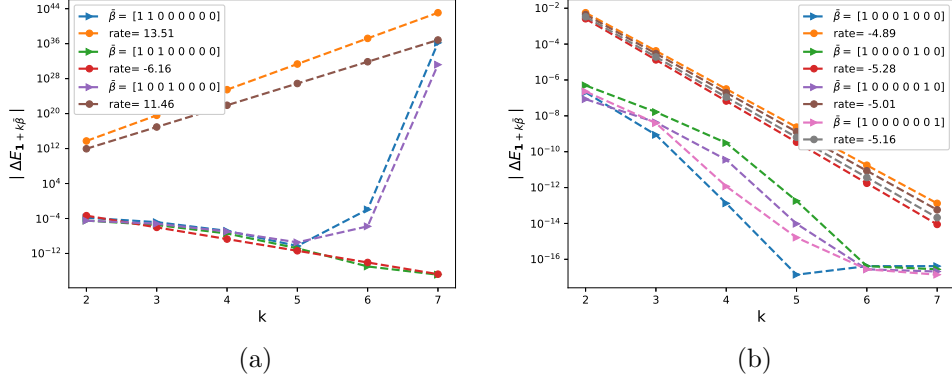


Figure 35: The rate of convergence of second order differences $|\Delta E_\beta|$ ($\beta = \mathbf{1} + k\bar{\beta}$), for $K = 1$, $H = 0.07$: a) for W^1 b) for W^2

our experiments, we observed that whenever the mixed differences is diverging the maximum value of the integrand evaluated at quadrature points seems to blow up. We plot in figure (36) the function evaluated with quadrature points without the gaussian weights. The integrand behavior without weights seems to blow up maybe with faster rate than how the weights of the Hermite quadrature is decaying. In order to solve the issue of the divergence of mixed difference, we need to understand the interplay between the weights and the function values.

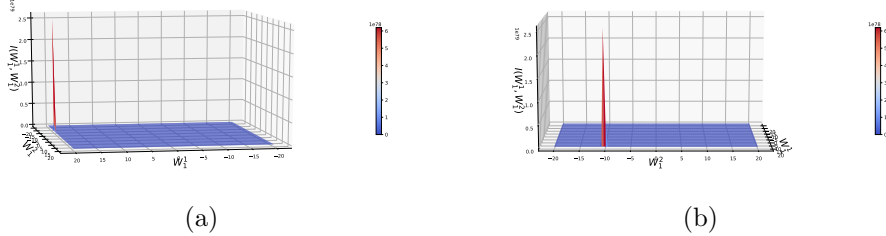


Figure 36: Two dimensional Plotting of the integrand I (in (8)) without the Gaussian weight for $H = 0.07$ and $N = 4$, function of W_1 coordinates (W_1^1, W_1^2)

4.4.3 Mixed differences for the case of set 1 in table 1

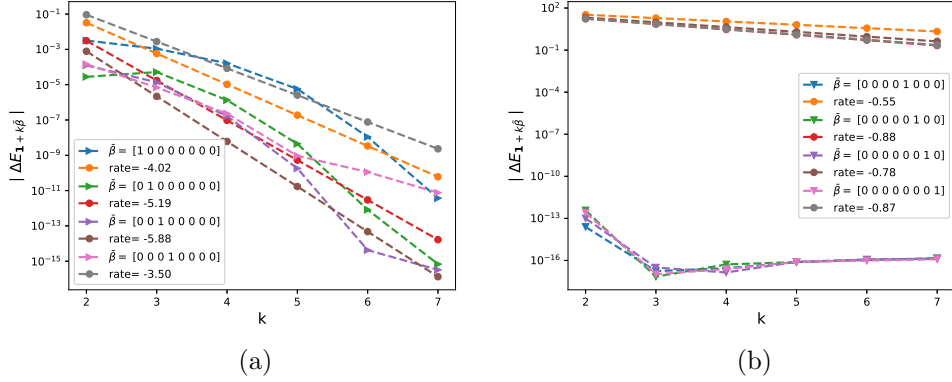


Figure 37: The rate of convergence of first order differences $|\Delta E_\beta|$ ($\beta = \mathbf{1} + k\bar{\beta}$), for $K = 1$, $H = 0.43$: a) for W^1 b) for W^2

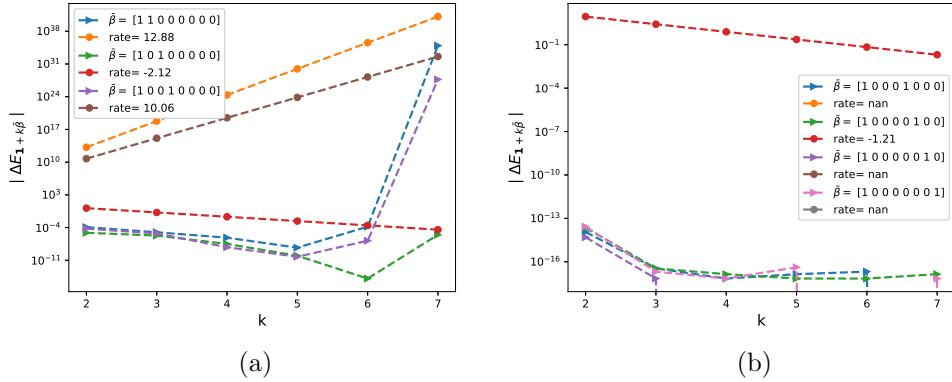


Figure 38: The rate of convergence of second order differences $|\Delta E_\beta|$ ($\beta = \mathbf{1} + k\bar{\beta}$), for $K = 1$, $H = 0.43$: a) for W^1 b) for W^2

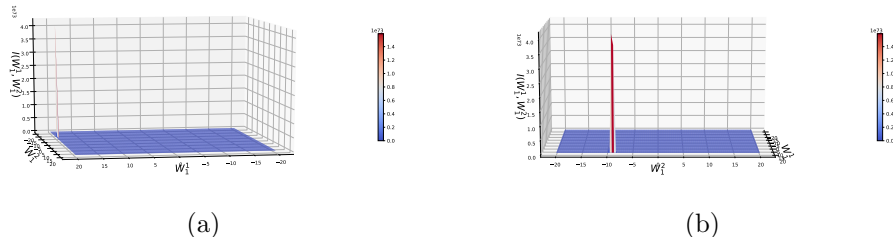


Figure 39: Two dimensional Plotting of the integrand I (in (8)) without the Gaussian weight for $H = 0.43$ and $N = 4$, function of W_1 coordinates (W_1^1, W_1^2)

4.4.4 Mixed differences for the case of set 3 in table 1

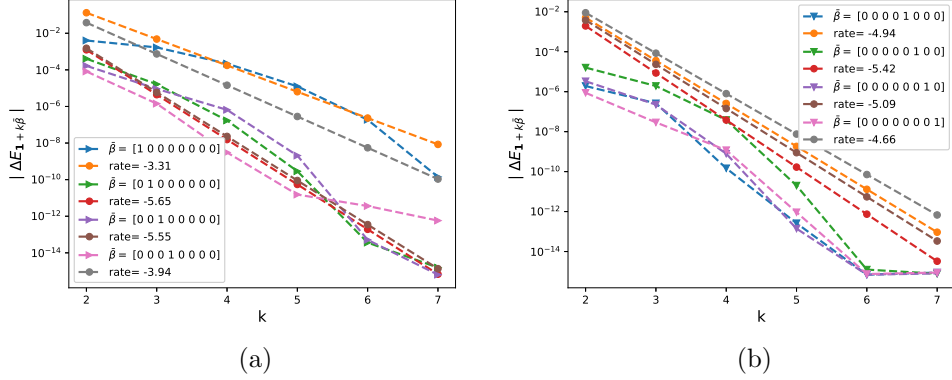


Figure 40: The rate of convergence of first order differences $|\Delta E_\beta|$ ($\beta = \mathbf{1} + k\bar{\beta}$), for $K = 0.8$, $H = 0.07$: a) for W^1 b) for W^2

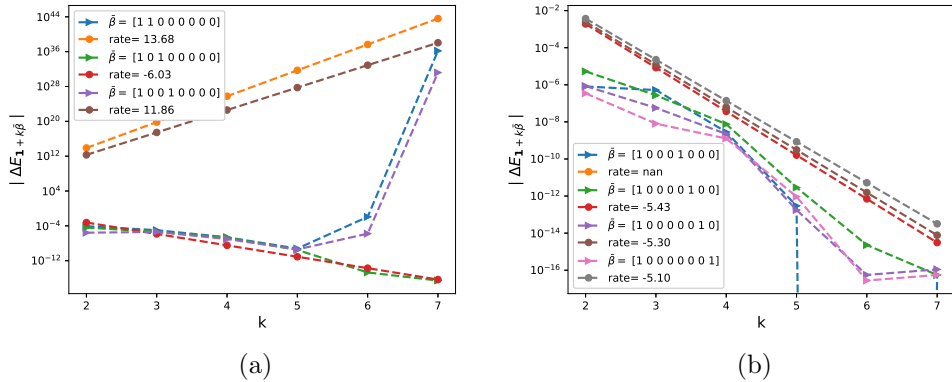


Figure 41: The rate of convergence of second order differences $|\Delta E_\beta|$ ($\beta = \mathbf{1} + k\bar{\beta}$), for $K = 0.8$, $H = 0.07$: a) for W^1 b) for W^2

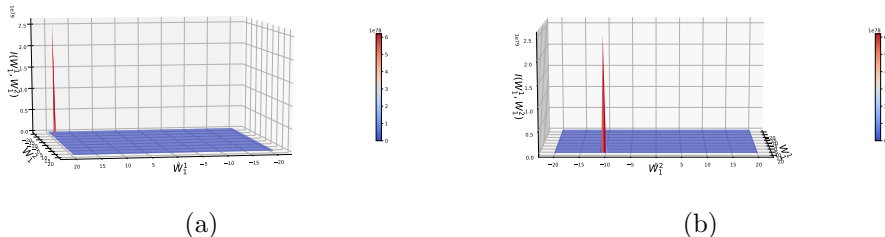


Figure 42: Two dimensional Plotting of the integrand I (in (8)) without the Gaussian weight for $H = 0.07$, $K = 0.8$ and $N = 4$, function of W_1 coordinates (W_1^1, W_1^2)

4.4.5 Mixed differences for the case of set 4 in table 1

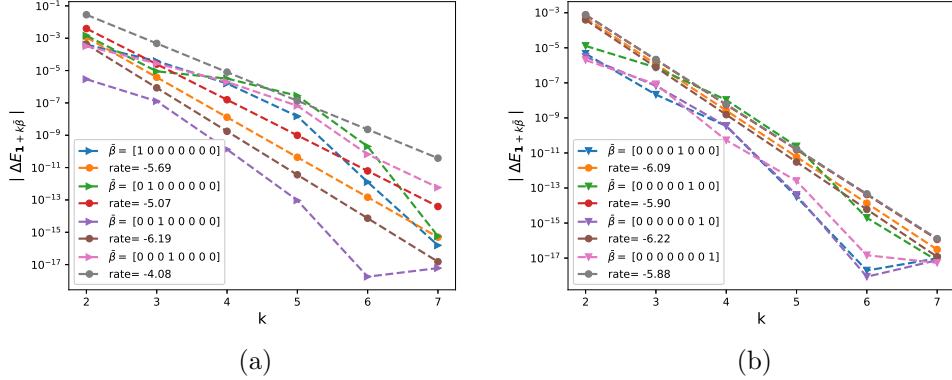


Figure 43: The rate of convergence of first order differences $|\Delta E_\beta|$ ($\beta = \mathbf{1} + k\bar{\beta}$), for $K = 1.2$, $H = 0.07$: a) for W^1 b) for W^2

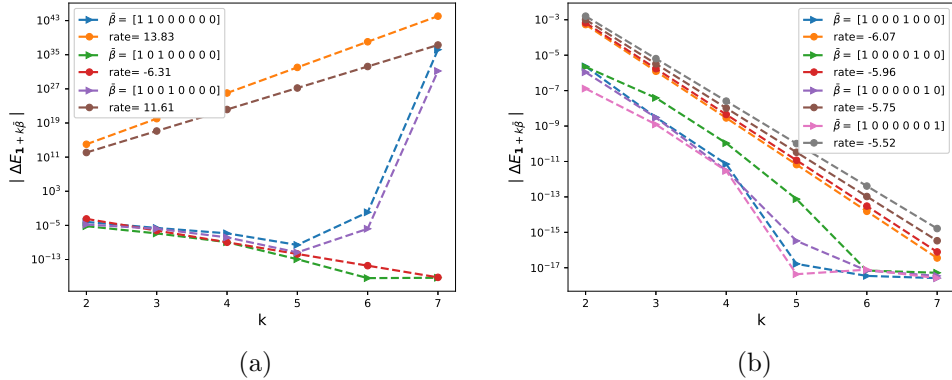


Figure 44: The rate of convergence of second order differences $|\Delta E_\beta|$ ($\beta = \mathbf{1} + k\bar{\beta}$), for $K = 1.2$, $H = 0.07$: a) for W^1 b) for W^2

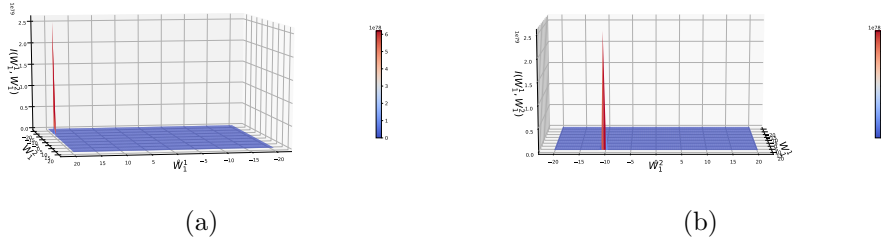


Figure 45: Two dimensional Plotting of the integrand I (in (8)) without the Gaussian weight for $H = 0.07$, $K = 1.2$ and $N = 4$, function of W_1 coordinates (W_1^1, W_1^2)

References Cited

- [1] Pierre Bajgrowicz, Olivier Scaillet, and Adrien Treccani. Jumps in high-frequency data: Spurious detections, dynamics, and news. *Management Science*, 62(8):2198–2217, 2015.

- [2] Christian Bayer, Peter Friz, and Jim Gatheral. Pricing under rough volatility. *Quantitative Finance*, 16(6):887–904, 2016.
- [3] Christian Bayer, Peter K Friz, Paul Gassiat, Joerg Martin, and Benjamin Stemper. A regularity structure for rough volatility. *arXiv preprint arXiv:1710.07481*, 2017.
- [4] Christian Bayer, Peter K Friz, Archil Gulisashvili, Blanka Horvath, and Benjamin Stemper. Short-time near-the-money skew in rough fractional volatility models. *arXiv preprint arXiv:1703.05132*, 2017.
- [5] Mikkel Bennedsen, Asger Lunde, and Mikko S Pakkanen. Decoupling the short-and long-term behavior of stochastic volatility. *arXiv preprint arXiv:1610.00332*, 2016.
- [6] Mikkel Bennedsen, Asger Lunde, and Mikko S Pakkanen. Hybrid scheme for brownian semistationary processes. *Finance and Stochastics*, 21(4):931–965, 2017.
- [7] Lorenzo Bergomi. Smile dynamics ii. 2005.
- [8] F. Biagini, Y. Hu, B. Øksendal, and T. Zhang. *Stochastic Calculus for Fractional Brownian Motion and Applications*. Probability and Its Applications. Springer London, 2008.
- [9] R. Carmona and M.R. Tehranchi. *Interest Rate Models: an Infinite Dimensional Stochastic Analysis Perspective*. Springer Finance. Springer Berlin Heidelberg, 2007.
- [10] Kim Christensen, Roel CA Oomen, and Mark Podolskij. Fact or friction: Jumps at ultra high frequency. *Journal of Financial Economics*, 114(3):576–599, 2014.
- [11] Laure Coutin. An introduction to (stochastic) calculus with respect to fractional brownian motion. In *Séminaire de Probabilités XL*, pages 3–65. Springer, 2007.
- [12] Martin Forde and Hongzhong Zhang. Asymptotics for rough stochastic volatility models. *SIAM Journal on Financial Mathematics*, 8(1):114–145, 2017.
- [13] Masaaki Fukasawa. Asymptotic analysis for stochastic volatility: martingale expansion. *Finance and Stochastics*, 15(4):635–654, 2011.
- [14] Jim Gatheral. *The volatility surface: a practitioner’s guide*, volume 357. John Wiley & Sons, 2011.
- [15] Jim Gatheral, Thibault Jaisson, Andrew Lesniewski, and Mathieu Rosenbaum. Volatility is rough, part 2: Pricing.
- [16] Jim Gatheral, Thibault Jaisson, and Mathieu Rosenbaum. Volatility is rough. *arXiv preprint arXiv:1410.3394*, 2014.
- [17] Paul Glasserman. *Monte Carlo methods in financial engineering*. Springer, New York, 2004.
- [18] Abdul-Lateef Haji-Ali, Fabio Nobile, Lorenzo Tamellini, and Raul Tempone. Multi-index stochastic collocation for random pdes. *Computer Methods in Applied Mechanics and Engineering*, 306:95–122, 2016.

- [19] Antoine Jacquier, Claude Martini, and Aitor Muguruza. On vix futures in the rough bergomi model. *Quantitative Finance*, 18(1):45–61, 2018.
- [20] Antoine Jacquier, Mikko S Pakkanen, and Henry Stone. Pathwise large deviations for the rough bergomi model. *arXiv preprint arXiv:1706.05291*, 2017.
- [21] Benoit B Mandelbrot and John W Van Ness. Fractional brownian motions, fractional noises and applications. *SIAM review*, 10(4):422–437, 1968.
- [22] Tina Marquardt et al. Fractional lévy processes with an application to long memory moving average processes. *Bernoulli*, 12(6):1099–1126, 2006.
- [23] Ryan McCrickerd and Mikko S Pakkanen. Turbocharging monte carlo pricing for the rough bergomi model. *arXiv preprint arXiv:1708.02563*, 2017.
- [24] David Nualart. *The Malliavin calculus and related topics*, volume 1995. Springer, 2006.
- [25] Marc Romano and Nizar Touzi. Contingent claims and market completeness in a stochastic volatility model. *Mathematical Finance*, 7(4):399–412, 1997.

A Comparing relative errors: additional results

B additional results: measure change

B.1 Motivation for the need of measure change

In this Section, we motivate the need of measure change as a pre-processing step before applying the MISC solver.

B.1.1 Integrand plotting wrt different random inputs

In this section, we plot the integrand, given by the term inside the expectation in (8)(including the Gaussian density), wrt different random inputs (W^1, W^2). This is important to check if we need a measure change and if needed for which variables. We show the results for $H = 0.07$ and for two scenarios of number of time steps $N \in \{2, 4\}$ (similar plots are produced for $H = 0.43$ in Appendices (C.1,C.2)). We also show the two dimensional plots (See figures 48,??,??,??). As it seems from the plots, we just need change of measure wrt to W^1 coordinates and we do not need a measure chnage for W^2 coordinates.

N=2, H=0.07

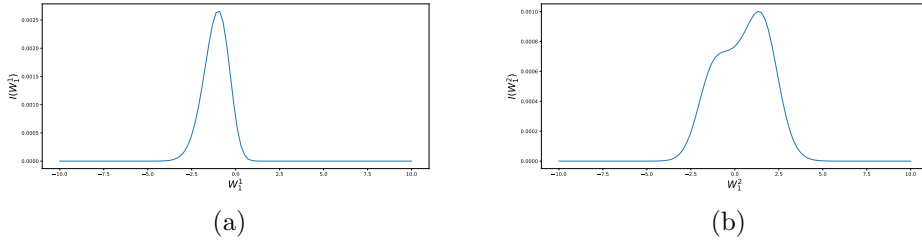


Figure 46: Plotting the integrand I (in (8)) as a function of W^1 coordinates for $H = 0.07$ and $N = 2$.

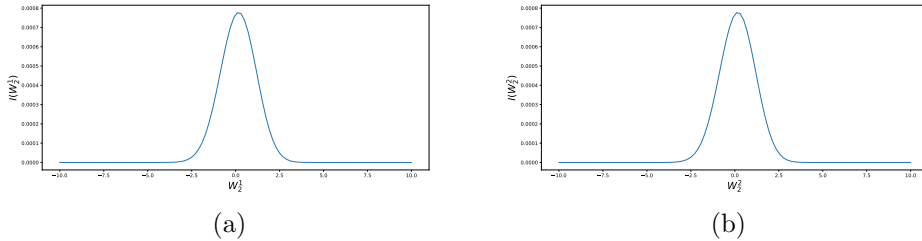


Figure 47: Plotting the integrand I (in (8)) as a function of W^2 coordinates for $H = 0.07$ and $N = 2$.

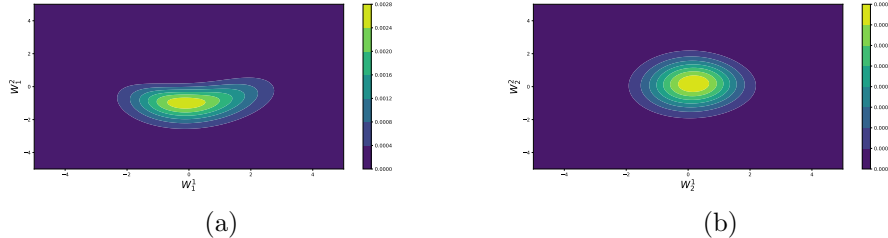


Figure 48: Two dimensional Plotting of the integrand I (in (8)) for $H = 0.07$ and $N = 2$, a) function of W_1 coordinates, b) function of W^2 coordinates

N=4, H=0.07

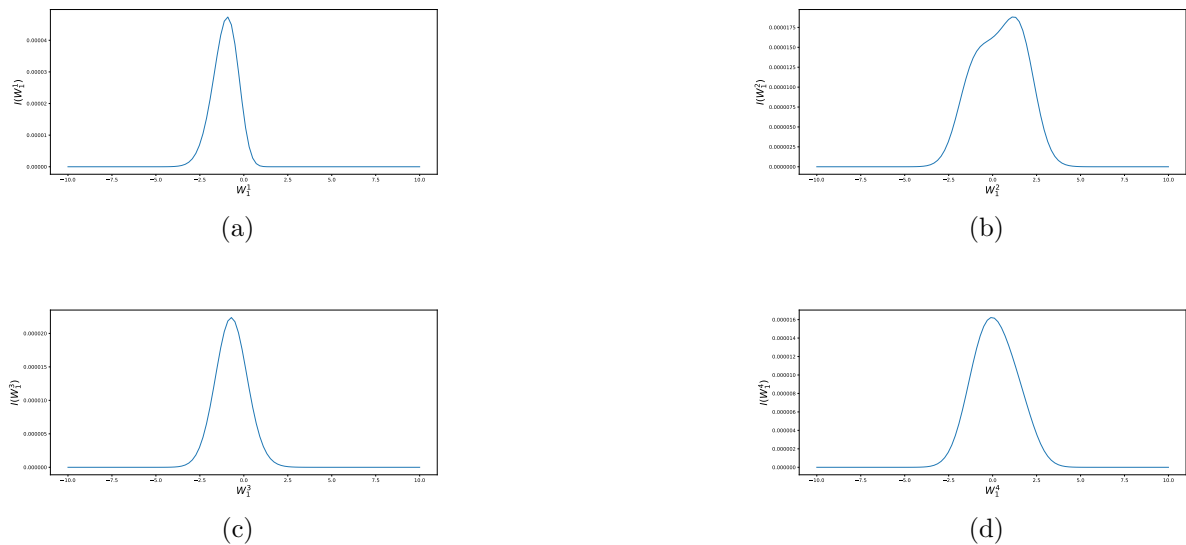


Figure 49: Plotting the integrand I (in (8)) as a function of W_1 coordinates for $H = 0.07$ and $N = 4$.

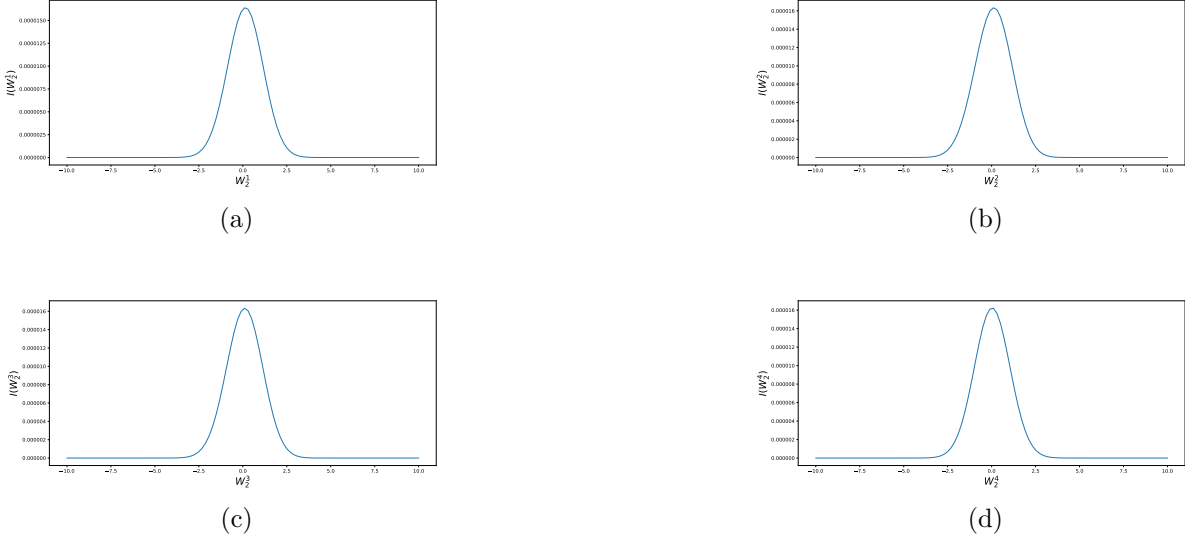


Figure 50: Plotting the integrand I (in (8)) as a function of W_2 coordinates for $H = 0.07$ and $N = 4$.

B.1.2 Comparing the mixed differences rates

In this section, we compare the mixed differences (first and second differences) rates for the standard case against the case where we do a partial change of measure wrt W_1 coordinates (see Section 3.2), for the case of $H = 0.07$ and $N = 4$ time steps. From figures (51,53,52,54), we may notice that we face a bad behavior for the second differences, for the case without change of measure, which may explain the observed instability by MISC. This bad behavior is resolved when doing the partial change of measure. We obtained better results when using a measure change based on spectral decomposition rather than Cholesky decomposition. therefore by doing the change of measure, we expect to obtain a more robust MISC solver.

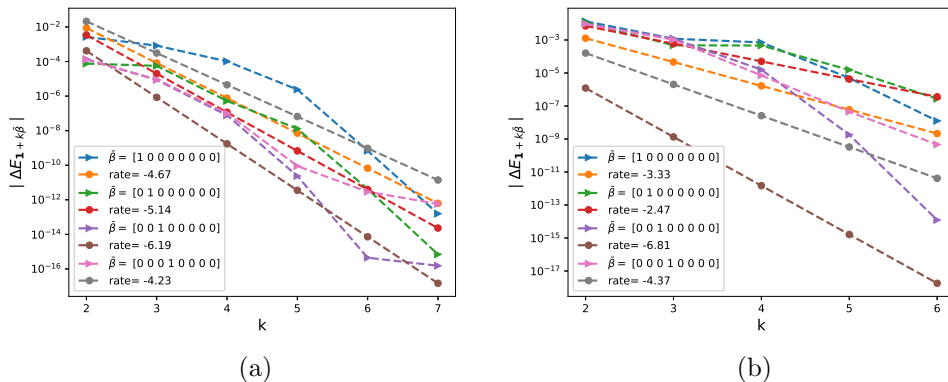


Figure 51: The rate of convergence of first order differences $|\Delta E_\beta|$ ($\beta = \mathbf{1} + k\bar{\beta}$), for W^1 , for $K = 1$, $H = 0.07$: a) Without measure change b) With measure change

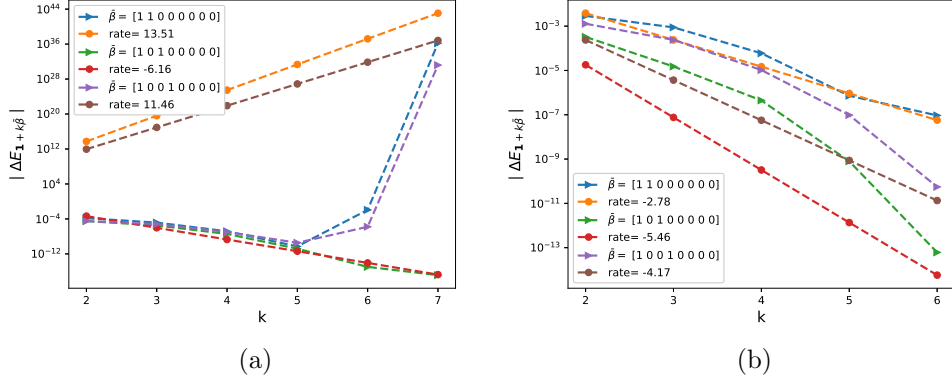


Figure 52: The rate of convergence of second order differences $|\Delta E_\beta|$ ($\beta = \mathbf{1} + k\bar{\beta}$), for W^1 , for $K = 1$, $H = 0.07$: a) Without measure change b) With measure change

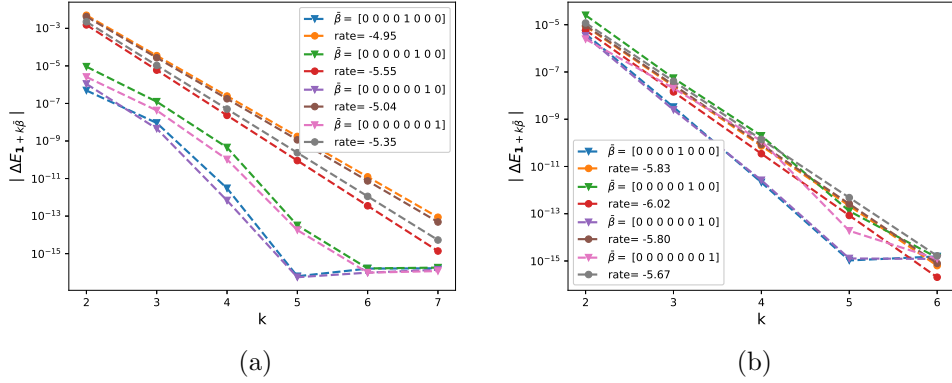


Figure 53: The rate of convergence of first order differences $|\Delta E_\beta|$ ($\beta = \mathbf{1} + k\bar{\beta}$), for W^2 , for $K = 1$, $H = 0.07$: a) Without measure change b) With measure change

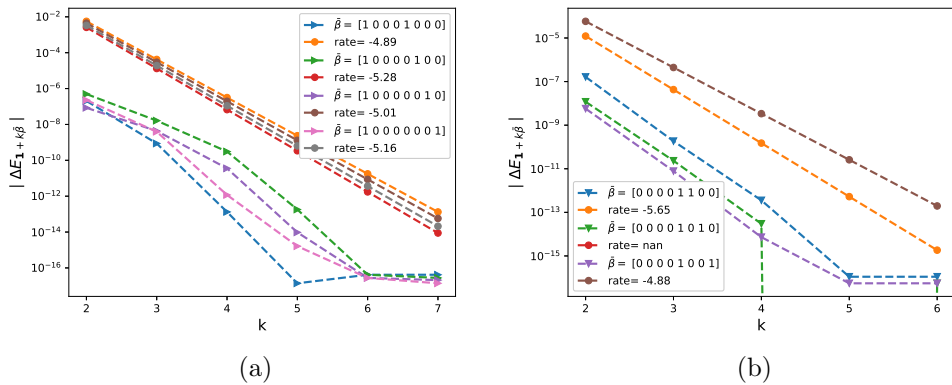


Figure 54: The rate of convergence of second order differences $|\Delta E_\beta|$ ($\beta = \mathbf{1} + k\bar{\beta}$), for W^2 , for $K = 1$, $H = 0.07$: a) Without measure change b) With measure change

B.2 Numerical results for the case with change of measure

B.2.1 Weak error plots

In this section, I include the results of weak error rates for the case with change of measure for both cases without and with Richardson extrapolation, for $H = 0.07$. The reference solution was computed with $N = 500$ time steps. We note that we limit the maximum number of changed coordinates up to 4, due to practical purposes related to the optimization procedure. We note that the weak errors plotted here corresponds to relative errors.

Without Richardson extrapolation

From figure 55), we see that for $H = 0.07$, we get a weak error of order Δt . The upper and lower bounds are 95% confidence interval. In table 52, we show the values of relative weak error. it is clear that compared to the values observed in table ??, we almost observe the same behavior, which may tell us that the change of measure procedure maybe not needed to improve results since we are adding complexity without observing gains in terms of the weak error.

Method \ Steps	2	4	8	16
MC method ($M = 10^6$)	0.5462	0.2686	0.1243	0.0411

Table 52: Relative error of Call option price of the different tolerances for different number of time steps. Case $K = 1$, $H = 0.07$, without Richardson extrapolation

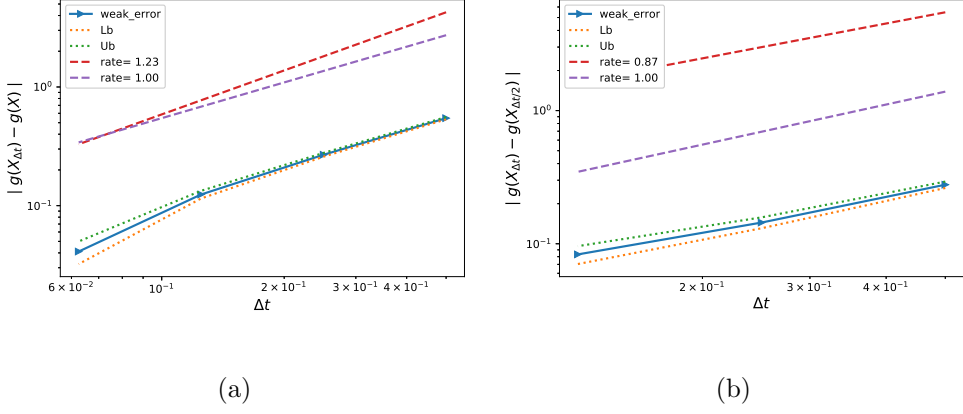


Figure 55: The rate of convergence of the weak error for $H = 0.07$ $K = 1$, without Richardson extrapolation, using MC with $M = 10^5$: a) $|E[g(X_{\Delta t})] - g(X)|$ b) $|E[g(X_{\Delta t}) - g(X_{\Delta t/2})]|$

With Richardson extrapolation (level 1)

From figure 56 , we see that for $H = 0.07$, we get a weak error of order Δt^2 . The upper and lower bounds are 95% confidence interval. In table 53, we show the corresponding results. Comparing to the results without change of measure (see figure 8 and table ??), we got worser weak error values after the change of measure. We provide a potential explanation of the possible cause of this in Section B.2.2.

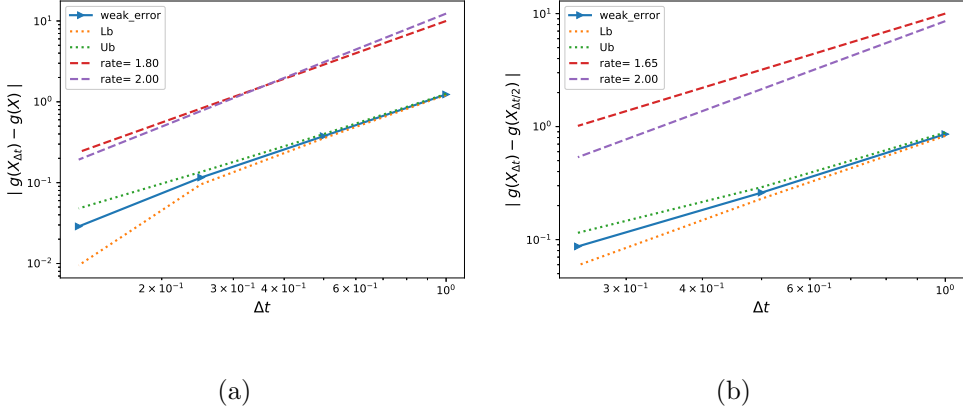


Figure 56: The rate of convergence of the weak error for $H = 0.07$ $K = 1$, with Richardson extrapolation, using MC with $M = 10^6$: a) $|E[2g(X_{\Delta t/2}) - g(X_{\Delta t})] - g(X)|$ b) $|E[3g(X_{\Delta t/2}) - g(X_{\Delta t}) - 2g(X_{\Delta t/4})]|$

Method \ Steps	1 - 2	2 - 4	4 - 8	8 - 16
MC method ($M = 10^6$)	1.2339	0.3763	0.1158	0.0288

Table 53: Relative error of Call option price of the different tolerances for different number of time steps. Case $K = 1$, $H = 0.07$, using Richardson extrapolation (level 1)

B.2.2 Plotting the Richardson integrand for the change of measure

In this section, We try to investigate the reason of having worse weak rates than the case without change of measure. We plot the Richardson integrand used for the change of measure, for $H = 0.07$ and for two cases of time steps in the coarse level of Richardson extrapolation ($N \in \{1, 2\}$) . We conclude from those plots that the extrapolated formula is not very appropriate since we have a more complex function (bi-modal functions or higher as we go deeper for the levels of Richardson extrapolation). As a result, we think it is better to focus on the case without applying a change of measure.

N=1, H=0.07

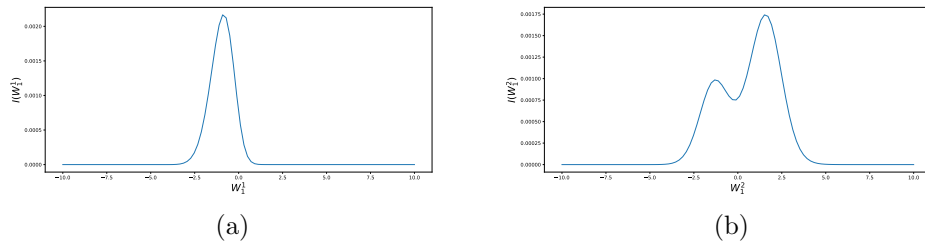


Figure 57: Plotting the integrand I (in (8)) when using Richardson extrapolation(level 1) as a function of W^1 coordinates for $H = 0.07$ and $N = 1$ in the coarser level.

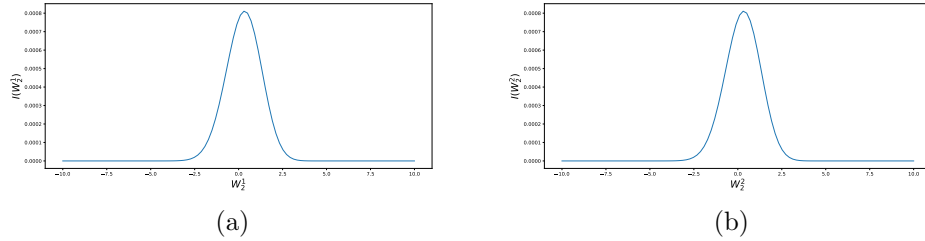


Figure 58: Plotting the integrand I (in (8)) when using Richardson extrapolation(level 1) as a function of W^2 coordinates for $H = 0.07$ and $N = 1$ in the coarser level.

N=2, H=0.07

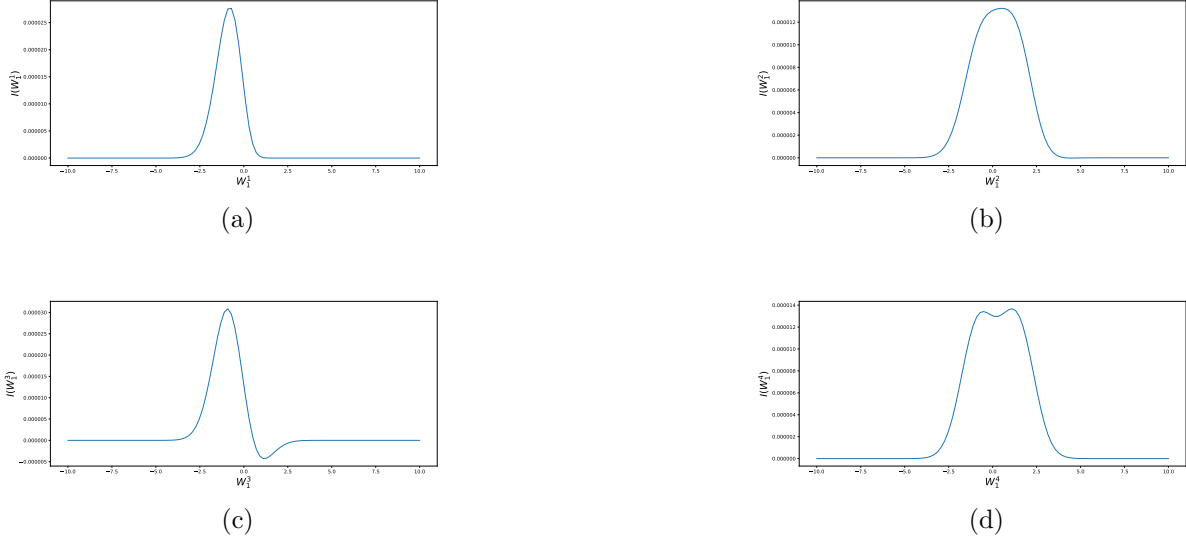


Figure 59: Plotting the integrand I (in (8)) when using Richardson extrapolation(level 1) as a function of W^1 coordinates for $H = 0.07$ and $N = 2$ in the coarser level.

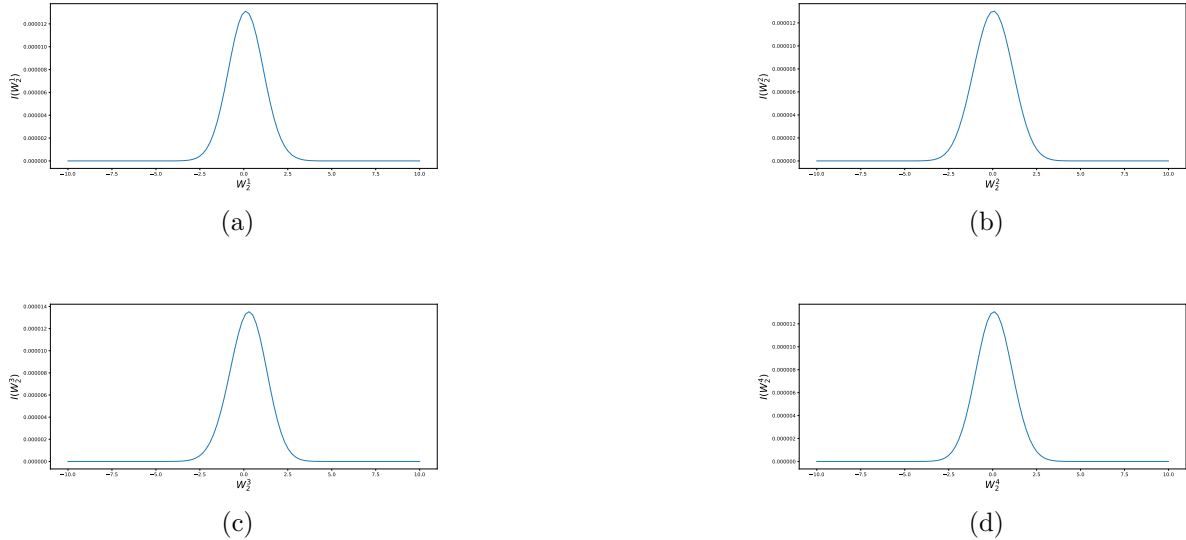


Figure 60: Plotting the integrand I (in (8)) when using Richardson extrapolation(level 1) as a function of W^2 coordinates for $H = 0.07$ and $N = 2$ in the coarser level.

C additional results

C.1 Integrand plotting wrt different random inputs N=2, H=0.43

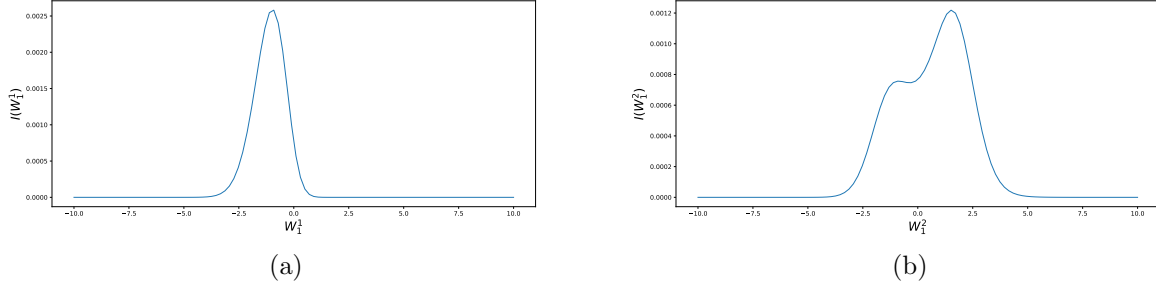


Figure 61: Plotting the integrand I (in (8)) as a function of W^1 coordinates for $H = 0.43$ and $N = 2$.

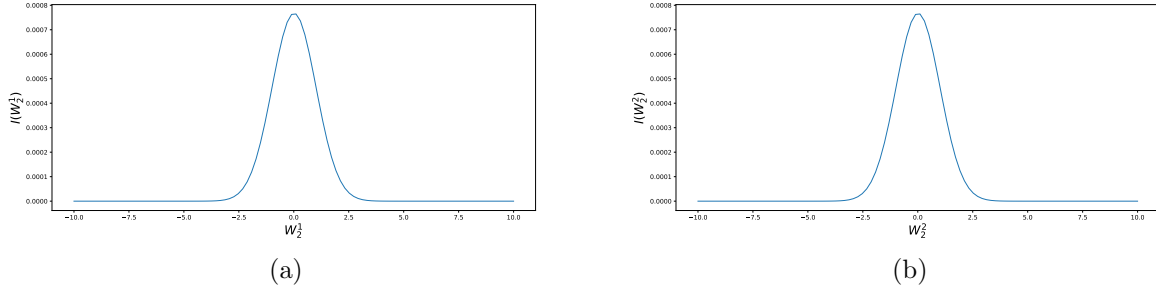


Figure 62: Plotting the integrand I (in (8)) as a function of W^2 coordinates for $H = 0.43$ and $N = 2$.

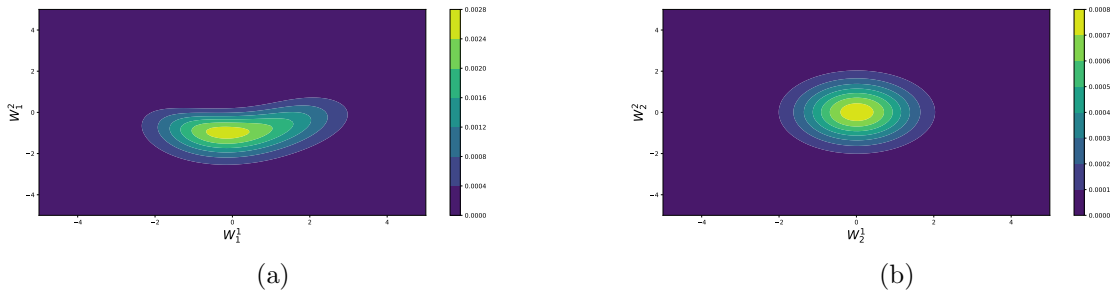


Figure 63: Two dimensional Plotting of the integrand I (in (8)) for $H = 0.43$ and $N = 2$, a) function of W^1 coordinates, b) function of W^2 coordinates

C.2 Integrand plotting wrt different random inputs: N=4, H=0.43

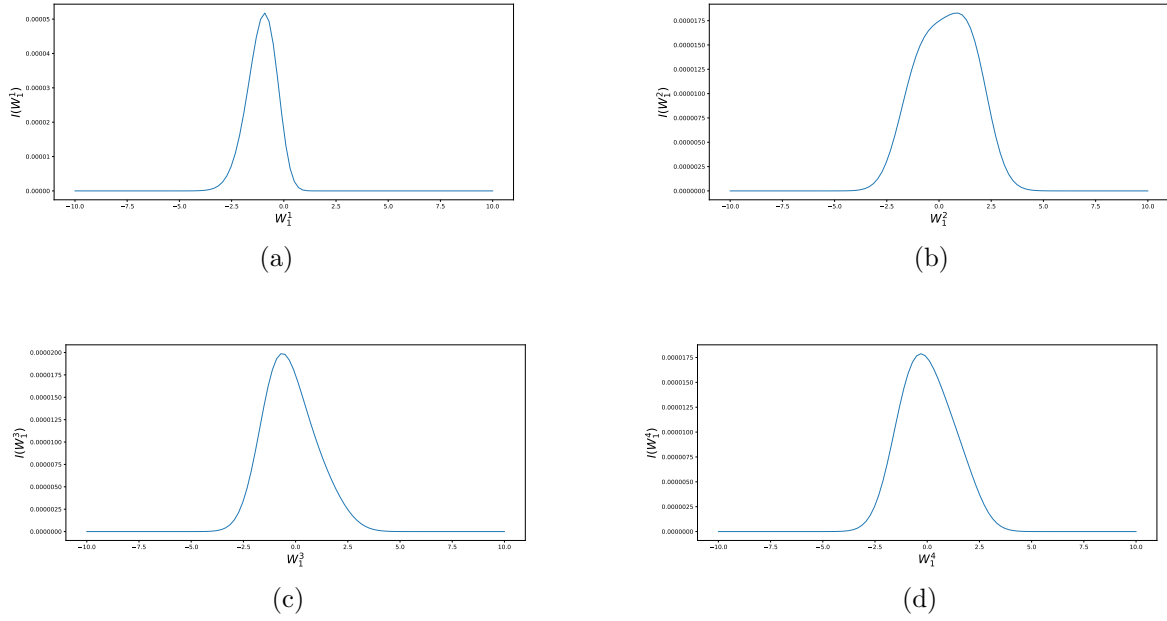


Figure 64: Plotting the integrand I (in (8)) as a function of W^1 coordinates for $H = 0.43$ and $N = 4$.

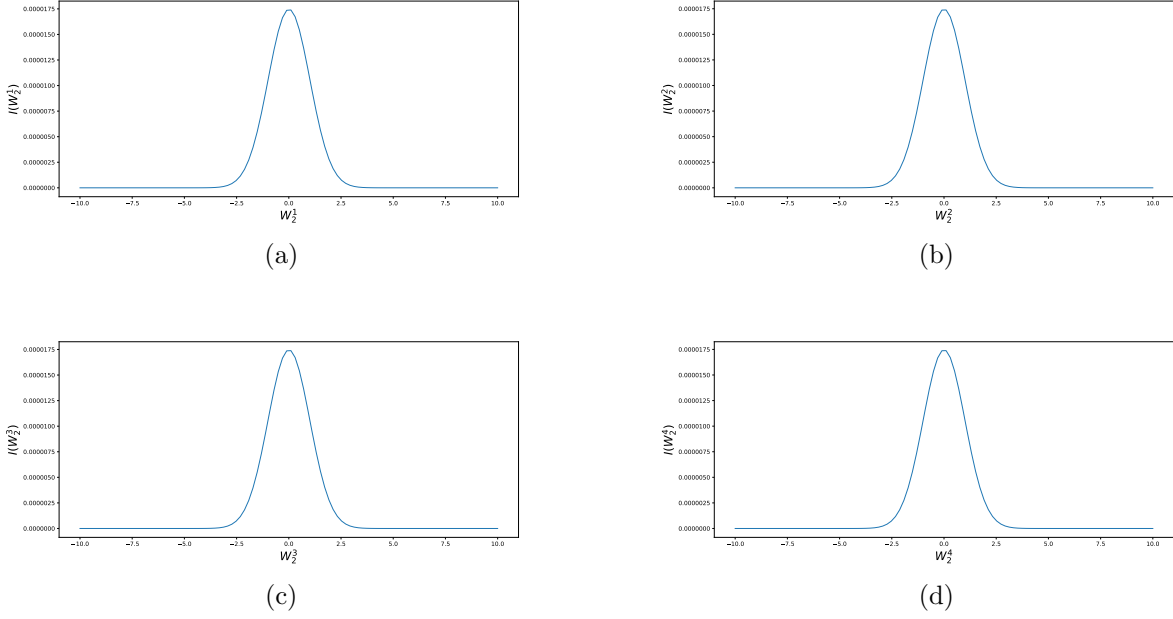


Figure 65: Plotting the integrand I (in (8)) as a function of W^2 coordinates for $H = 0.43$ and $N = 4$.

C.3 Motivation of the hierarchical representation and investigating the effect with respect to H

In this section, we motivate the idea of using hierarchical representation (Brownian bridge construction) for building W^1 and W^2 .

C.3.1 Totally Hierarchical

In this section, we do both hierarchical transformation, based on brownian bridges, for both directions W^1 and W^2 . We see clearly from figures (66,67) the advantage of building W^2 in a hierarchical fashion as W^1

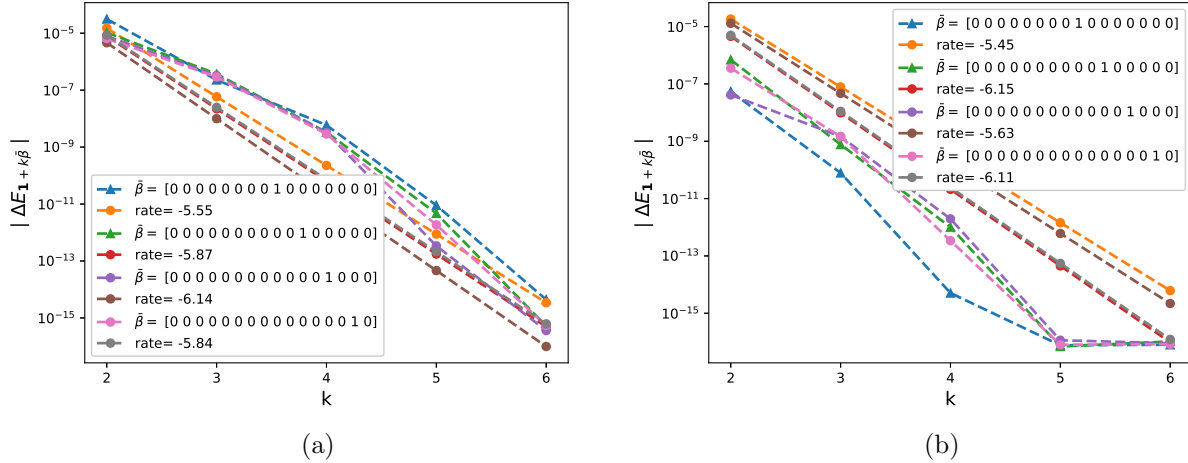


Figure 66: The rate of convergence of first order differences $|\Delta E_\beta|$ ($\beta = \mathbf{1} + k\bar{\beta}$) for $K = 1$: a) Without hierarchical for W_2 b) With hierarchical for W_2

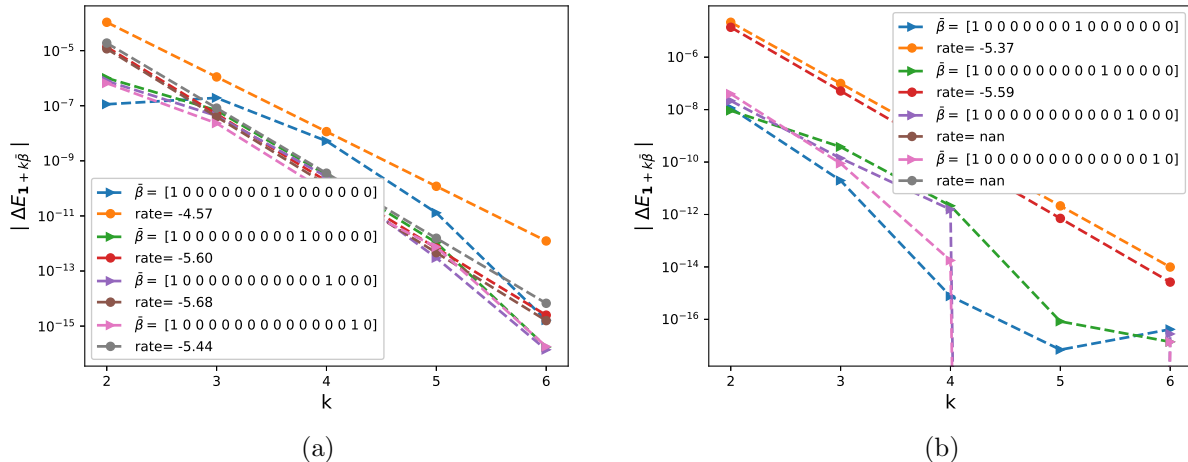


Figure 67: The rate of convergence of second order differences $|\Delta E_\beta|$ ($\beta = \mathbf{1} + k\bar{\beta}$) for $K = 1$: a) Without hierarchical for W_2 b) With hierarchical for W_2

C.3.2 Hierarchical

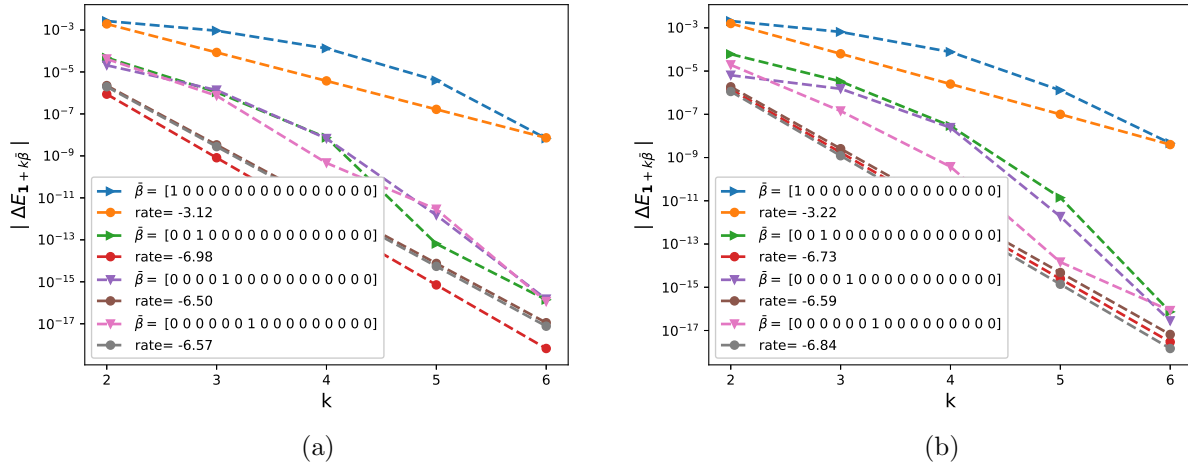


Figure 68: The rate of convergence of first order differences $|\Delta E_\beta|$ ($\beta = \mathbf{1} + k\bar{\beta}$) for $K = 1$: a) $H = 0.43$ b) $H = 0.07$

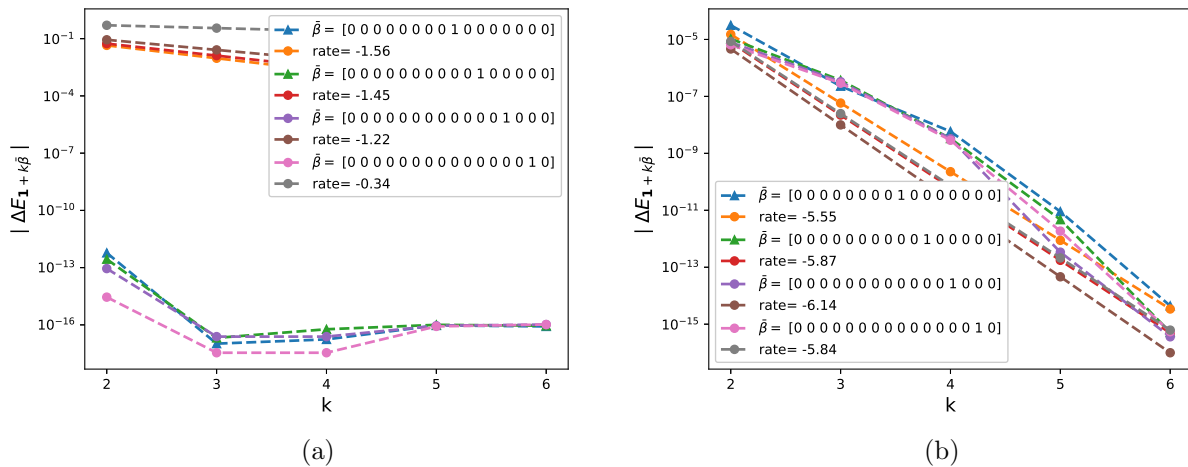


Figure 69: The rate of convergence of first order differences $|\Delta E_\beta|$ ($\beta = \mathbf{1} + k\bar{\beta}$) for $K = 1$: a) $H = 0.43$ b) $H = 0.07$

C.3.3 Non Hierarchical

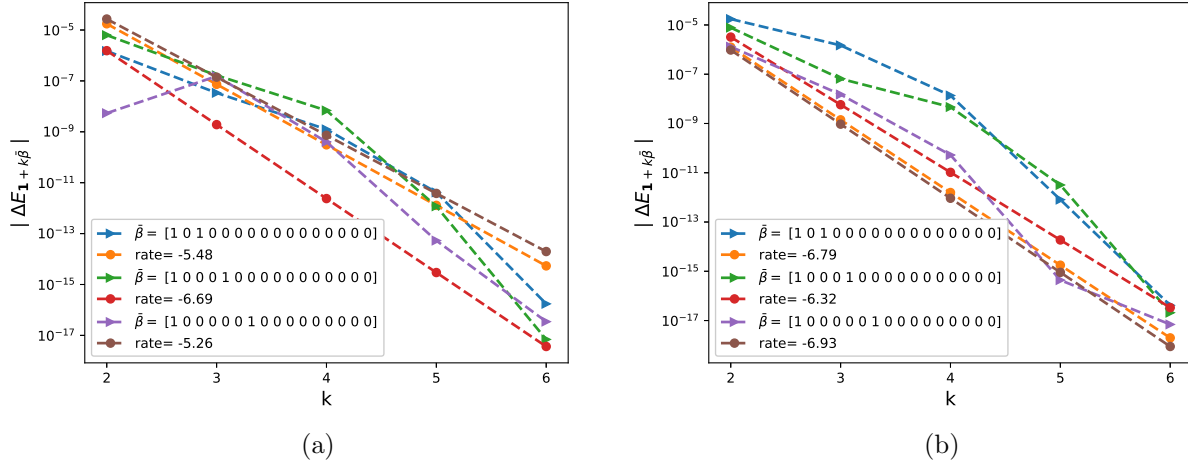


Figure 70: The rate of convergence of mixed order differences $|\Delta E_\beta|$ ($\beta = \mathbf{1} + k\bar{\beta}$) for $K = 1$: a) $H = 0.43$ b) $H = 0.07$

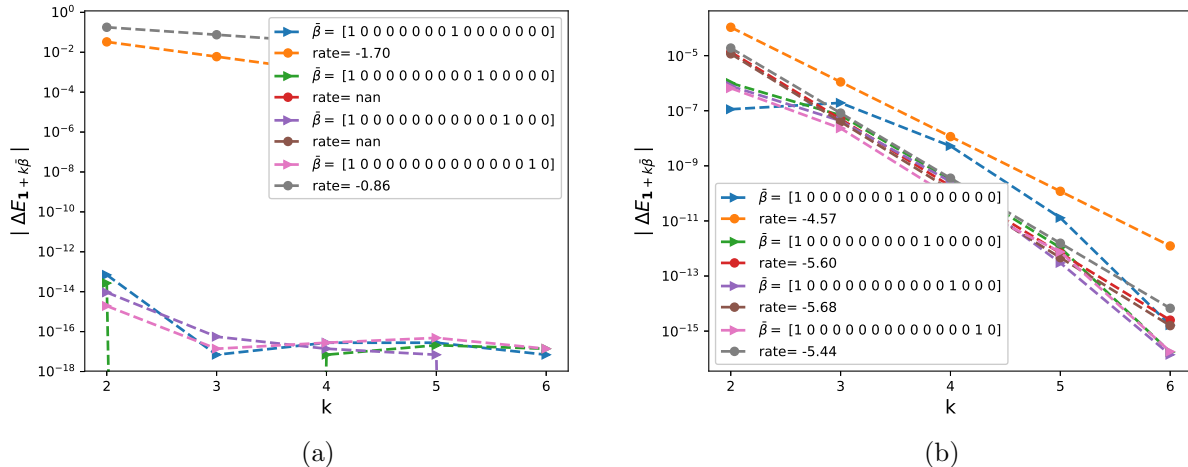


Figure 71: The rate of convergence of mixed order differences $|\Delta E_\beta|$ ($\beta = \mathbf{1} + k\bar{\beta}$) for $K = 1$: a) $H = 0.43$ b) $H = 0.07$

C.4 Investigating mixed differences wrt ρ

N=4, K=1

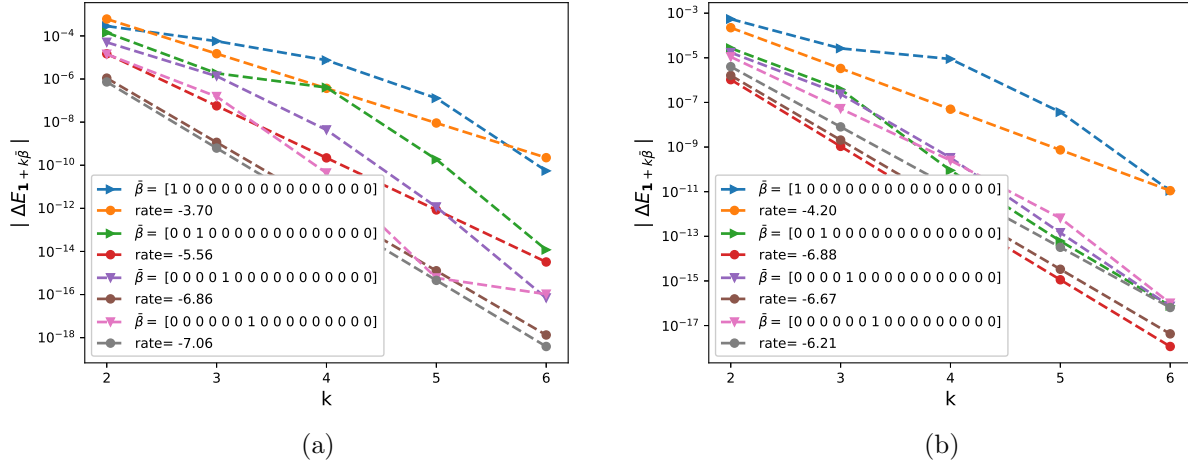


Figure 72: The rate of convergence of first order differences $|\Delta E_\beta|$ ($\beta = \mathbf{1} + k\bar{\beta}$) for $K = 1$: a) $H = 0.43$ b) $H = 0.07$

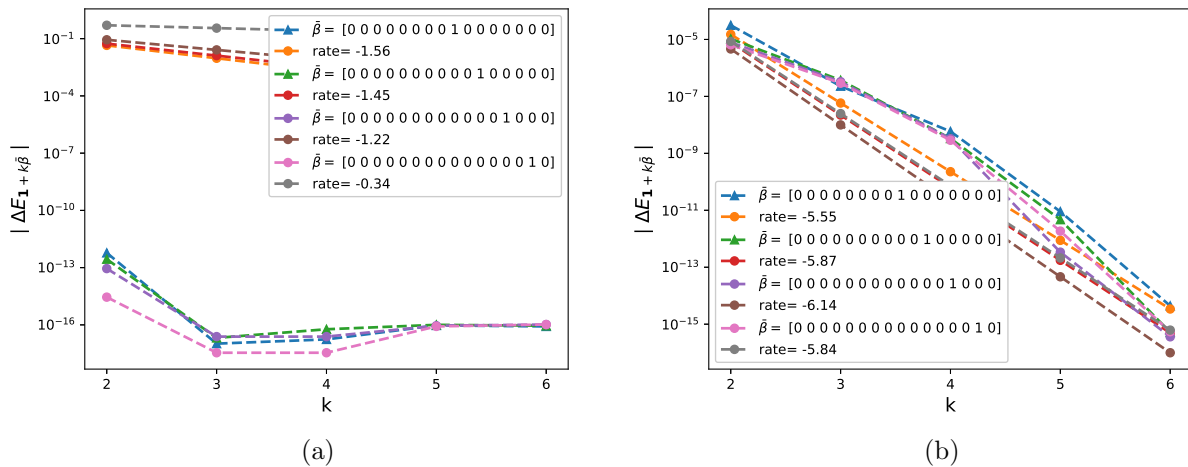


Figure 73: The rate of convergence of first order differences $|\Delta E_\beta|$ ($\beta = \mathbf{1} + k\bar{\beta}$) for $K = 1$: a) $H = 0.43$ b) $H = 0.07$

N=8, K=1

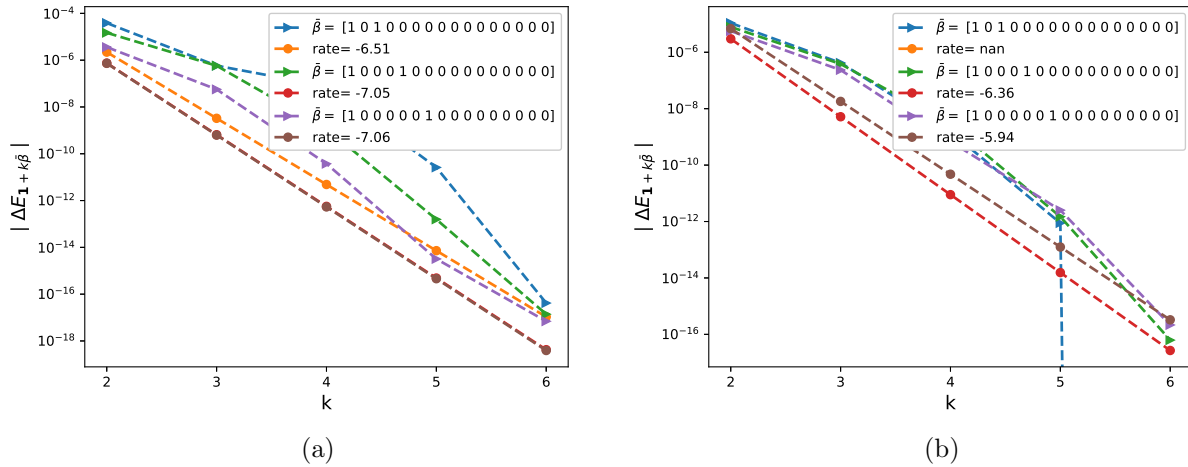


Figure 74: The rate of convergence of mixed order differences $|\Delta E_\beta|$ ($\beta = \mathbf{1} + k\bar{\beta}$) for $K = 1$: a) $H = 0.43$ b) $H = 0.07$

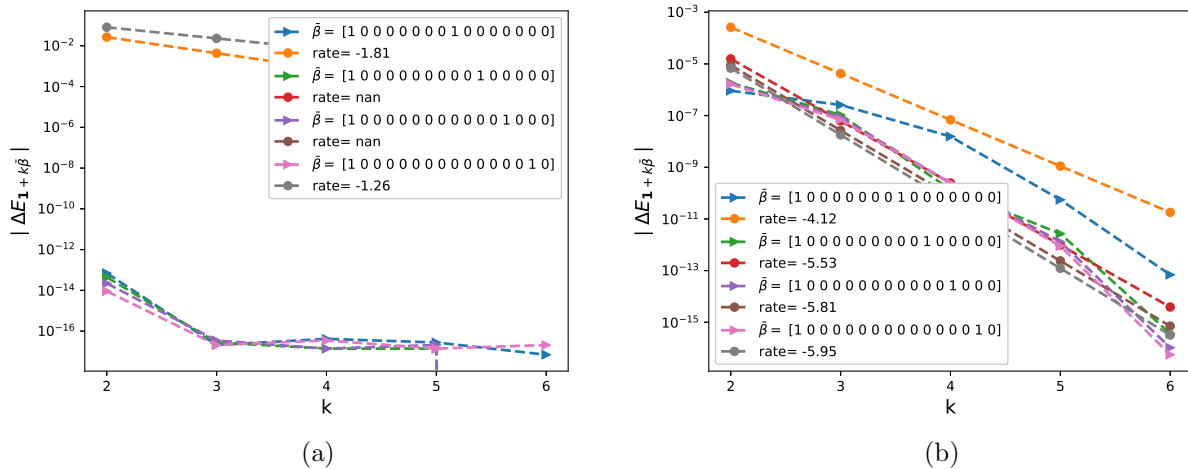


Figure 75: The rate of convergence of mixed order differences $|\Delta E_\beta|$ ($\beta = \mathbf{1} + k\bar{\beta}$) for $K = 1$: a) $H = 0.43$ b) $H = 0.07$

N=4, K=0.8

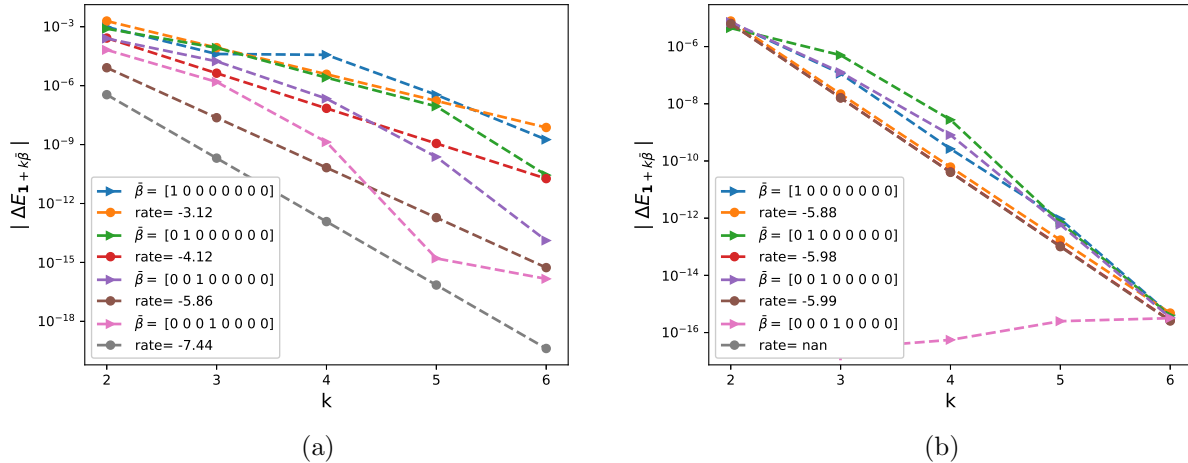


Figure 76: The rate of convergence of first order differences $|\Delta E_\beta|$ ($\beta = \mathbf{1} + k\bar{\beta}$) for $K = 1$: a) $\rho = -0.9$ b) $\rho = 0$.

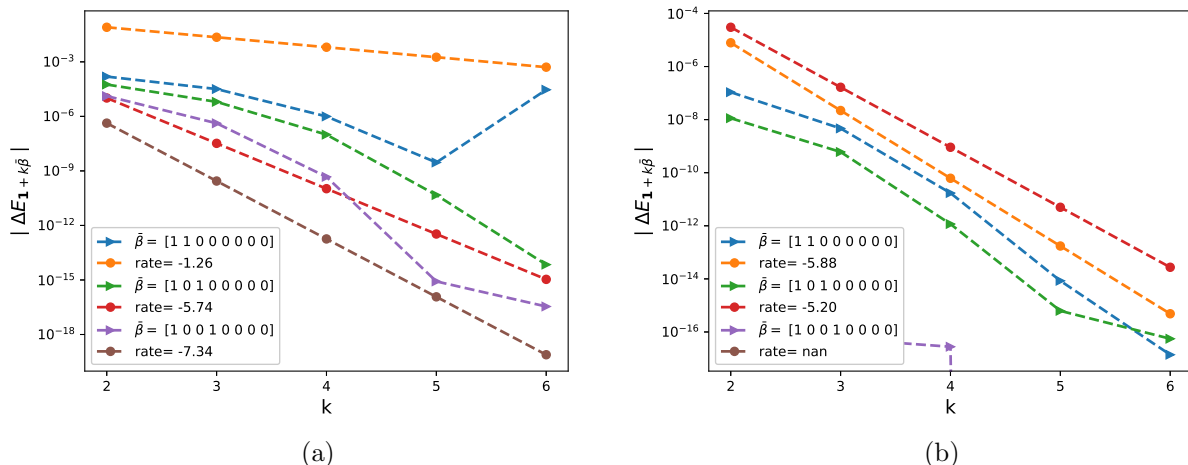


Figure 77: The rate of convergence of mixed order differences $|\Delta E_\beta|$ ($\beta = \mathbf{1} + k\bar{\beta}$): a) $\rho = -0.9$ b) $\rho = 0$.

N=8, K=0.8

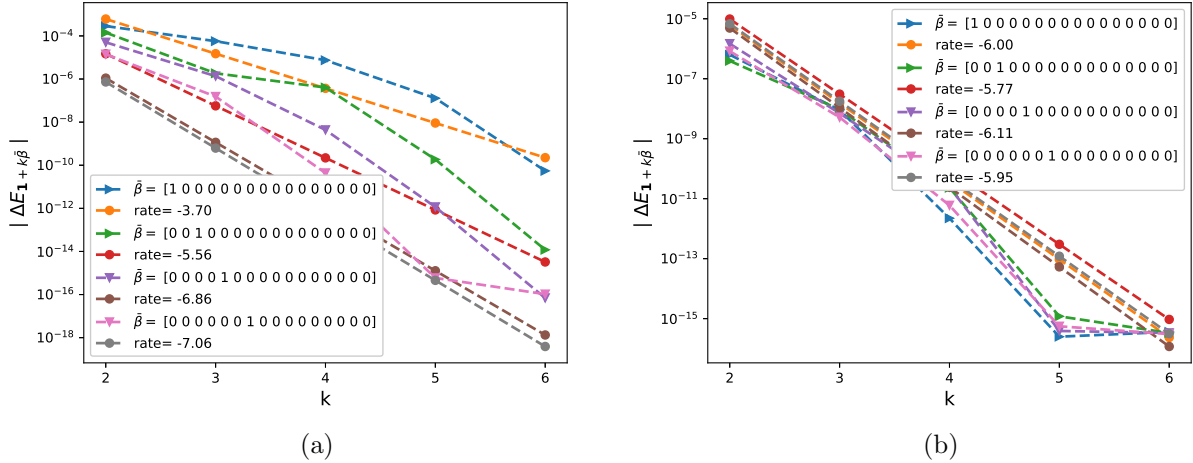


Figure 78: The rate of convergence of first order differences $|\Delta E_\beta|$ ($\beta = \mathbf{1} + k\bar{\beta}$): a) $\rho = -0.9$ b) $\rho = 0$.

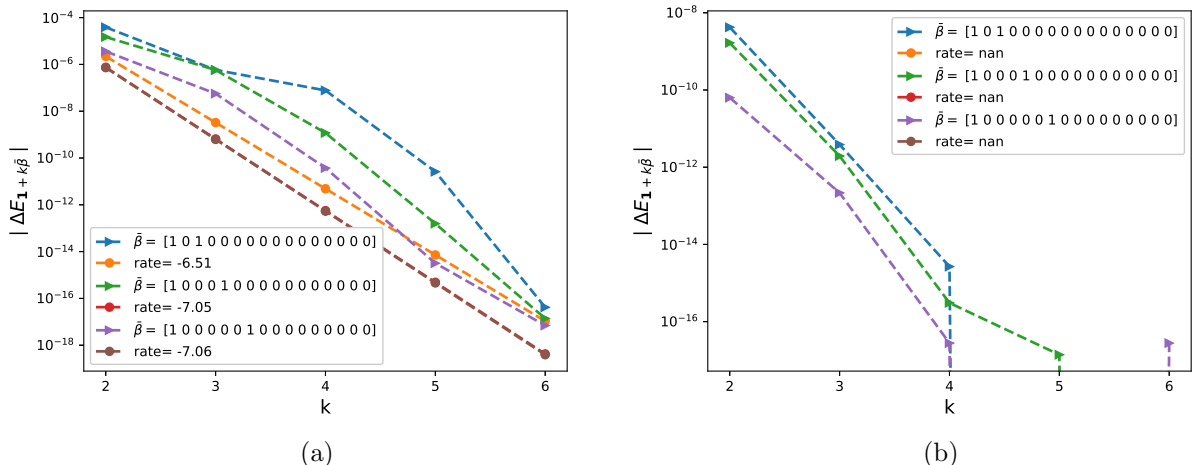


Figure 79: The rate of convergence of mixed order differences $|\Delta E_\beta|$ ($\beta = \mathbf{1} + k\bar{\beta}$): a) $\rho = -0.9$ b) $\rho = 0$.

C.5 Investigating mixed differences wrt ξ

N=4, K=1

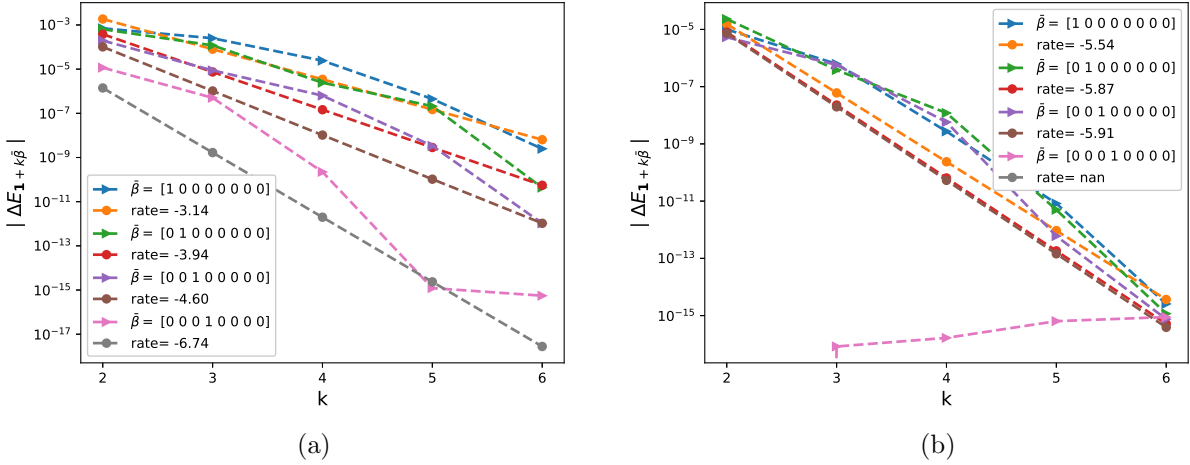


Figure 80: The rate of convergence of first order differences $|\Delta E_\beta|$ ($\beta = \mathbf{1} + k\bar{\beta}$): a) $\rho = -0.9$ b) $\rho = 0$.

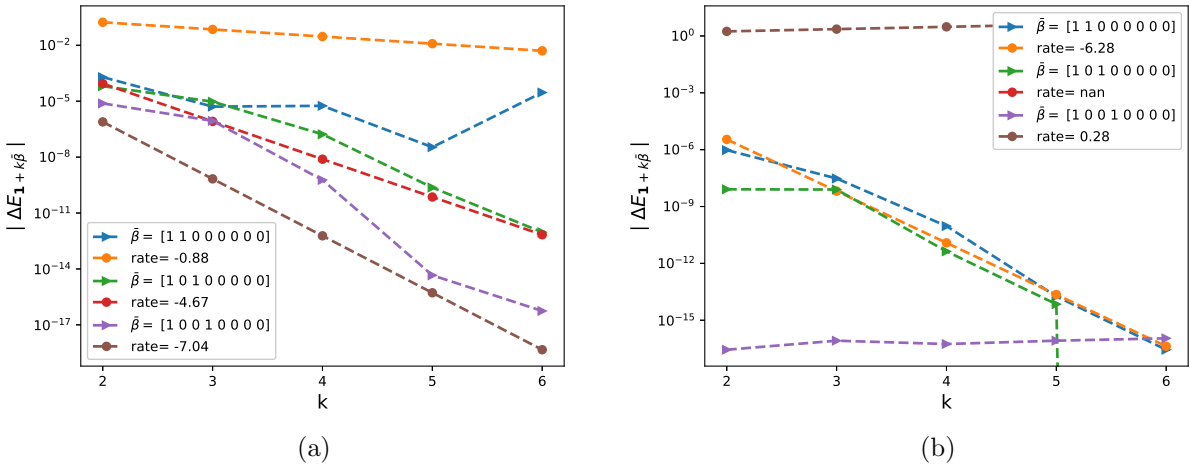


Figure 81: The rate of convergence of mixed order differences $|\Delta E_\beta|$ ($\beta = \mathbf{1} + k\bar{\beta}$): a) $\rho = -0.9$ b) $\rho = 0$.

N=8, K=1

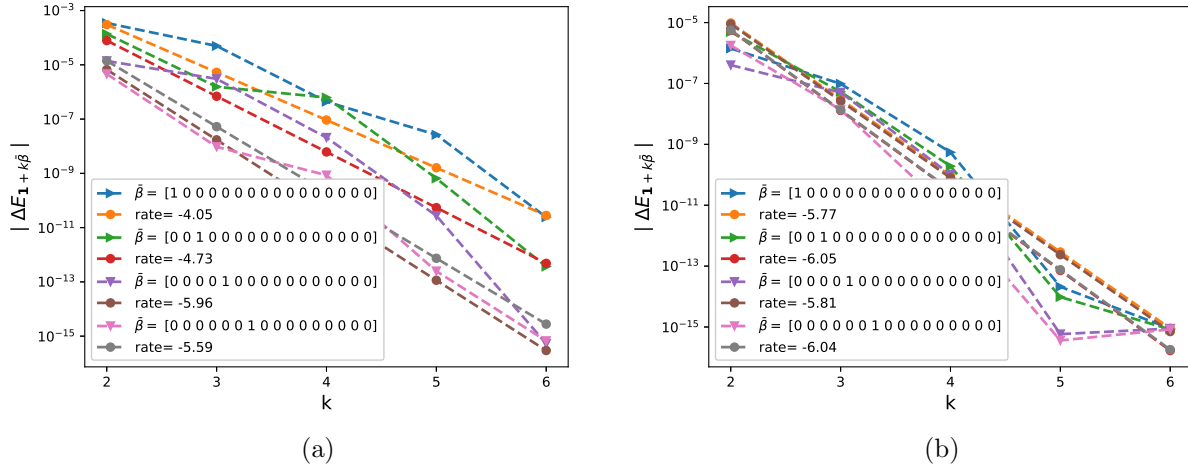


Figure 82: The rate of convergence of first order differences $|\Delta E_\beta|$ ($\beta = \mathbf{1} + k\bar{\beta}$): a) $\rho = -0.9$ b) $\rho = 0$.

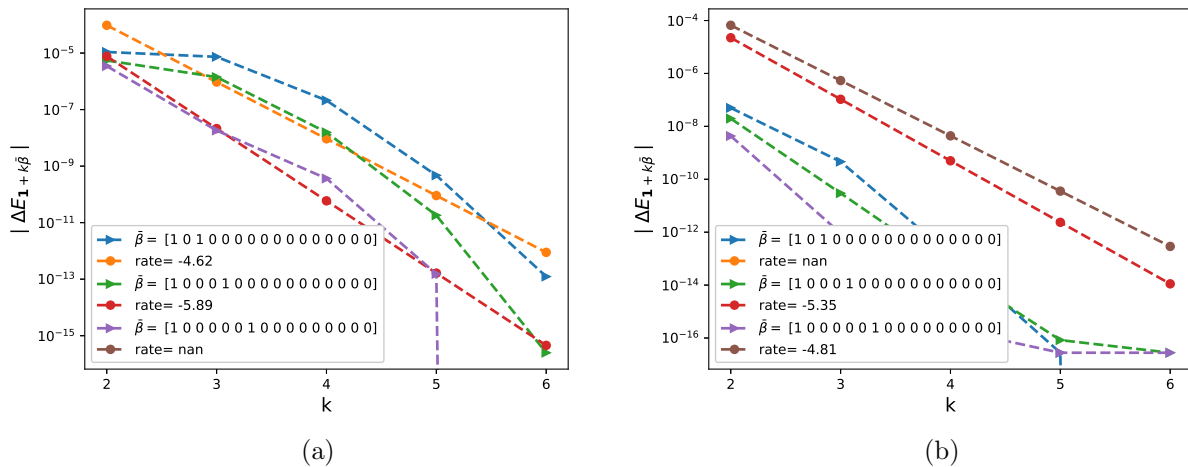


Figure 83: The rate of convergence of mixed order differences $|\Delta E_\beta|$ ($\beta = \mathbf{1} + k\bar{\beta}$): a) $\rho = -0.9$ b) $\rho = 0$.

N=4, K=0.8

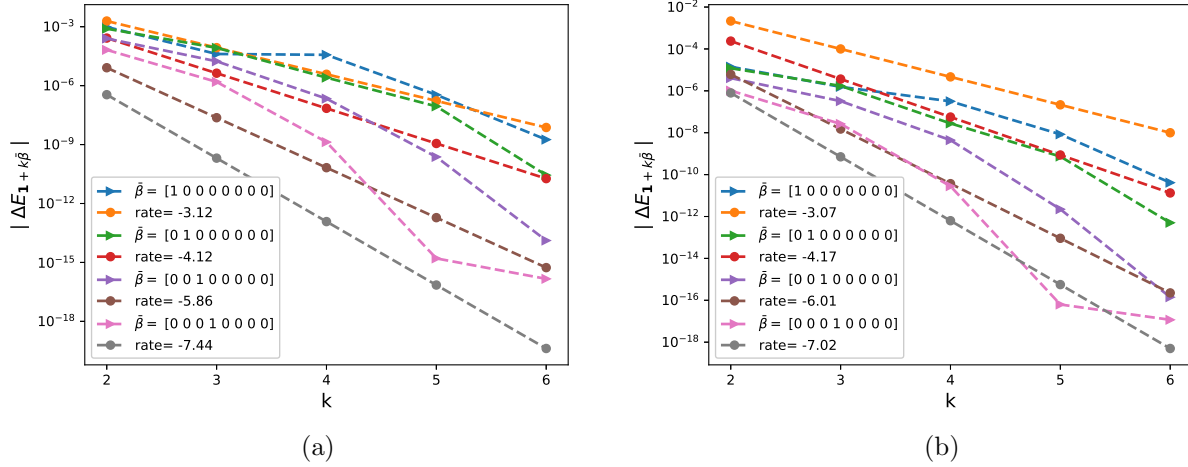


Figure 84: The rate of convergence of first order differences $|\Delta E_\beta|$ ($\beta = \mathbf{1} + k\bar{\beta}$): a) $\xi = 0.235^2$ b) $\xi = 10^{-5}$

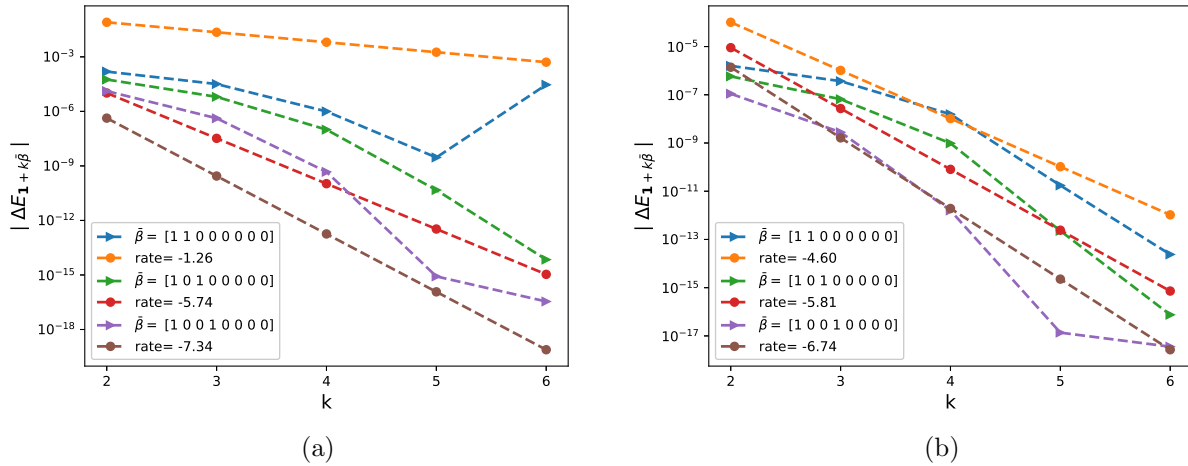


Figure 85: The rate of convergence of mixed order differences $|\Delta E_\beta|$ ($\beta = \mathbf{1} + k\bar{\beta}$): a) $\xi = 0.235^2$ b) $\xi = 10^{-5}$

N=8, K=0.8

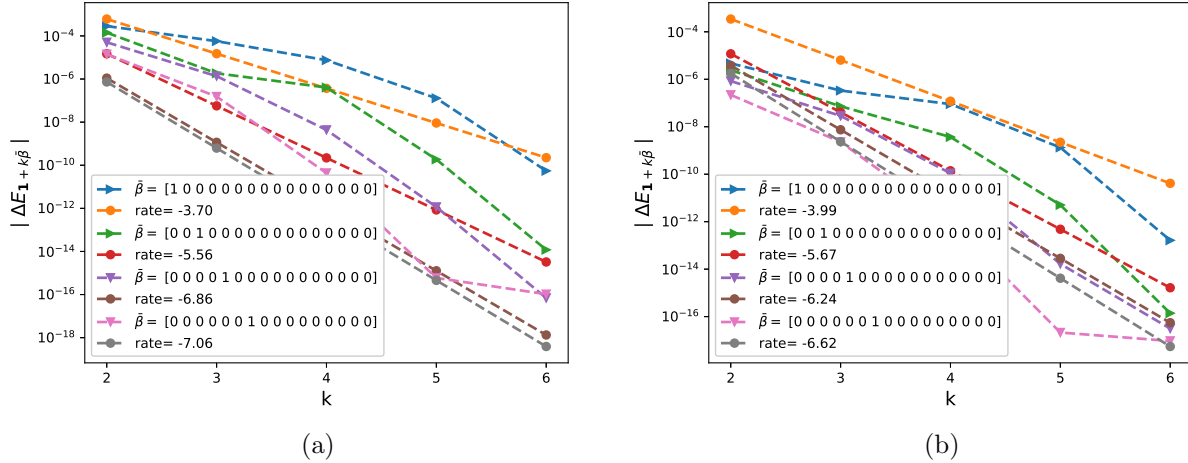


Figure 86: The rate of convergence of first order differences $|\Delta E_\beta|$ ($\beta = \mathbf{1} + k\bar{\beta}$): a) $\xi = 0.235^2$ b) $\xi = 10^{-5}$

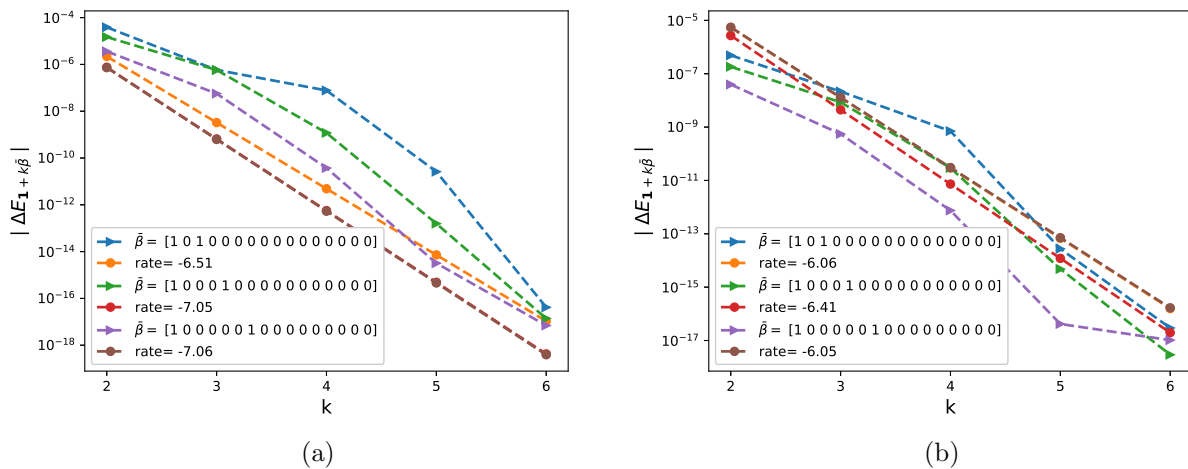


Figure 87: The rate of convergence of mixed order differences $|\Delta E_\beta|$ ($\beta = \mathbf{1} + k\bar{\beta}$): a) $\xi = 0.235^2$ b) $\xi = 10^{-5}$

C.6 Investigating mixed differences wrt moneyness K

Case $H = 0.43$

$N = 8$

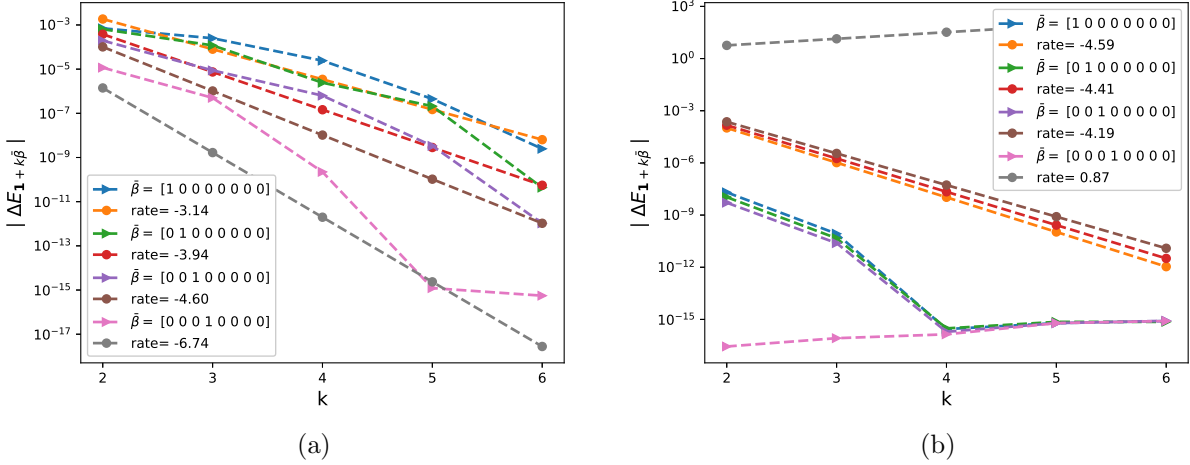


Figure 88: The rate of convergence of first order differences $|\Delta E_\beta|$ ($\beta = \mathbf{1} + k\bar{\beta}$): a) $\xi = 0.235^2$ b) $\xi = 10^{-5}$

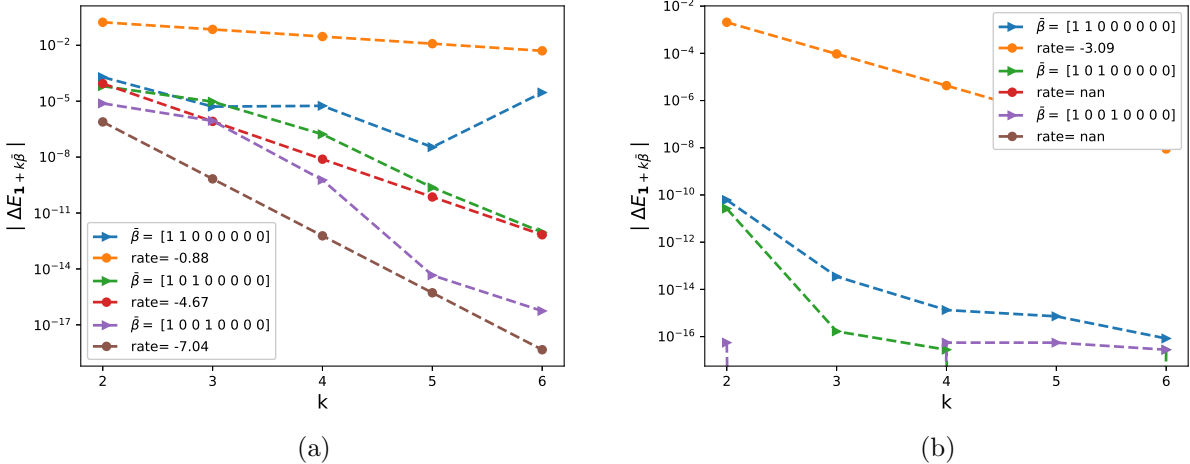


Figure 89: The rate of convergence of mixed order differences $|\Delta E_\beta|$ ($\beta = \mathbf{1} + k\bar{\beta}$): a) $\xi = 0.235^2$ b) $\xi = 10^{-5}$

$N = 16$

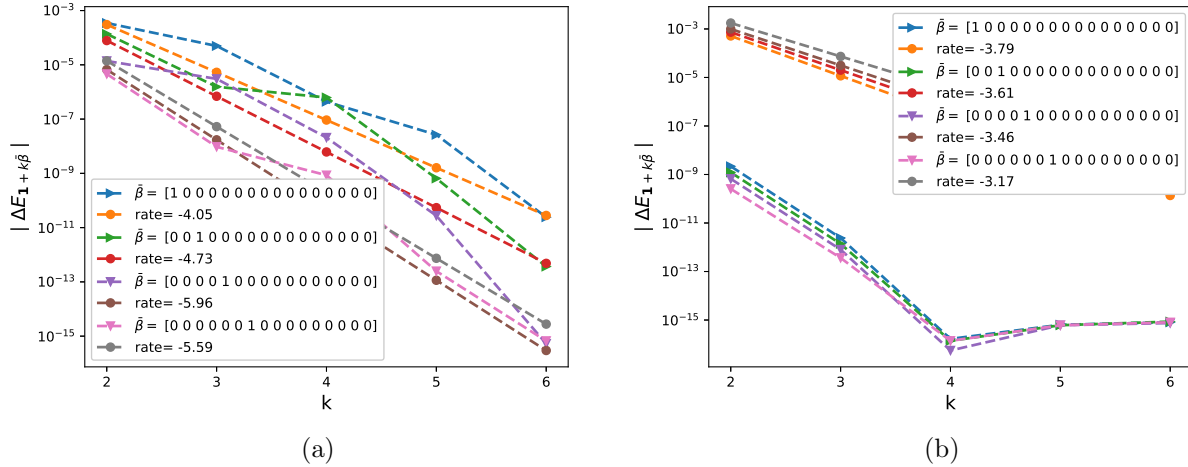


Figure 90: The rate of convergence of first order differences $|\Delta E_\beta|$ ($\beta = \mathbf{1} + k\bar{\beta}$): a) $\xi = 0.235^2$ b) $\xi = 10^{-5}$

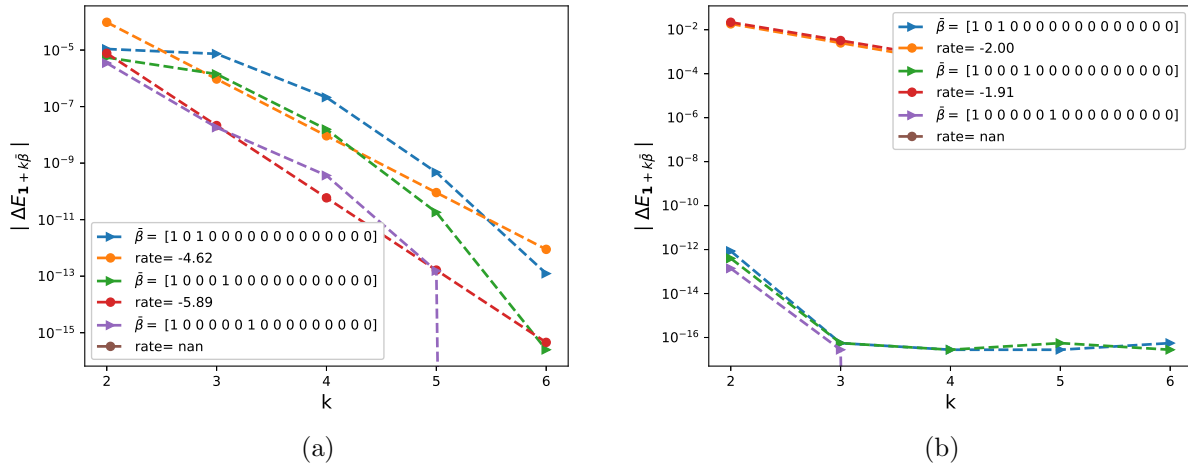


Figure 91: The rate of convergence of mixed order differences $|\Delta E_\beta|$ ($\beta = \mathbf{1} + k\bar{\beta}$): a) $\xi = 0.235^2$ b) $\xi = 10^{-5}$

Case $H = 0.07$

$N = 8$

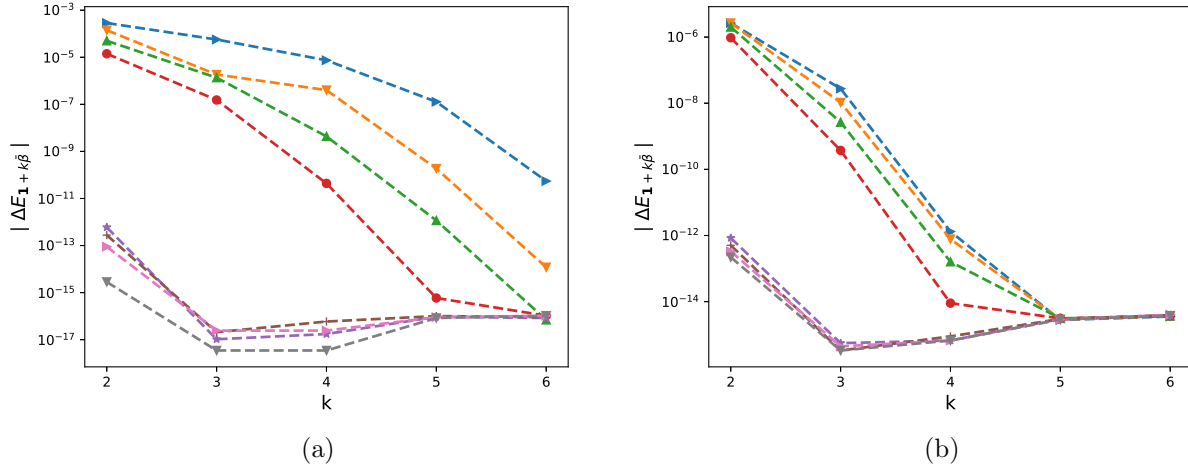


Figure 92: The rate of convergence of first order differences $|\Delta E_\beta|$ ($\beta = \mathbf{1} + k\bar{\beta}$): a) $K = 1$ b) $K = \exp(-4)$.

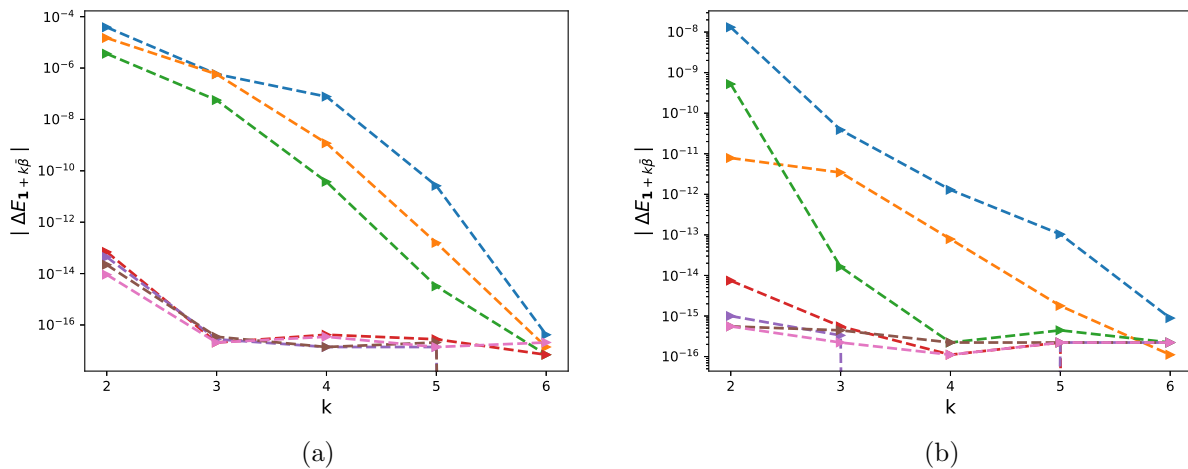


Figure 93: The rate of convergence of second order differences $|\Delta E_\beta|$ ($\beta = \mathbf{1} + k\bar{\beta}$): a) $K = 1$ b) $K = \exp(-4)$.

$N = 16$

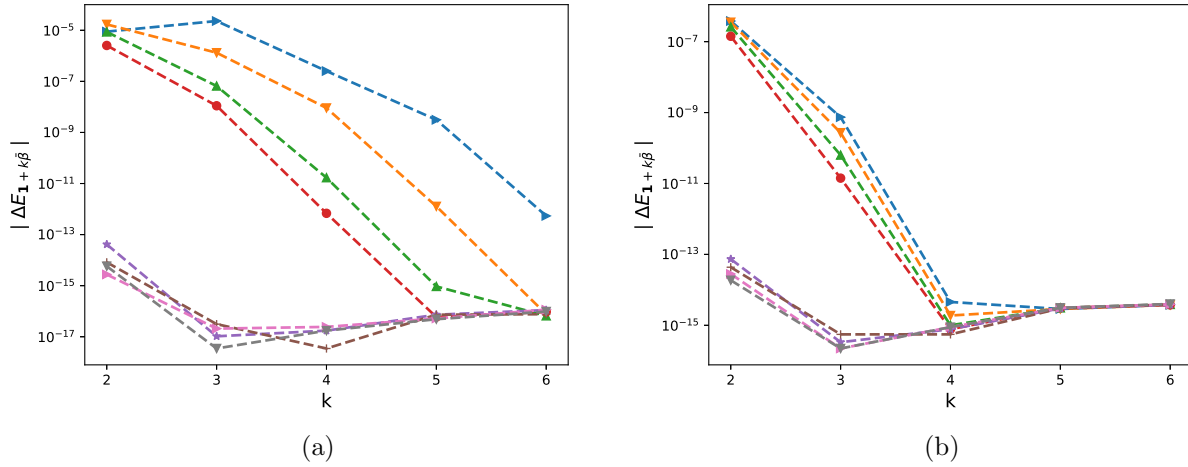


Figure 94: The rate of convergence of first order differences $|\Delta E_\beta|$ ($\beta = \mathbf{1} + k\bar{\beta}$): a) $K = 1$ b) $K = \exp(-4)$.

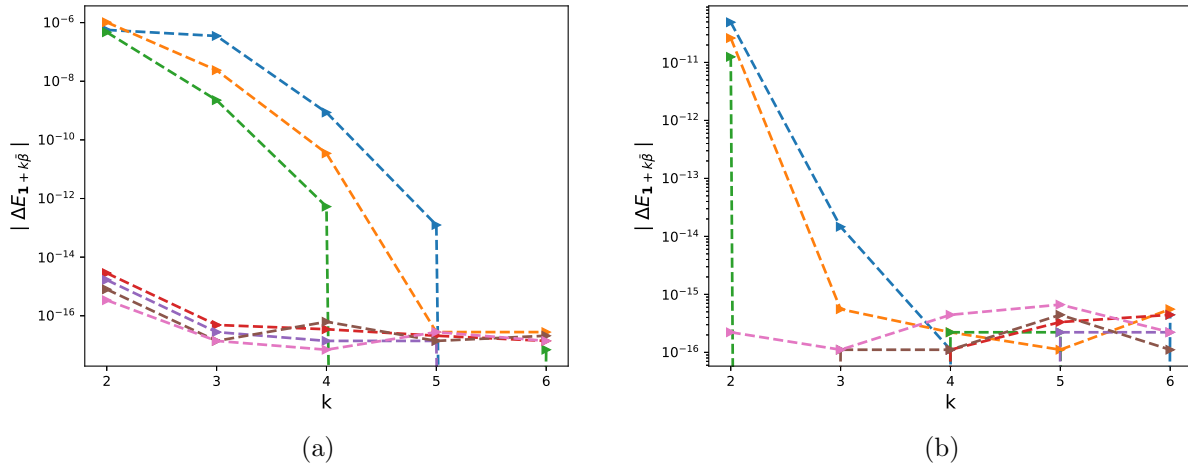


Figure 95: The rate of convergence of second order differences $|\Delta E_\beta|$ ($\beta = \mathbf{1} + k\bar{\beta}$): a) $K = 1$ b) $K = \exp(-4)$.

C.7 Convergence plots using MISC ($H = 0.43$)

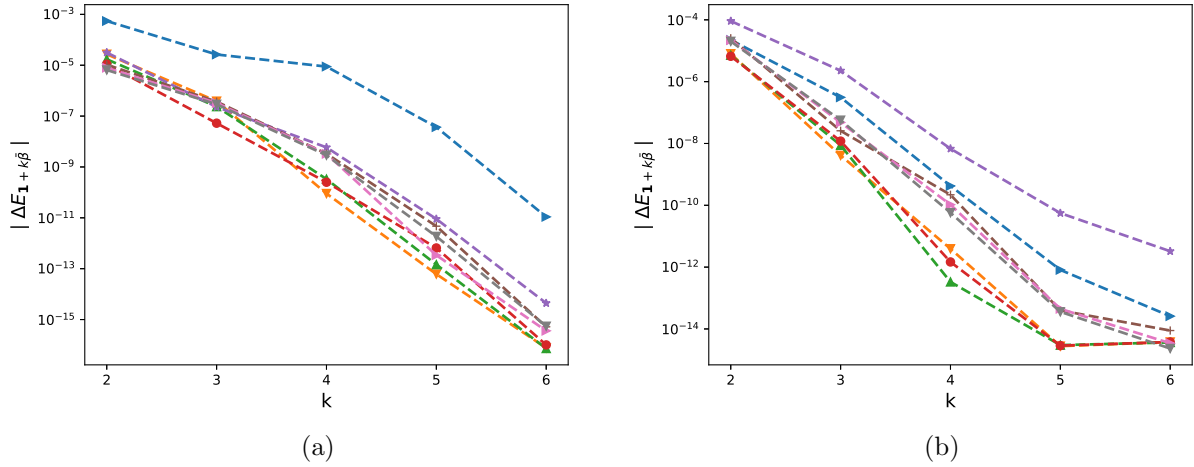


Figure 96: The rate of convergence of first order differences $|\Delta E_\beta|$ ($\beta = \mathbf{1} + k\bar{\beta}$): a) $K = 1$ b) $K = \exp(-4)$.

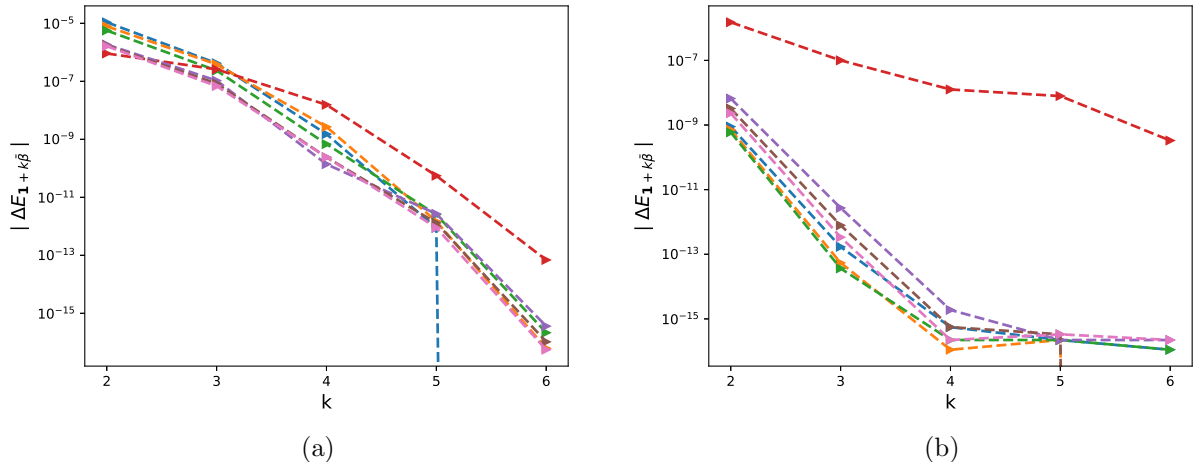


Figure 97: The rate of convergence of second order differences $|\Delta E_\beta|$ ($\beta = \mathbf{1} + k\bar{\beta}$): a) $K = 1$ b) $K = \exp(-4)$.

Case of 2 time steps, $K = e^{-4}$

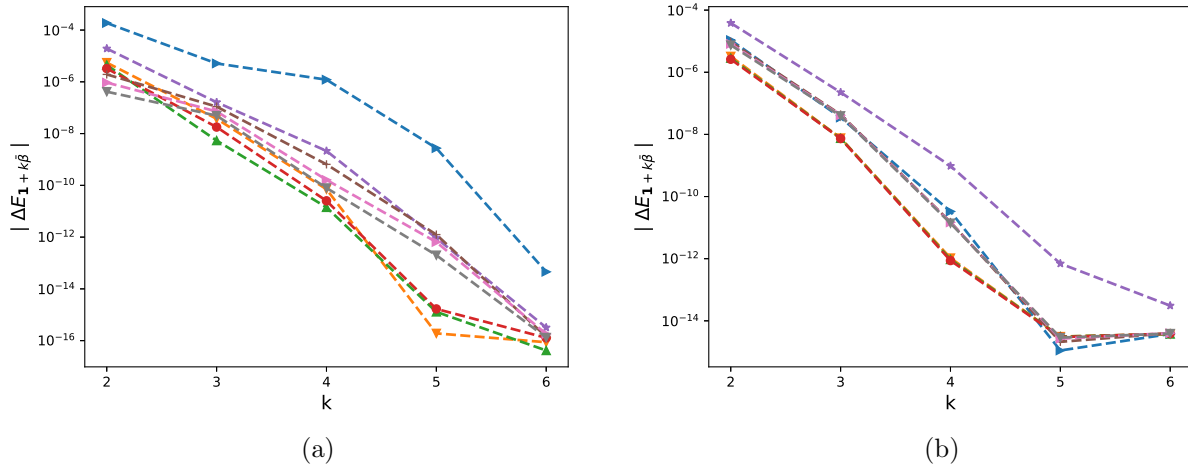


Figure 98: The rate of convergence of first order differences $|\Delta E_\beta|$ ($\beta = \mathbf{1} + k\bar{\beta}$): a) $K = 1$ b) $K = \exp(-4)$.

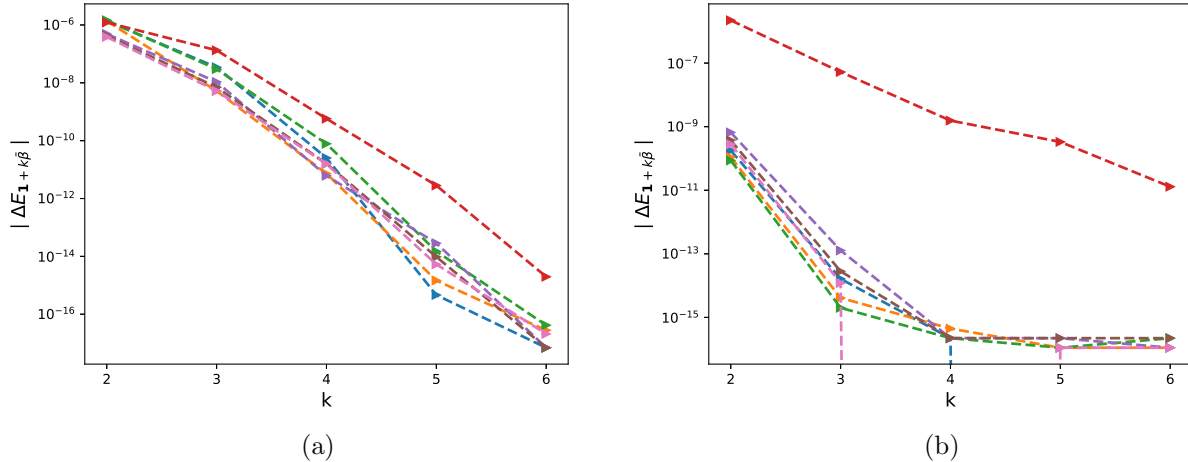
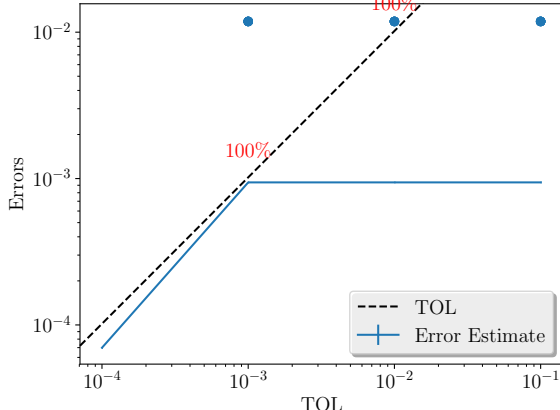
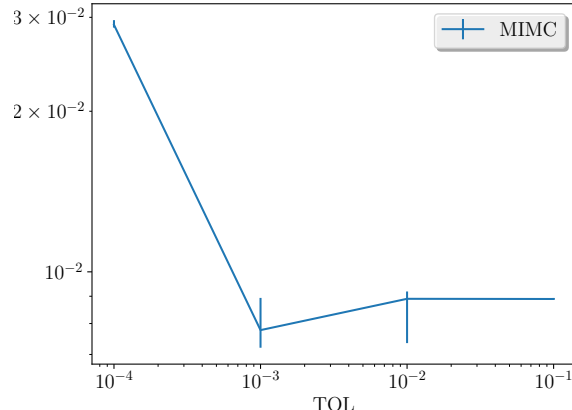


Figure 99: The rate of convergence of second order differences $|\Delta E_\beta|$ ($\beta = \mathbf{1} + k\bar{\beta}$): a) $K = 1$ b) $K = \exp(-4)$.

Case of 2 time steps, $K = 1.2$

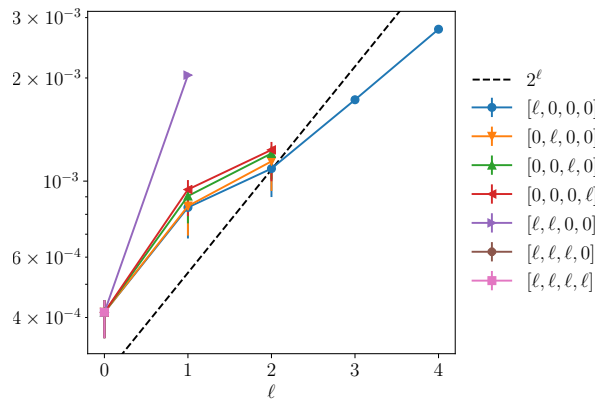


(a) Error estimate

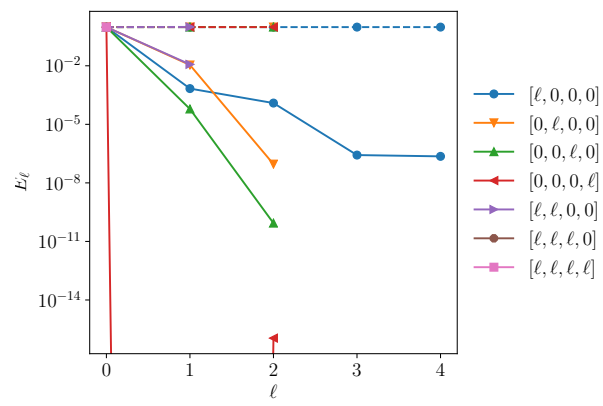


(b) Average running time as a function of TOL

Figure 100: Convergence and complexity results for the call payoff with rBergomi model.



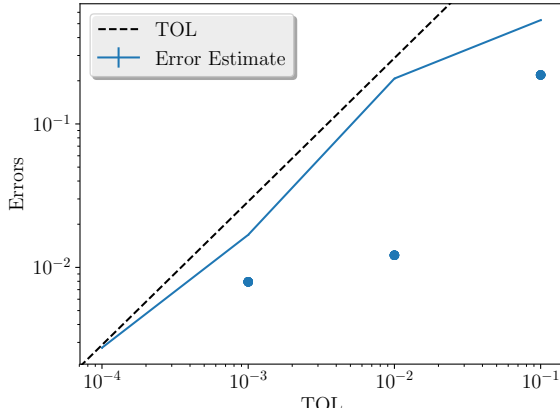
(a) Average Computational time per level



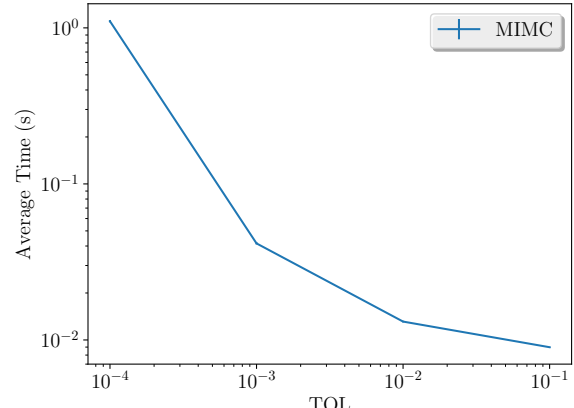
(b) The convergence rate of mixed differences per level

Figure 101: Convergence and work rates for discretization levels the call payoff with rBergomi model.

Case of 4 time steps, $K = e^{-4}$

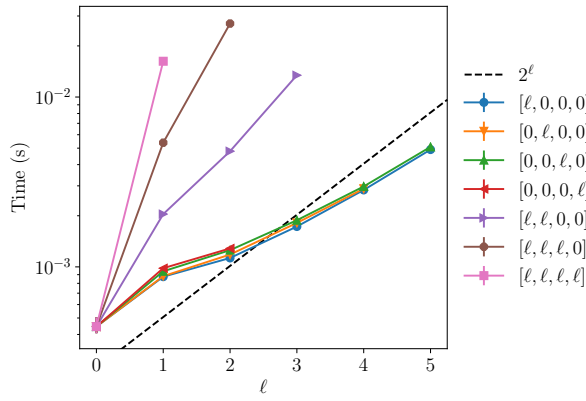


(a) Error estimate

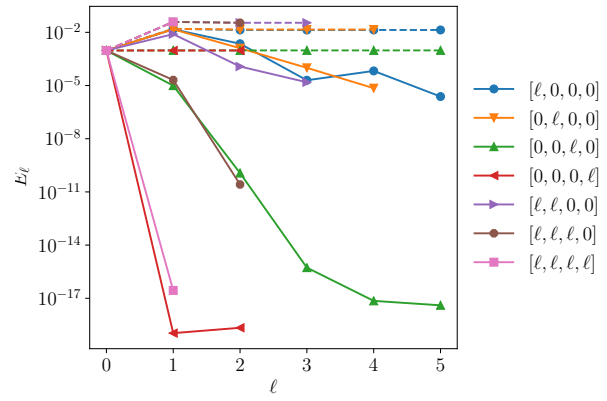


(b) Average running time as a function of TOL

Figure 102: Convergence and complexity results for the call payoff with rBergomi model.



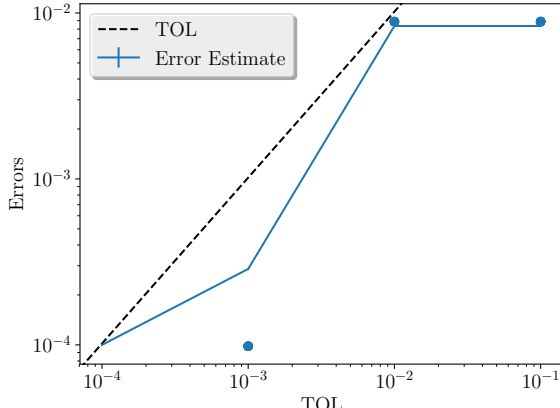
(a) Average Computational time per level



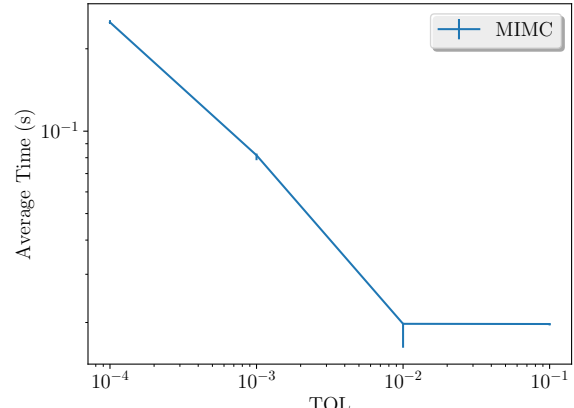
(b) The convergence rate of mixed differences per level

Figure 103: Convergence and work rates for discretization levels the call payoff with rBergomi model.

Case of 4 time steps, $K = 1.2$

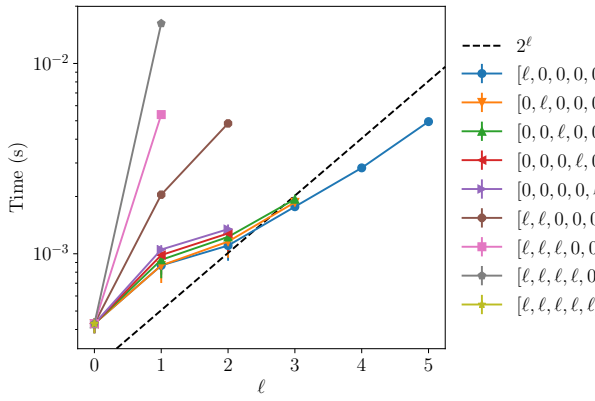


(a) Error estimate

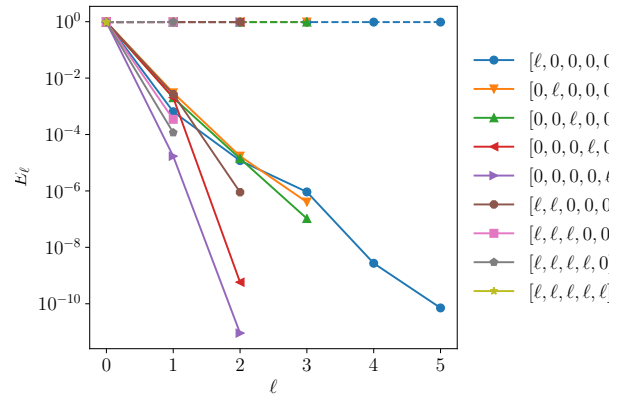


(b) Average running time as a function of TOL

Figure 104: Convergence and complexity results for the call payoff with rBergomi model.



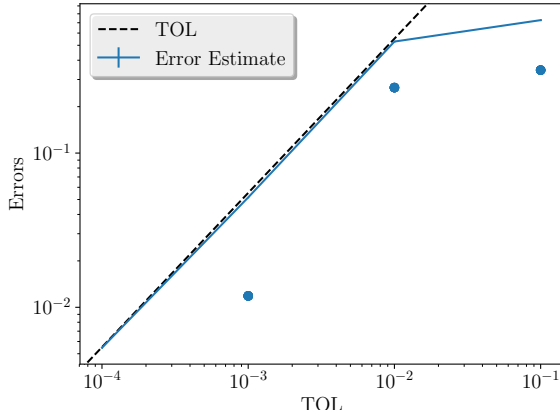
(a) Average Computational time per level



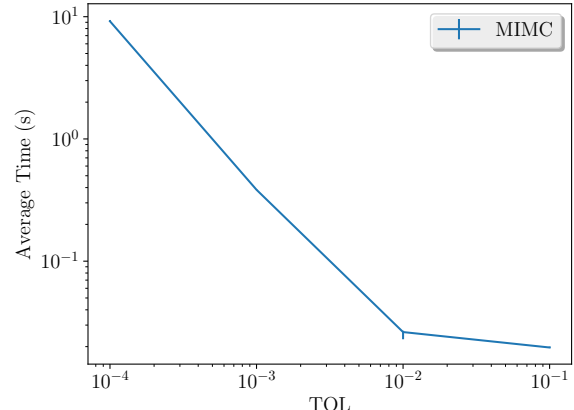
(b) The convergence rate of mixed differences per level

Figure 105: Convergence and work rates for discretization levels the call payoff with rBergomi model.

Case of 8 time steps, $K = e^{-4}$

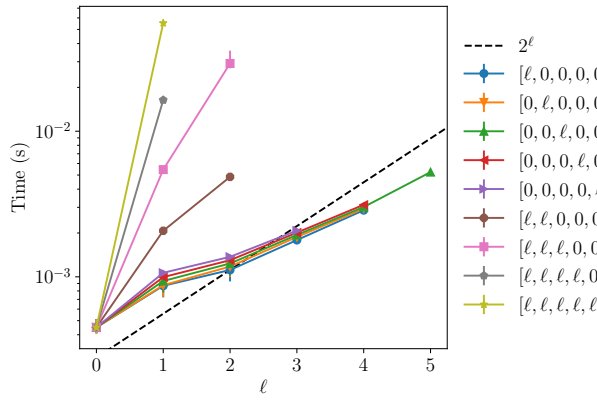


(a) Error estimate

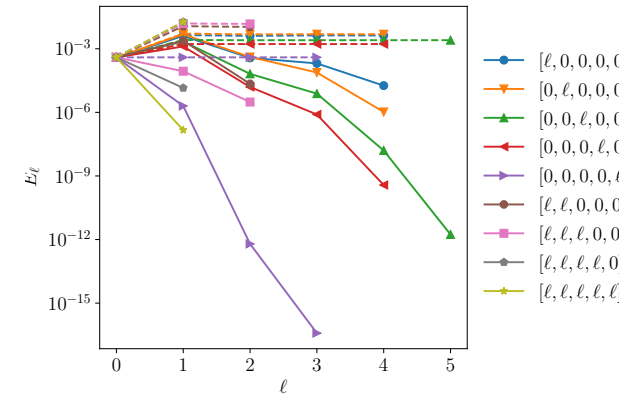


(b) Average running time as a function of TOL

Figure 106: Convergence and complexity results for the call payoff with rBergomi model.



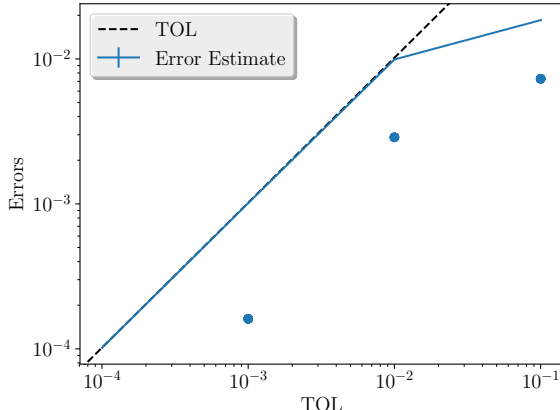
(a) Average Computational time per level



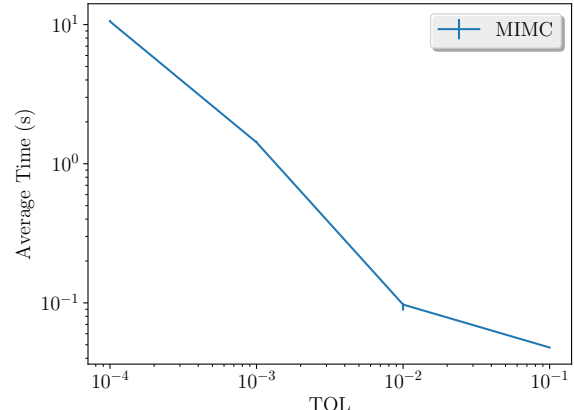
(b) The convergence rate of mixed differences per level

Figure 107: Convergence and work rates for discretization levels the call payoff with rBergomi model.

Case of 8 time steps, $K = 1.2$

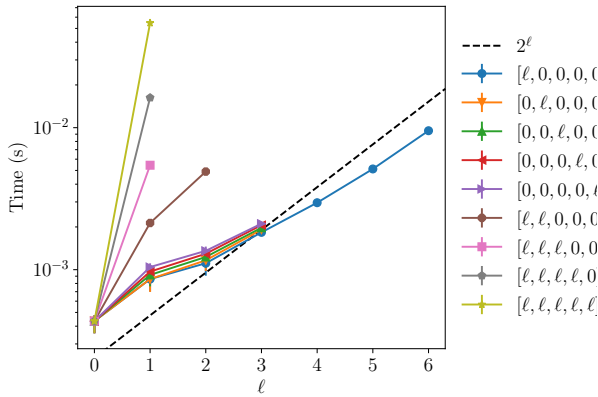


(a) Error estimate

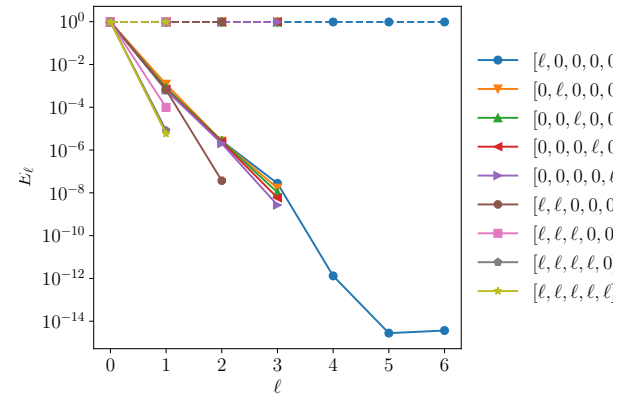


(b) Average running time as a function of TOL

Figure 108: Convergence and complexity results for the call payoff with rBergomi model.



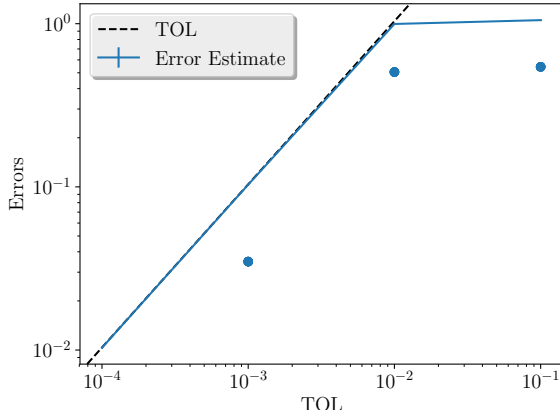
(a) Average Computational time per level



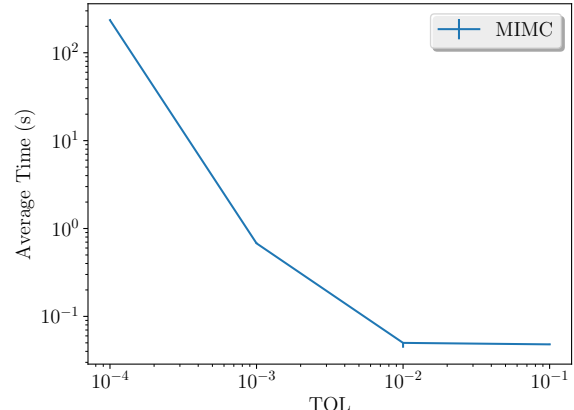
(b) The convergence rate of mixed differences per level

Figure 109: Convergence and work rates for discretization levels the call payoff with rBergomi model.

Case of 16 time steps, $K = e^{-4}$

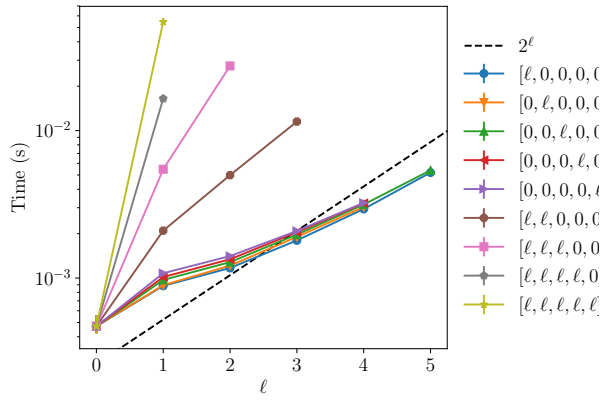


(a) Error estimate

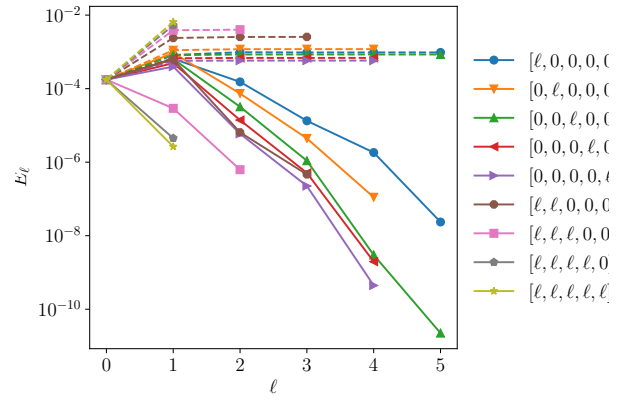


(b) Average running time as a function of TOL

Figure 110: Convergence and complexity results for the call payoff with rBergomi model.



(a) Average Computational time per level



(b) The convergence rate of mixed differences per level

Figure 111: Convergence and work rates for discretization levels the call payoff with rBergomi model.

Case of 16 time steps, $K = 1.2$

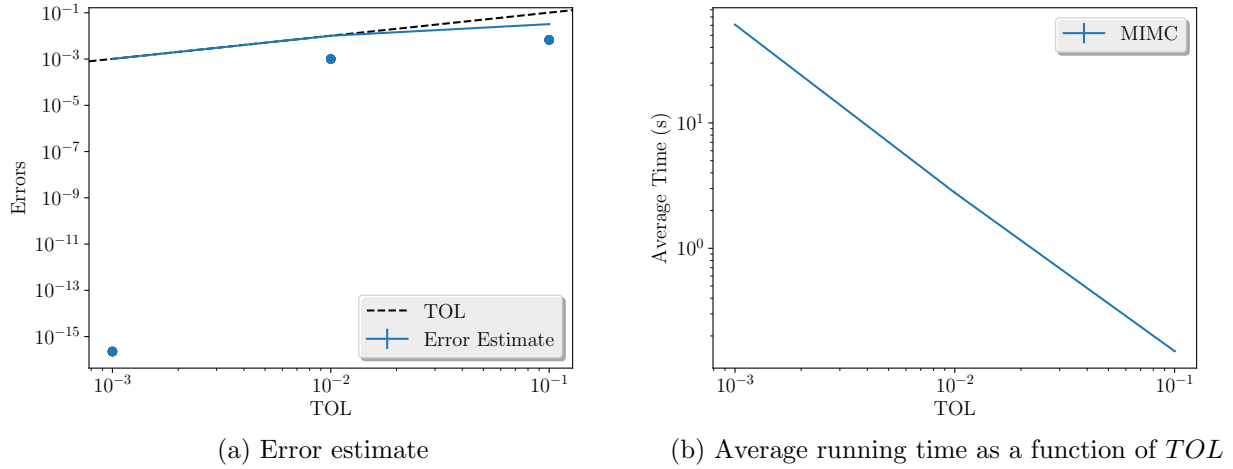


Figure 112: Convergence and complexity results for the call payoff with rBergomi model.

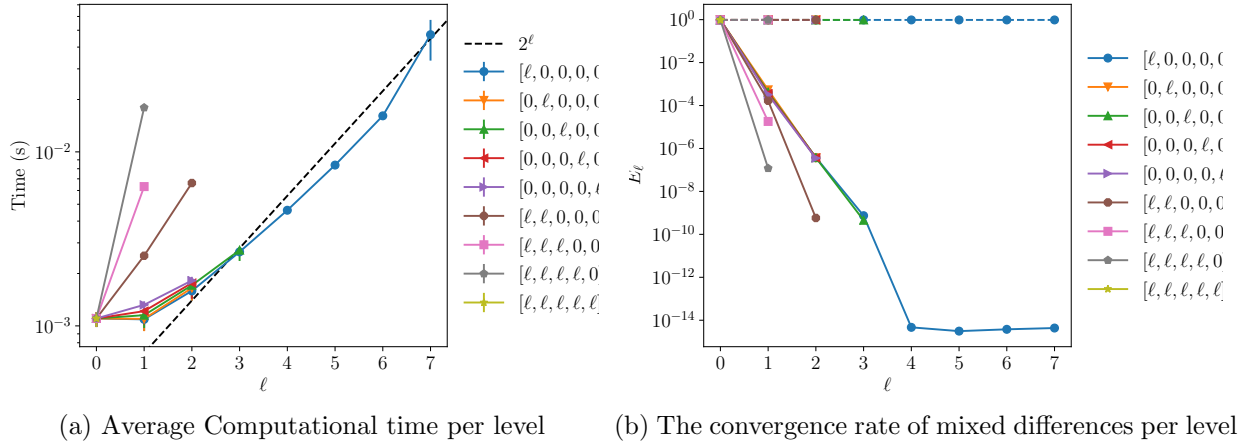
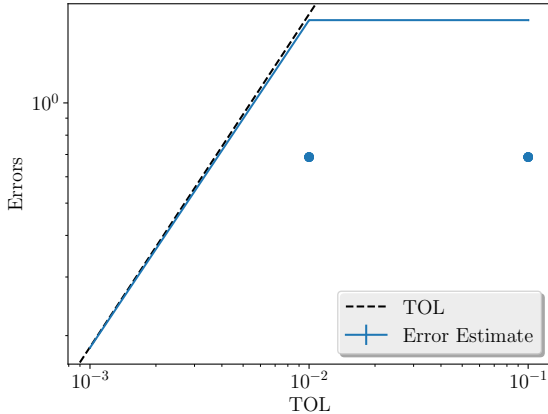


Figure 113: Convergence and work rates for discretization levels the call payoff with rBergomi model.

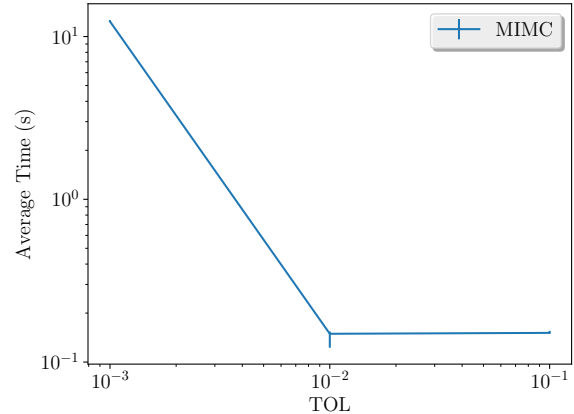
C.8 MISCE plots

C.9 Non Hierarchical

H=0.43

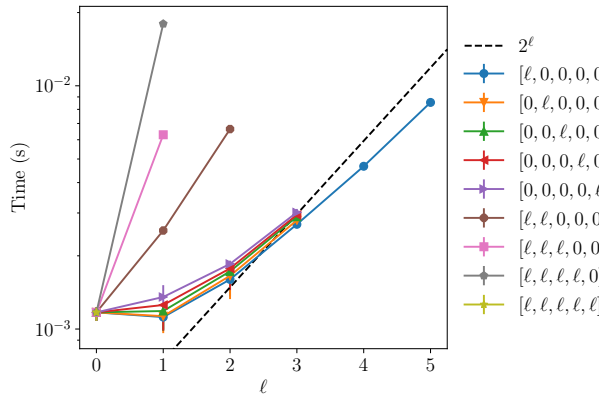


(a) Error estimate

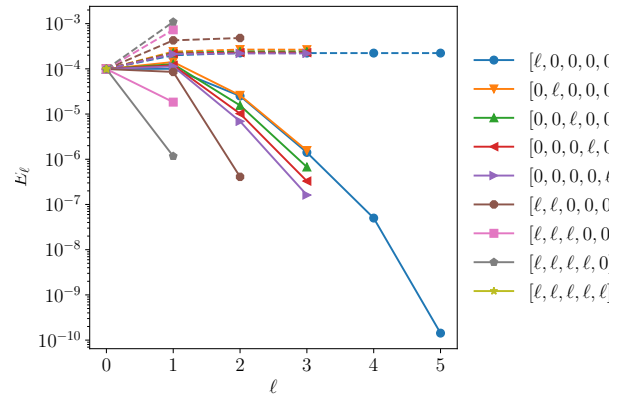


(b) Average running time as a function of TOL

Figure 114: Convergence and complexity results for the call payoff with rBergomi model.



(a) Average Computational time per level



(b) The convergence rate of mixed differences per level

Figure 115: Convergence and work rates for discretization levels the call payoff with rBergomi model.

Case of 8 time steps

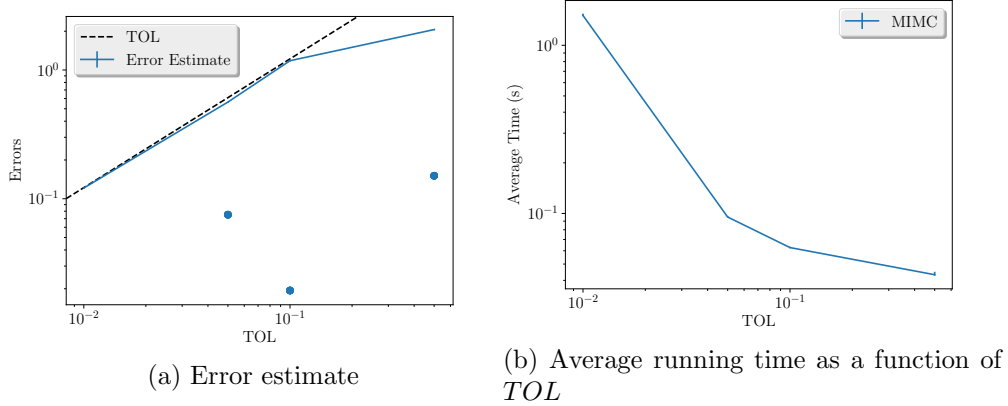


Figure 116: Convergence and complexity results for the call payoff with rBergomi model for $K = 1$, $H = 0.43$ and $N = 8$.

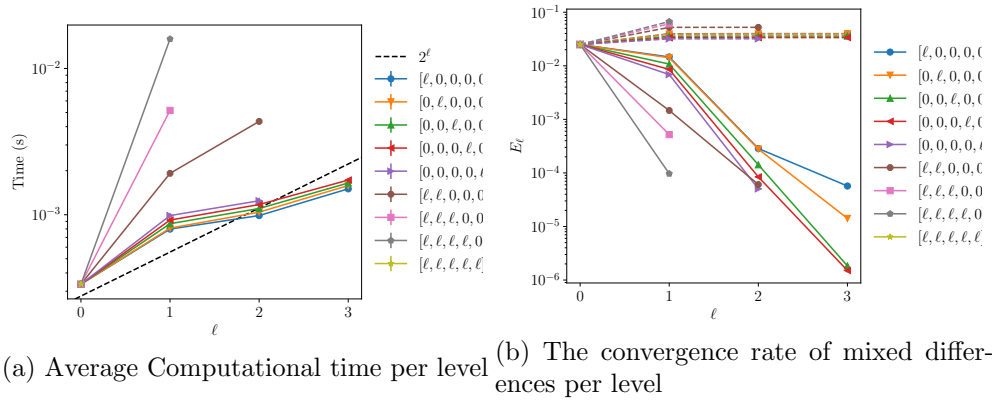


Figure 117: Convergence and work rates for discretization levels the call payoff with rBergomi model for $K = 1$, $H = 0.43$ and $N = 8$.

Case of 16 time steps

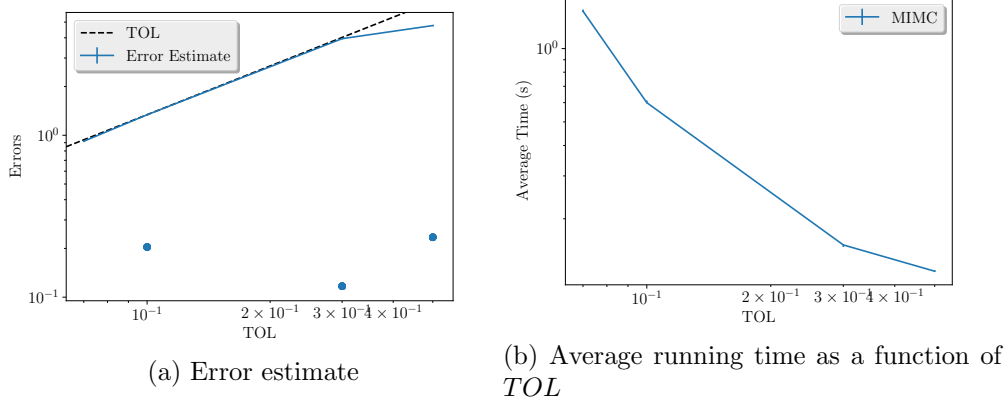


Figure 118: Convergence and complexity results for the call payoff with rBergomi model for $K = 1$, $H = 0.43$ and $N = 16$.

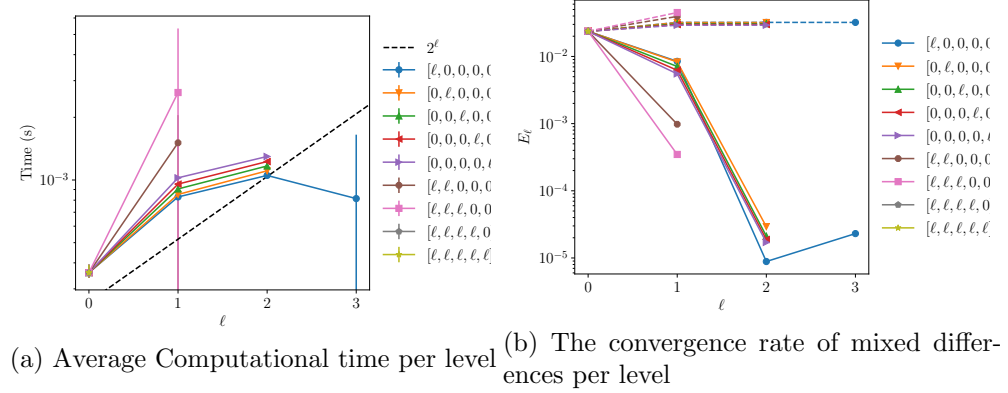


Figure 119: Convergence and work rates for discretization levels the call payoff with rBergomi model for $K = 1$, $H = 0.43$ and $N = 16$.

H=0.07

Case of 8 time steps

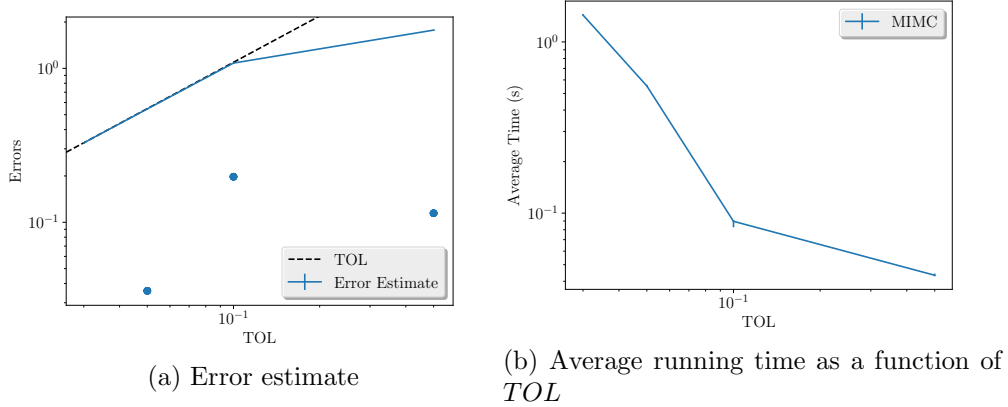


Figure 120: Convergence and complexity results for the call payoff with rBergomi model for $K = 1$, $H = 0.07$ and $N = 8$.

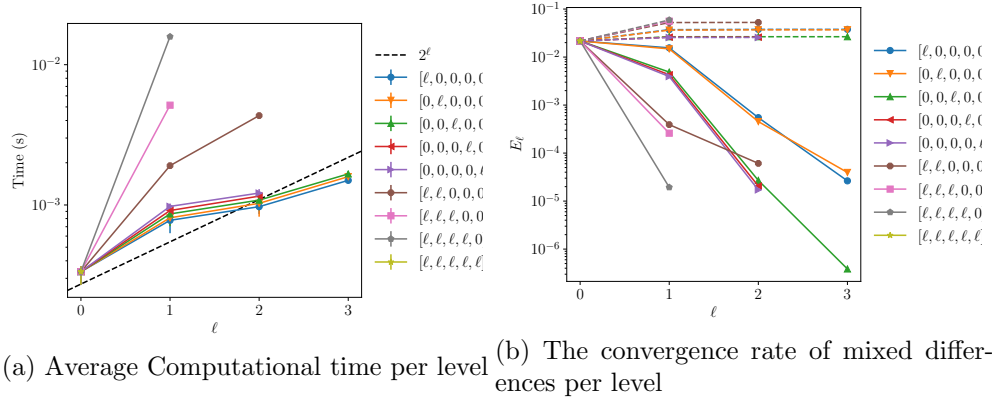


Figure 121: Convergence and work rates for discretization levels the call payoff with rBergomi model for $K = 1$, $H = 0.07$ and $N = 8$.

Case of 16 time steps

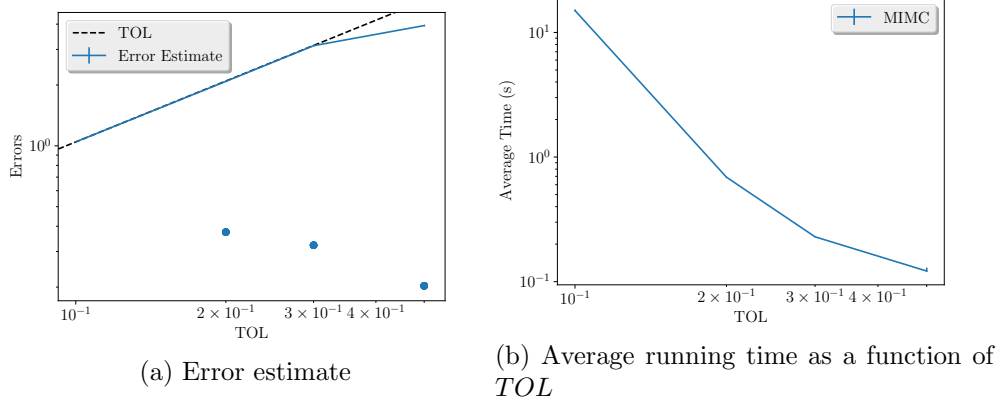


Figure 122: Convergence and complexity results for the call payoff with rBergomi model for $K = 1$, $H = 0.07$ and $N = 16$.

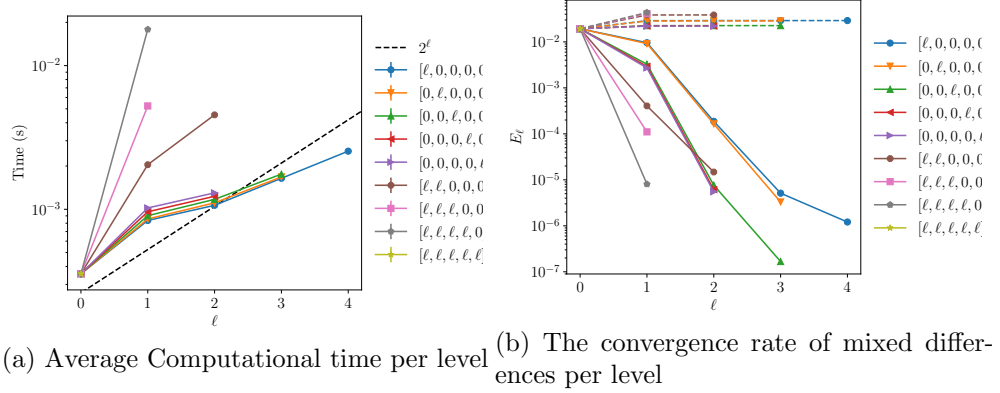


Figure 123: Convergence and work rates for discretization levels the call payoff with rBergomi model for $K = 1$, $H = 0.07$ and $N = 16$.

C.10 Hierarchical

H=0.43

Case of 8 time steps

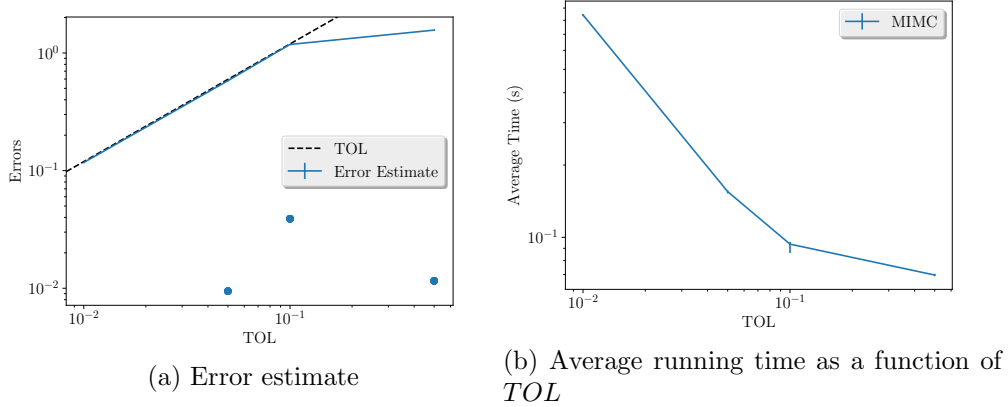


Figure 124: Convergence and complexity results for the call payoff with rBergomi model for $K = 1$, $H = 0.43$ and $N = 8$.

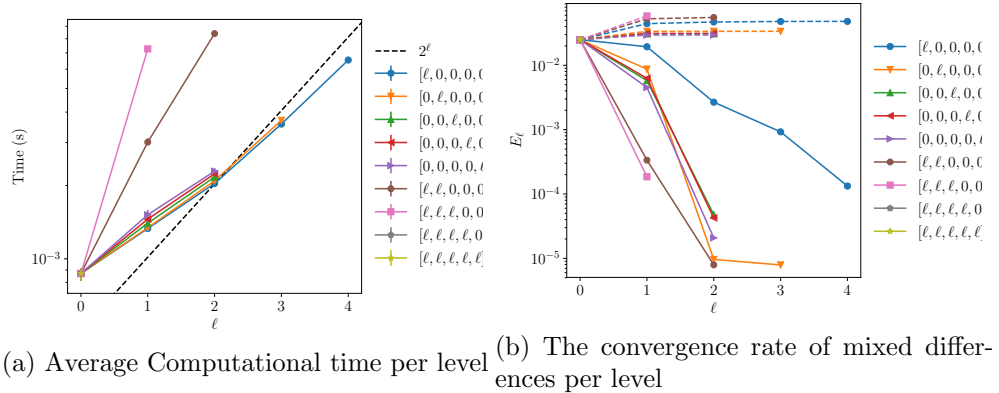


Figure 125: Convergence and work rates for discretization levels the call payoff with rBergomi model for $K = 1$, $H = 0.43$ and $N = 8$.

Case of 16 time steps

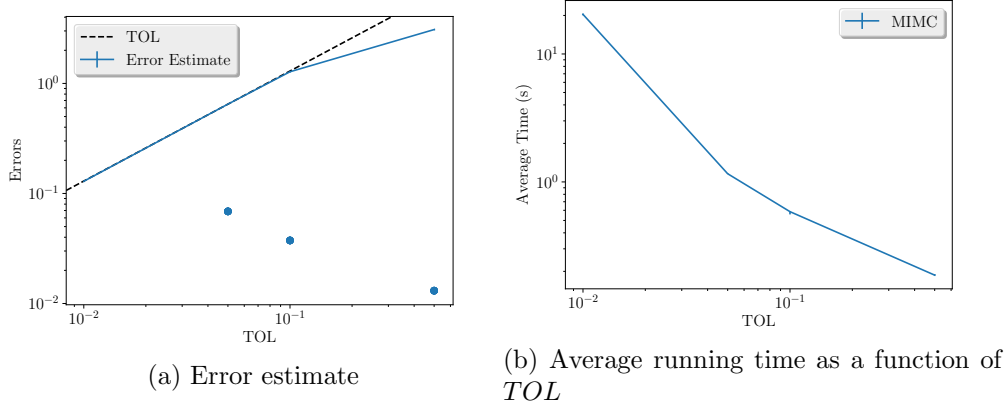


Figure 126: Convergence and complexity results for the call payoff with rBergomi model for $K = 1$, $H = 0.43$ and $N = 16$.

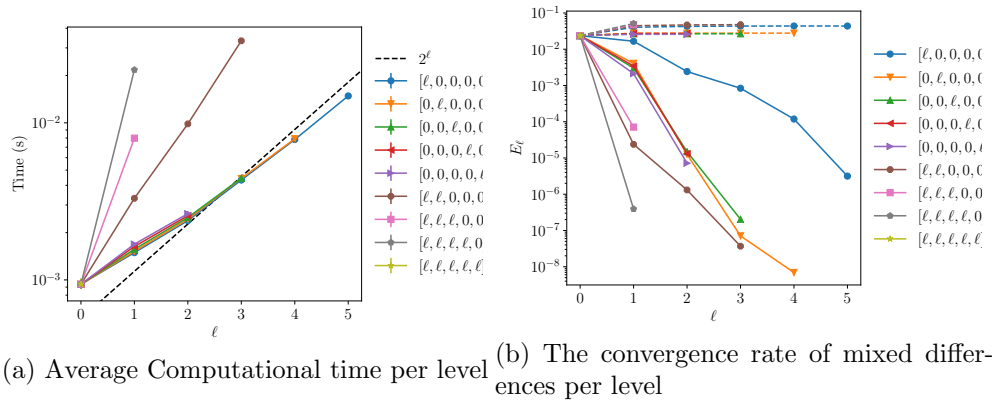


Figure 127: Convergence and work rates for discretization levels the call payoff with rBergomi model for $K = 1$, $H = 0.43$ and $N = 16$.

H=0.07

Case of 8 time steps

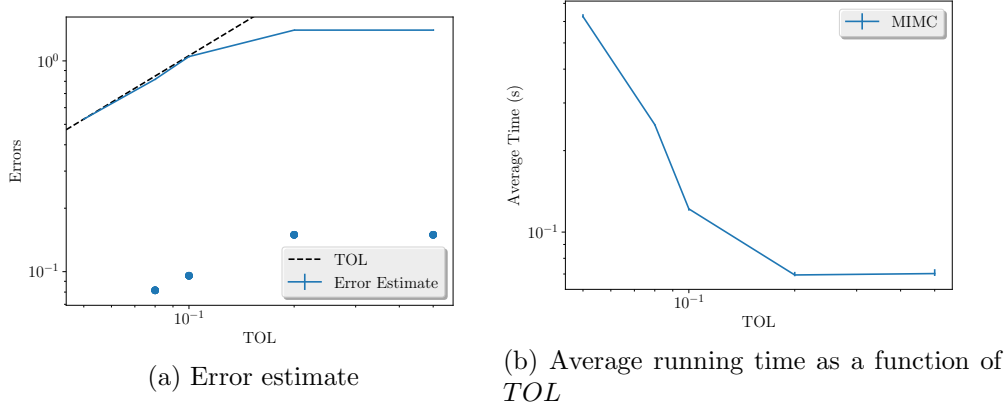


Figure 128: Convergence and complexity results for the call payoff with rBergomi model for $K = 1$, $H = 0.07$ and $N = 8$.

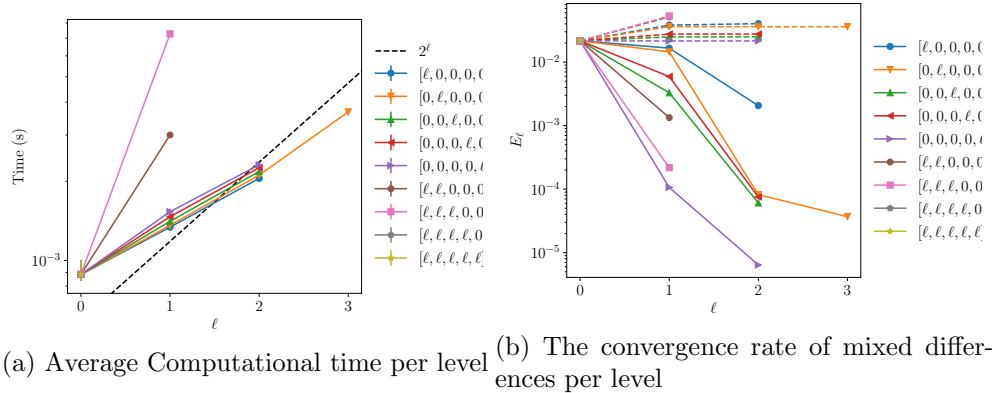


Figure 129: Convergence and work rates for discretization levels the call payoff with rBergomi model for $K = 1$, $H = 0.07$ and $N = 8$.

Case of 16 time steps

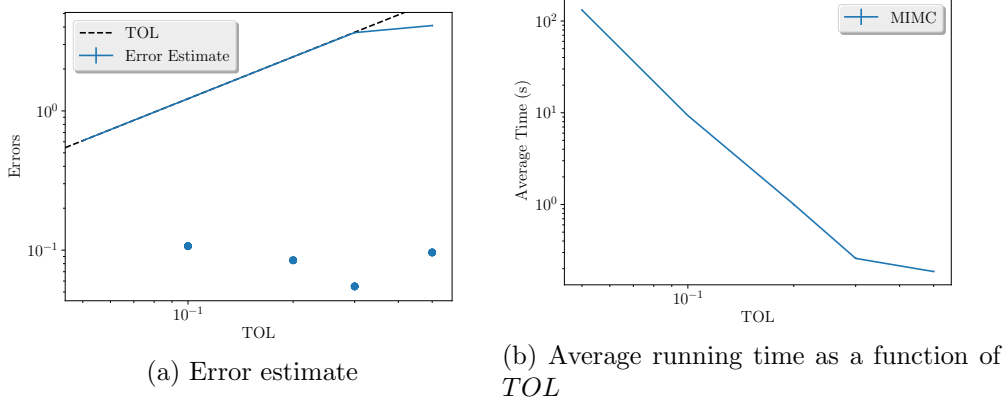


Figure 130: Convergence and complexity results for the call payoff with rBergomi model for $K = 1$, $H = 0.07$ and $N = 16$.

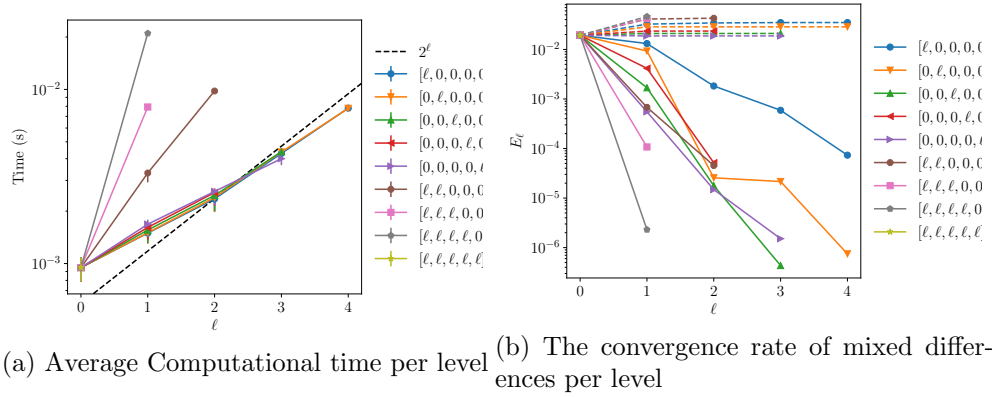


Figure 131: Convergence and work rates for discretization levels the call payoff with rBergomi model for $K = 1$, $H = 0.07$ and $N = 16$.

C.11 Comparing call options prices

C.11.1 Without Hierarchical representation

Case $H = 0.43$

Case $H = 0.07$

Method \ Steps	2	4	8	16
MISC ($Tol = 5.10^{-1}$)	0.1057	0.0988	0.0944	0.0921
MISC ($Tol = 10^{-1}$)	0.1057	0.0988	0.0836	0.0594
MISC ($Tol = 5.10^{-2}$)	0.1057	0.0976	0.0758	0.0781
MISC ($Tol = 10^{-2}$)	0.1113	0.0940	0.0820	—
MC method ($M = 10^6$)	0.1079 ($1.55e-04$)	0.0921 ($9.65e-05$)	0.0822 ($7.61e-05$)	0.0769 ($6.65e-05$)

Table 54: Call option price of the different methods for different number of time steps. Case $K = 1$

Method \ Steps	2	4	8	16
MISC ($Tol = 5.10^{-1}$)	0.1065	0.0900	0.0809	0.0762
MISC ($Tol = 10^{-1}$)	0.1065	0.0900	0.0733	0.0956
MISC ($Tol = 5.10^{-2}$)	0.1065	0.0898	0.0881	—
MISC ($Tol = 10^{-2}$)	0.1226	0.1022	0.0933	—
MC method ($M = 10^6$)	0.1216 ($1.05e-03$)	0.1020 ($1.86e-04$)	0.0912 ($1.35e-04$)	0.0854 ($1.08e-04$)

Table 55: Call option price of the different methods for different number of time steps. Case $K = 1$